Kurile-Kamchatka and **Al**eutean **M**arginal Sea - Island **Ar**c Systems

Program and Abstracts

Workshop in Russian-German Cooperation. May 16 - 20, 2011 Trier, Germany

Vol. 2011
Heft 2011

KALMAR - Bilateral Workshop on Russian-German Cooperation on Kurile-Kamchatka and the Aleutean Marginal Sea-Island Arc Systems

Editor
Herausgeberin

Dr. Christel van den Bogaard, Prof. Wolf-ChristianDullo
IFM-GEOMAR, Leibniz-Institut für Meereswissenschaften
Wischhofstr. 1-3, 24149 Kiel
Tel.: +49 (0) 431 6002647, Fax: +49 (0) 431 6002960

Editorial staff
Redaktion

Dr. Christel van den Bogaard, Jutta Bothmann
IFM-GEOMAR, Leibniz-Institut für Meereswissenschaften

Printed by
Druck

G + D Grafik + Druck, Kiel

Bundesministerium
für Bildung
und Forschung

KALMAR Workshop

funded by

German Ministry of Education and Research
Russian Ministry of Education and Science

organized by

PARTICIPANTS

Abelmann, Andrea	AWI, Bremerhaven, Germany
Almeev, Renat	Leibniz University, Hannover, Germany
Baranov, Boris	IO RAS, Moscow, Russia
Barckhausen, Udo	BGR, Hannover, Germany
Botcharnikov, Roman	Leibniz University, Hannover, Germany
Bubenshchikova, Natalya	IO RAS, Moscow, Russia
Derkachev, Alexander	POI FEB RAS, Vladivostok, Russia
Delisle, Georg	BGR, Hannover, Germany
Diekmann, Bernhard	AWI, Potsdam, Germany
Dirksen, Oleg	IVS FEB RAS, Petropavlovsk-Kamchatsky, Russia
Dirksen, Veronika	IVS FEB RAS, Petropavlovsk-Kamchatsky, Russia
Dullo, Wolf-Christian	IFM-GEOMAR, Kiel, Germany
Freitag, Ralf	BGR, Hannover, Germany
Freundt, Armin	IFM-GEOMAR, Kiel, Germany
Gaedicke, Christoph	BGR, Hannover, Germany
Gorbarenko, Sergey	POI FEB RAS, Vladivostok, Russia
Hoernle, Kaj	IFM-GEOMAR, Kiel, Germany
Holtz, Francois	Leibniz University, Hannover, Germany
Ivanova, Elena	IO RAS, Moscow, Russia
Korsun, Sergei	IO RAS, Moscow, Russia
Kozhurin, Andrey	Geological Institute, RAS, Moscow, Russia
Krüger, Kirstin	IFM-GEOMAR, Kiel, Germany
Lehmkuhl, Frank	RWTH, Aachen, Germany
Levitan, Mikhail	GEOKHI RAS, Moscow, Russia
Malakhov, Mikhail	NEISRI RAS, Magadan, Russia
Matul, Alexander	IO RAS, Moscow, Russia
Max, Lars	AWI, Bremerhaven, Germany
Mironov, Nikita	GEOKHI RAS, Moscow, Russia
Nürnberg, Dirk	IFM-GEOMAR, Kiel, Germany
Ovsepyan, Ekaterina	IO RAS, Moscow, Russia
Pinegina, Tatyana	IVS FEB RAS, Petropavlovsk-Kamchatsky, Russia
Ponomareva, Vera	IVS FEB RAS, Petropavlovsk-Kamchatsky, Russia
Portnyagin, Maxim	IFM-GEOMAR, Kiel, Germany
Riethdorf, Jan-Rainer	IFM-GEOMAR, Kiel, Germany
Schwarz-Schampera, Ulrich	BGR, Hannover, Germany
Silantyev, Sergei	GEOKHI RAS, Moscow, Russia
Sirokko, Frank	University of Mainz, Mainz, Germany
Smirnova, Maria	IO RAS, Moscow, Russia
Stauch, Georg	RWTH, Aachen, Germany
Tanner, Barbara	PTJ, Warnemünde, Germany
Tiedemann, Ralf	AWI, Bremerhaven, Germany
Tsukanov, Nikolay	IO RAS, Moscow, Russia
van den Bogaard, Christel	IFM-GEOMAR, Kiel, Germany
Wanke, Maren	IFM-GEOMAR, Kiel, Germany
Weiss, Richard	USC, Columbia, USA
Werner, Reinhard	IFM-GEOMAR, Kiel, Germany
Yogodzinski, Gene	USC, Columbia, USA

CONTENT

PROGRAM

MONDAY, 16. MAY 2011

16:00 – 16:30 **Registration** – Hotel Nells Park, Trier

17:00 **Icebreaker**

TUESDAY, 17. MAY 2011

Opening

09:00 – 9:30 **Prof. Dr. Wolf-Christian Dullo**
German Project leader of KALMAR

Prof. Dr. Boris Baranov
Russian Project leader of KALMAR

Dr. Christel van den Bogaard
Coordination of KALMAR

Session 1

09:30 – 10:30 **INTERPROJECT DISCUSSION GROUPS + POSTERS**

Tectonic structure, geodynamic evolution and neotectonics at the active plate margin of Kamchatka and the Kamchatka Triple Junction

Volcanic and magmatic evolution of the Kamchatka-Aleutian Triple Junction

Pleistocene-Holocene climate development on Kamchatka and in the subarctic NW Pacific Ocean

Coffee Break

11:00 – 12:30 **Session 1 continued**

Lunch Break
Poster Session

Session 2

14:30 – 15:30 **THEMES AND AREAS FOR FUTURE JOINT COLLABORATION AND RESEARCH**

Coffee Break

16:00 **Prof. Dr. Frank Sirokko –** *(University of Mainz, Germany)*
Invited talk –
Maar deposits in the West Eifel, Germany –
High resolution quaternary climate archives.

WEDNESDAY, 18. MAY 2011

Full-day excursion to the Vulkan Eifel

08:30 – 23:00 Start at Nell's Park Hotel
Lunch at Ulmener Maar
Dinner at Vulkanbrauerei Mendig

West Eifel guided by Prof. Dr. Frank Sirokko *(Unversity of Mainz, Germany)*
East and West Eifel guided by PD. Dr. Armin Freundt *(IFM-GEOMAR Kiel, Germany)*

THURSDAY, 19. MAY 2011

Opening
Session 3

09:00 – 9:25 **Prof. Dr. Wolf-Christian Dullo**
German Project leader of KALMAR
Prof. Dr. Boris Baranov
Russian Project leader of KALMAR

Introduction to the KALMAR Project

Tectonic structure, geodynamic evolution and neotectonics at the active plate margin of Kamchatka and the Kamchatka Triple Junction

09:25 – 09:50 *Ralf Freitag (BGR Hannover, Germany), Dorthe Pflanz (University Jena), Nikolay Tsukanov (IO Moscow, Russia), Christoph Gaedicke (BGR Hannover, Germany), Matthias Krbetschek (University Freiberg, Germany) Boris Baranov (IO Moscow, Russia), Nikola Seliverstov (IVS Petropavlovsk-Kamchatsky, Russia)*
Exhumation and surface uplift at the Kamchatka-Aleutian triple junction area - Results from KALMAR neotectonics group (TP1)

09:50 – 10:05 *Andrey Kozhurin (Geological Institute Moscow, Russia), Tatiana Pinegina (IVS Petropavlovsk-Kamchatsky, Russia)*
Active fault study in the Kamchatsky Peninsula, Kamchatka-Aleutian junction

10:05 – 10:30 *Christoph Gaedicke, Udo Barckhausen, Dieter Franke, Ralf Freitag, Ingo Heyde, Stefan Ladage, Rüdiger Lutz (BGR Hannover, Germany), Nikolay Tsukanov (IO Moscow, Russia), Thomas Pletsch (BGR Hannover, Germany), Evgeny Sukhoveev (POI Vladivostok, Russia), Hauke Thöle (BGR Hannover, Germany)*
SO201 Leg 1a KALMAR – Geophysical Measurements in the North-west Pacific: An Overview

Coffee Break

11:00 – 11:15 *Boris Baranov (IO Moscow, Russia), Reinhard Werner (IFM-GEOMAR Kiel, Germany), Nikolay Tsukanov (IC Moscow, Russia), Maxim Portnyagin (IFM-GEOMAR, Germany), Gene Yogodzinski (U of South Carolina, USA)*
1. Multi-beam investigations in the SO-201 Cruise, Leg 2

Volcanic and magmatic evolution of the Kamchatka-Aleutian Triple Junction

11:15 – 11:30 *Kaj Hoernle, Maxim Portnyagin, Reinhard Werner (IFM-GEOMAR Kiel, Germany), Gennady Avdeiko (IVS Petropavlovsk-Kamchatsky, Russia), Boris Baranov (IO Moscow, Russia), Vera Ponomareva (IVS Petropavlovsk-Kamchatsky, Russia) and TP3 team*
KALMAR contribution to the understanding of spatial and temporal magmatic evolution of the Kamchatka-Aleutian junction

11:30 – 11:45 *Maxim Portnyagin (IFM-GEOMAR Kiel, Germany), Alexander Sobolev, Nikita Mironov (GEOKHI Moscow, Russia), Natalya Gorbach (IVS Petropavlovsk-Kamchatsky, Russia), Dmitri Kuzmin (MPI Mainz, Germany), Kaj Hoernle (IFM-GEOMAR Kiel, Germany)*
The origin of primary magmas at the Kamchatka-Aleutian Arc junction by melting of mixed pyroxenite and peridotite mantle sources

11:45 – 12:00 *Gene Yogodzinski, Joshua Turka, Shawn Arndt (U of South Carolina, USA), Peter Kelemen (Columbia University, USA), Maxim Portnyagin, Kaj Hoernle (IFM-GEOMAR Kiel, Germany)*
Geochemistry of Seafloor Lavas of the Western Aleutian Arc

12:00 – 12:15 *Maren Wanke (CAU Kiel, Germany), Maxim Portnyagin, Reinhard Werner, Folkmar Hauff, Kaj Hoernle (IFM-GEOMAR Kiel, Germany), Dieter Garbe-Schönberg (CAU Kiel, Germany)*
New geochemical data provide evidence for an island-arc origin of the Bowers and Shirshov Ridges (Bering Sea, NW Pacific)

Lunch Break
Poster Session

14:00 – 14:15 *Vera Ponomareva (IVS Petropavlovsk-Kamchatsky,Russia) for the KALMAR Tephra Team*
Overview of tephra studies in the KALMAR project: Integrating terrestrial, lake and marine records

Pleistocene-Holocene climate development on Kamchatka and in the subarctic NW Pacific Ocean

14:15 – 14:30 *Ralf Tiedemann (AWI-Bremerhaven, Germany)*, *Dirk Nürnberg (IFM-GEOMAR Kiel, Germany), Andrea Abelmann (AWI-Bremerhaven, Germany)*, *Wolf-Christian Dullo (IFM-GEOMAR Kiel, Germany), Sergey Gorbarenko, Alexander Derkachev (POI Vladivostok, Russia), Mikhail Malakhov (NEISRI Magadan, Russia), Alexander Matul (IO Moscow, Russia), Elena Ivanova (IO Moscow, Russia), Sergey Korsun (IO Moscow, Russia), Jan-Rainer Riethdorf (IFM-GEOMAR Kiel, Germany), Lars Max (AWI-Bremerhaven, Germany)*
Timing, nature, and processes of Holocene to Pleistocene climatic and oceanographic changes in the NW-Pacific

14:30 – 14:45 *Alexander Matul (IO Moscow, Russia), Andrea Abelmann (AWI-Bremerhaven, Germany) Khadyzhat Saidova, Maria Smirnova, Tatyana Khusid (IO Moscow, Russia)*
Late Quaternary paleoceanography in the southeastern Bering Sea

14:45 – 15:00 *Jan-Rainer Riethdorf (IFM-GEOMAR Kiel, Germany), Lars Max (AWI-Bremerhaven, Germany), Dirk Nürnberg (IFM-GEOMAR Kiel, Germany), Ralf Tiedemann (AWI-Bremerhaven, Germany)*
Late Pleistocene to Holocene changes in sea surface temperature, marine productivity and terrigenous fluxes in the western Bering Sea

15:00 – 15:25 *Bernhard Diekmann (AWI-Potsdam, Germany), Annette Bleibtreu (University of Potsdam, Germany), Bernhard Chapiglin (AWI-Potsdam, Germany), Verena de Hoog (University of Potsdam, Germany), Oleg Dirksen, Veronica Dirksen (IVS Petropavlovsk-Kamchatsky, Russia), Ulrike Hoff, Hans-Wolfgang Hubberten, Conrad Kopsch, Hanno Meyer, Larisa Nazarova (AWI-Potsdam, Germany), Christel van den Bogaard (IFM-GEOMAR Kiel, Germany)*
Holocene Palaeoenvironment on Kamchatka

15:25 – 15:40 *Oleg Dirksen (IVS Petropavlovsk-Kamchatsky, Russia), Christel van den Bogaard (IFM-GEOMAR Kiel, Germany) Tohru Danhara (FT Co. Kyoto, Japan) Bernhard Diekmann (AWI Potsdam, Germany)*
Holocene terraces and landslide events in northern and southern Kamchatka: evidence of sharp tectonic and volcanic unrest at 2800-2900 ^{14}C BP

Coffee Break
Poster Session

16:00 – 16:30 Discussion and Posters

16:30 – 17:00 *Wolf-Christian Dullo (IFM-GEOMAR Kiel, Germany) Boris Baranov (IO Moscow, Russia)*
Closure of session / Summary

Conference Dinner

17:30 Meet at Amphitheater
Walk through vineyards

FRIDAY, 20. MAY 2011

Session 4

Themes and areas for future joint collaboration and research

09:00 – 09:20 *Wolf-Christian Dullo (IFM-GEOMAR Kiel, Germany) Boris Baranov (IO Moscow, Russia)*
Outlook and Future Perspectives

09:20 – 09:35 *Georg Stauch (RWTH Aachen, Germany), Olga Glushkova (NEISRI Magadan Russia), Frank Lehmkuhl (RWTH Aachen, Germany), Bernhard Diekmann (AWI Potsdam, Germany)*
Quaternary Glaciations in NE Russia

09:35 – 09:50 *Tatiana Pinegina (IVS Petropavlovsk-Kamchatsky, Russia), Andrey Kozhurin (Geological Institute Moscow, Russia)*
Tsunami and active tectonics along the western margin of the Bering Sea - impact on the coastal zone environment and evolution

09:50 – 10:05 *Ulrich Schwarz-Schampera (BGR Hannover, Germany), Nikolay Tsukanov (IO Moscow, Russia), Christoph Gaedicke (BGR Hannover, Germany), Boris Baranov (IO Moscow, Russia), Gennadi Cherkachev (VNII St. Petersburg, Russia), Nikolay Seliverstov (IVS Petropavlovsk-Kamchatsky, Russia)*
Epithermal alteration of volcanic rocks of Kamchatka – onshore, offshore

10:05 – 10:20 *Renat Almeev (Leibniz Universität Hannover, Germany), Alexei Ariskin (GEOKHI Moscow, Russia), Roman Botcharnikov, Francois Holtz, Tatiana Shishkina (Leibniz University Hannover, Germany), Maxim Portnyagin (IFM-GEOMAR Kiel, Germany), Jun-Ichi Kimura (JAMSTEC, Japan), Alexey Ozerov (IVS Petropavlovsk-Kamchatsky, Russia)*
Modeling magma differentiation processes in volcanic systems

10:20 – 10:35 *Kirstin Krüger, Matthew Toohey (IFM-GEOMAR Kiel, Germany), Davide Zachettin, Claudia Timmreck (MPI-M Hamburg, Germany)*
Climate effects of large explosive volcanism: tropical versus high latitude eruptions

Coffee Break

11:00 – 11:10 *Wolf-Christian Dullo (IFM-GEOMAR Kiel, Germany)*
Boris Baranov (IO Moscow, Russia)
Closure of session / Summary

End of Meeting

Poster Sessions

Tectonic structure, geodynamic evolution and neotectonics at the active plate margin of Kamchatka and the Kamchatka Triple Junction

Udo Barckhausen (BGR Hannover, Germany), Sina Muff (CAU Kiel, Germany), Christoph Gaedicke (BGR Hannover, Germany)
The Cretaceous Normal Superchron in the Northwest Pacific

Georg Delisle, Michael Zeibig (BGR Hannover, Germany)
Marine heat flow measurements offshore Kamchatka – results and interpretation

Ralf Freitag, Christoph Gaedicke (BGR Hannover, Germany), Nikolay Tsukanov (IO Moscow, Russia), Udo Barckhausen, Dieter Franke, Ingo Heyde, Stefan Ladage, Rüdiger Lutz, Michael Schnabel (BGR Hannover, Germany)
The Krusenstern Fault, NW Pacific: A Reactivated Cretaceous Transform Fault?

Ralf Freitag, Dorthe Pflanz (University Jena), Christoph Gaedicke (BGR Hannover, Germany), Nikolay Tsukanov, Boris Baranov (IO Moscow, Russia), Matthias Krbetschek (University Freiberg, Germany)
Surface uplift and rock exhumation of morphotectonic blocks at the active fore-arc of Kamchatka, Russia

Ingo Heyde, Dieter Franke, Ralf Freitag, Christoph Gaedicke, (BGR Hannover, Germany) Nikolay Tsukanov (IO Moscow, Russia)
Marine geophysical measurements in the northernmost part of the Emperor Seamount Chain in the Northwest Pacific

Nikolay Tsukanov (IO Moscow, Russia), Christoph Gaedicke, Ralf Freitag (BGR Hannover, Germany), Karina Dozorova (IO Moscow, Russia),
Structure of the uppermost sedimentary layers in Kamchatka and Aleutian island arcs junction area and northern Emperor Seamounts and Emperor Trough - new insights from high resolution echosound data (SO201 Leg 1a, Leg 2 KALMAR)

Volcanic and magmatic evolution of the Kamchatka-Aleutian Triple Junction

Boris Baranov (IO RAS Moscow, Russia), Reinhard Werner (IFM-GEOMAR Kiel, Germany)
Structure and regional stress of the Vulkanologov Massif (Western Bering Sea) based on swath bathymetric surveys

Roman Botcharnikov, Tatiana Shishkina, Renat Almeev, Francois Holtz (Leibniz University Hannover, Germany), Maxim Portnyagin (IFM-GEOMAR Kiel, Germany)
Evaluation of storage conditions and degassing processes for natural magmas: An effective combination of natural observations and experimental methods

Alexander Derkachev, Nataliya Nikolaeva (POI Vladivostok, Russia)
Heavy mineral assemblages of the tephra layers found in sediments from the Bering Sea and the north-western Pacific Ocean

Alexander Derkachev (POI Vladivostok, Russia), Maxim Portnyagin (IFM-GEOMAR Kiel, Germany), Vera Ponomareva (IVS Petropavlovsk-Kamchatsky, Russia), Sergey Gorbarenko (POI FEB Vladivostok, Russia), Mikhail Malakhov (NEISRI Magadan, Russia), Dirk Nürnberg, Jan-Rainer Riethdorf (IFM-GEOMAR Kiel, Germany), Ralf Tiedemann (AWI Bremerhaven, Germany), Christel van den Bogaard (IFM-GEOMAR Kiel, Germany)
Marker tephra layers in the Holocene-Pleistocene deposits of the Bering Sea and the north-western Pacific Ocean

Natalia Gorbach (IVS Petropavlovsk-Kamchatsky, Russia) Maxim Portnyagin (IFM-GEOMAR Kiel, Germany)
Evolution of the Late Pleistocene Old Shiveluch Volcano, Kamchatka

Stepan Krasheninnikov, Maxim Portnyagin (IFM-GEOMAR Kiel, Germany)
Parental melts of Avachinskiy volcano (Kamchatka) inferred from data on melt inclusions

Elisaveta Krasnova (GEOKHI Moscow, Russia), Maxim Portnyagin (IFM-GEOMAR Kiel, Germany), Sergei Silantiev (GEOKHI Moscow, Russia), Reinhard Werner, Folkmar Hauff, Kaj Hoernle (IFM-GEOMAR Kiel, Germany)
Petrology and geochemistry of mantle rocks from the Stalemate Fracture Zone (NW Pacific)

Olga Kuvikas (IVS Petropavlovsk-Kamchatsky, Russia), Maxim Portnyagin (IFM-GEOMAR Kiel, Germany), Vera Ponomareva (IVS Petropavlovsk-Kamchatsky, Russia)
Compositional variations of volcanic glasses from Kamchatka

Nikita Mironov (GEOKHI Moscow, Russia), Maxim Portnyagin (IFM-GEOMAR Kiel, Germany)
Deep roots of Klyuchevskoy volcano, Kamchatka

Nikita Mironov (GEOKHI Moscow, Russia), Maxim Portnyagin (IFM-GEOMAR Kiel, Germany)
Volatile flux from Klyuchevskoy volcano, Kamchatka

Anastasiya Plechova, Nikita Mironov (GEOKHI Moscow, Russia), Maxim Portnyagin (IFM-GEOMAR Kiel, Germany)
Diatom stratigraphy and paleogeography of the Western Bering
Fluxes of volatiles from volcanoes of Kamchatka

Vera Ponomareva (IVS Petropavlovsk-Kamchatsky, Russia), Maxim Portnyagin (IFM-GEOMAR Kiel, Germany), Alexander Derkachev (POI Vladivostok, Russia), Maarten Blaaw (Queens Universtiy Belfast, UK), Andrey Kozhurin, Maria Pevzner (Geological Institute Moscow, Russia), Tatiana Pinegina (IVS Petropavlovsk-Kamchatsky, Russia), Dieter Garbe-Schönberg (CAU Kiel, Germany) Christel van den Bogaard (IFM-GEOMAR Kiel, Germany)
Tephra links for the NW Pacific, Asian mainland and Kamchatka regions

Maxim Portnyagin, Folkmar Hauff, Kaj Hoernle (IFM-GEOMAR Kiel, Germany), Gene Yogodzinski (USC Columbia, USA), Reinhard Werner (IFM-GEOMAR Kiel, Germany), Boris Baranov (IO Moscow, Russia), Dieter Garbe-Schönberg (CAU Kiel, Germany)
Geochemical systematics of submarine glasses from the Volcanologists Massif, Far Western Aleutian Arc

Sergei Silantyev, Elisaveta Krasnova (GEOKHI Moscow, Russia), Maxim Portnyagin (IFM-GEOMAR Kiel, Germany), Alexey Novoselov (GEOKHI Moscow, Russia)
Silification of peridotites from the Stalemate Fracture Zone, NW Pacific: Tectonic and geochemical applications

Maren Wanke (CAU Kiel, Germany), Maxim Portnyagin, Reinhard Werner, Folkmar Hauff, Kaj Hoernle (IFM-GEOMAR Kiel, Germany), Dieter Garbe-Schönberg (CAU Kiel, Germany)
Effect of seawater alteration on trace element geochemistry of submarine basalts from the Bowers Ridge, Bering Sea

Pleistocene-Holocene climate development on Kamchatka and in the subarctic NW Pacific Ocean

Natalia Bubenshchikova (IO Moscow, Russia), Dirk Nürnberg (IFM-GEOMAR Kiel, Germany), Ralf Tiedemann (AWI Bremerhaven, Germany)
Spatial and temporal variability of an oxygen minimum zone in the marginal NW-Pacific during the last deglaciation to Holocene: indications from benthic foraminiferal and biogeochemical data

Marina Cherepanova (IBS Vladivostok, Russia), Sergey Gorbarenko (POI Vladivostok, Russia), Mikhail Malakhov (NEISRI Magadan, Russia), Dirk Nürnberg (IFM-GEOMAR Kiel, Germany)
Diatom stratigraphy and paleogeography of the Western Bering Sea over the past 170 ka

Veronika Dirksen (IVS Petropavlovsk-Kamchatsky, Russia), Bernhard Diekmann (AWI Potsdam, Germany)
New Holocene pollen record from Sokoch Lake, southern Kamchatka, and its paleoclimatic implications

Wolf-Christian Dullo (IFM-GEOMAR Kiel, Germany), Sergey Shapovalov (IO Moscow, Russia)
Hydrography of the NW Pacific off Kamchatka and of the SW Bering Sea

Ulrike Hoff, Bernhard Diekmann (AWI Potsdam, Germany)
Fossil diatom assemblages in mid- to late Holocene lake sediments of central Kamchatka, Russia

Galina Kazarina, Maria Smirnova (IO Moscow, Russia)
Diatoms in the Late Quaternary sediments of sediment core SO201-2-101-KL, Shirshov Ridge, the northwestern Bering Sea

Sergei Korsun, Tatiana Khusid (IO Moscow, Russia)
Living and dead benthic foraminifera in the Bering Sea

Mikhail Levitan, Tatyana Kuzmina, Irma Roshchina, Kirill Syromyatnikov (GEOKHI Moscow, Russia), Ralf Tiedemann, (AWI Bremerhaven, Germany), Dirk Nürnberg (IFM-GEOMAR Kiel, Germany), Lars Max (AWI Bremerhaven, Germany)
First results of component, grain-size and XRF analyses for sediment core SO201-2-101-KL (Shirshov Ridge)

Mikhail Malakhov (NEISRI Magadan, Russia), Sergey Gorbarenko (POI Vladivostok, Russia), Dirk Nürnberg (IFM-GEOMAR Kiel, Germany), Ralf Tiedemann (AWI Bremerhaven, Germany), Galina Malakhova (POI Vladivostok, Russia), Jan-Rainer Riethdorf (IFM-GEOMAR Kiel, Germany), Aleksandr

Bosin (POI Vladivostok, Russia), Marina Cherepanova (PIG Vladivostok, Russia)
Climate change, sea ice and productivity responses in magnetic parameters of sediments from Western Bering Sea and NW Pacific

Mikhail Malakhov (NEISRI Magadan, Russia), Sergey Gorbarenko (POI Vladivostok, Russia) Dirk Nürnberg (IFM-GEOMAR Kiel, Germany), Ralf Tiedemann (AWI Bremerhaven, Germany) Galina Malakhova (NEISRI Magadan, Russia), Jan-Rainer Riethdorf (IFM-GEOMAR Kiel, Germany)
Geomagnetic reletive paleointensity of sediment cores of the Western Bering Sea and NW Pacific

Alexander Matul, Khadyzhat Saidova, Tatyana Khusid, Maria Chekhovskaya, Natalia Oskina, Maria Smirnova, Sergei Korsun (IO Moscow, Russia)
Late Quaternary micropaleontology and paleoceanography in the southeastern Beringia

Ekaterina Ovsepyan, Elena Ivanova, Ivar Murdmaa, Tatyana Alekseeva (IO Moscow, Russia), Alexander Bosin (POI Vladivostok, Russia)
Glacial – interglacial environmental changes on the Shirshov Ridge, Western Bering Sea: micropaleontological and sedimentary records from Core SO 201-2-85KL

Ralf Tiedemann (AWI Bremerhaven, Germany), Dirk Nürnberg (IFM-GEOMAR Kiel, Germany), Lars Max, Jan-Rainer Riethdorf (IFM-GEOMAR Kiel, Germany), Julia Gottschalk (University of Bremen Germany), Andrea Abelmann (AWI Bremerhaven, Germany), Sergey Gorbarenko (POI Vladivostok, Russia), Elena Ivanova, Alexander Matul (IO RAS Moscow, Russia)
Oceanic and atmospheric teleconnections between the North Pacific and the North Atlantic during the past 25 ka

ABSTRACTS

– in alphabetical order by names of first authors –

New biogenic opal-based proxies used for paleoceanographic reconstructions in the subarctic Pacific realm

Andrea Abelmann[1], Bernhard Chapligin[1], Oliver Esper[1], Alexander Matul[2], Ralf Tiedemann[1]

[1] AWI, Alfred Wegener Institute for Polar and Marine Research, Am Handelshafen 12, 27570 Bremerhaven,Germany; email: Andrea.Abelmann@awi.de
[2] IO RAS, P.P. Shirshov Institute of Oceanology RAS, Nakhimovsky prospekt 36, 117997 Moscow, Russia

The subarctic Pacific and its adjacent seas have a significant impact on global climate development and its variation concerning oceanographic, atmospheric, biological and glacial processes. The contemporary subarctic Pacific is a CO_2 source because of the upwelling of CO_2 rich deep water (Takahashi et al. 2002). In spite of high nutrient concentrations in surface waters it is one of the three HNLC regions (high-nutrient, low-chlorophyll) of the World Ocean, which is ascribed to the limitation of the trace element iron (Tsuda et al. 2003). This is in contrast to the Bering Sea, the Sea of Okhotsk and the NW-Pacific waters off Japan and the Kurile Arc, characterized by high biological productivity (Sorokin 1995) resulting in enhanced CO_2 drawdown (Takahashi et al. 2002). This pattern can be related to eolian iron deposition and inputs from near-shore areas (Fung et al. 2000; Lam, Bishop 2008). These productivity regimes may have changed during glacial periods through iron fertilization via dust, extent of the summer and winter sea ice field, oceanic circulation and lowered sea level.

The Bering Sea and Sea of Okhotsk are main areas for the formation of North Pacific Intermediate Water (NPIW), which spreads out to the equator and significantly influences the thermohaline circulation and distribution of nutrients (You 2003, Sarmiento et al. 2004). As the production of NPIW is closely related to sea ice, it is suggested that the formation of NPIW was enhanced during glacial periods (Keigwin 1998; Tanaka, Takahashi 2005). The extension of the glacial sea ice on the other hand, may have forced the development of sea surface stratification that may have affected the biological productivity.

In order to further elucidate and understand past physical and biological processes and their impact/response on the climate development in the yet not well-studied polar North Pacific realm we applied a combination of new and traditional proxies, which rely on the biogenic opal preserved in the sediment record. We present the first $\delta^{30}Si$ and $\delta^{18}O$ data of diatom opal from the Bering Sea, measured at the same aliquot of sample. After careful accomplishment of a step-wise preparation technique for the separation of diatoms into different size fractions, we used the high-temperature laser fluorination of samples in a BrF_5 atmosphere to produce oxygen and SiF_4 gas, followed by analysis of a gas source isotope ratio massspectrometer (IRMS) similar to the method established by Leng and Sloane (2008). The combination of $\delta^{30}Si$ and $\delta^{18}O$ diatom opal measurements are crucial for the proper understanding of the variability of physical surface ocean conditions and related nutrient utilization at glacial/interglacial time scales that are prerequisite of the understanding of past carbon cycling and related global climate development. This is complemented by a combination of traditional paleobiological and geochemical proxies providing information on the variability of surface water temperature, sea ice extent, biological productivity regimes, biogenic export and input of neritic components based on radiolarian and diatom assemblage composition and biogenic opal concentration. The data are from Core SO202-2-77-KL recovered from the Shirshov Ridge in the Bering Sea and will be compared to data obtained from the subarctic Pacific and Sea of Okhotsk to reconstruct the impact of climatic changes on the past oceanographic and biological systems.

References

Fung IY, Meyn SK, Tegen I, Doney SC, John JG, Bishop JKB (2000) Iron supply and demand in the upper ocean. Global Biogeochemical Cycles 14 (1), 281-295

Keigwin LD (1998) Glacial-age hydrography of the far northwest Pacific. Paleoceanography 13(4): 323-339

Lam PJ, Bishop JKB (2008) The continental margin is a key source of iron to the HNLC North Pacific Ocean. Geophysical Research Letters 35 art. no.-L07608

Leng MJ, Sloane HJ (2008) Combined oxygen and silicon isotope analysis of biogenic silica. J. Quat. Sci. 23, 313-319

Sarmiento JL, Gruber N, Brzezinski MA, Dunne JP (2004) High-latitude controls of thermocline nutrients and low latitude biological productivity, Nature 427, 56-60

Sorokin Y (1995) Primary production in the Bering Sea. In: Kotenev BN, Sapozhnikoiv VV (eds) Complex studies of the Bering Sea ecosystem, Moscow, VNIRO Press: 264-276 (in Russian)

Tanaka S, Takahashi K (2005) Late Quaternary paleoceanographic changes in the Bering Sea and the western subarctic Pacific based on radiolarian assemblages. Deep-Sea Research II 52: 2131- 2149

Takahashi T, Sutherland S, Sweeney C (2002) Global sea-air CO_2 flux based on climatological surface ocean pCO_2, and seasonal biological and temperature effects. Deep-Sea Res. II 49, 1601-1622

Tsuda A, et al. (2003) A mesoscale iron enrichment in the western subarctic Pacific induces a large centric diatom bloom. Science 300, 958-961

You Y (2003) The pathway and circulation of North Pacific Intermediate Water. Geophys. Res. Lett. 30(24), 2291, doi:10.1029/2003GL018561

Modeling magma differentiation processes in volcanic systems: Key examples from Kamchatka island arc (Klyuchevskoy, Bezymianny and Mutnovsky volcanoes)

Renat Almeev[1], Alexei Ariskin[2], Roman Botcharnikov[1], Francois Holtz[1], Tatiana Shishkina[1], Maxim Portnyagin[2,5], Jun-Ichi Kimura[3], Alexey Ozerov[4]

[1] Leibniz University of Hannover, Callinstr. 3, 30419, Hannover, Germany; email: ralmeev@mineralogie.uni-hannover.de
[2] GEOKHI RAS, V.I.Vernadsky Institute of Geochemistry and Analytical Chemistry RAS, Kosygin St. 19, 119991 Moscow, Russia
[3] Institute for Research on Earth Evolution, JAMSTEC, 2-15 Natsushima-cho, Yokosuka 237-0061, Japan
[4] VS FEB RAS, Institute of Volcanology and Seismology FEB RAS, Piip Boulevard 9, 683006 Petropavlovsk-Kamchatsky, Russia
[5] IFM-GEOMAR, Leibniz Institute of Marine Sciences, Wischhofstrasse 1-3, 24148 Kiel, Germany

The key aspect of understanding magma differentiation processes is related to the mechanisms and thermodynamic conditions (P-T-$f$$O_2$-$a$$H_2O$) at which primary and parental basaltic magmas can generate derivative magmas resulting in the formation of tholeiitic, calc-alkaline, and other magmatic series. The liquid lines of descent are controlled by the compositions and proportions of fractionating minerals. Several thermodynamic and empirical models have been developed to predict melting-crystallization relations in basaltic to rhyolitic melts in a wide range of thermodynamic conditions in closed to open magmatic systems (*e.g.* MELTs, COMAGMAT, Petrolog). In practice, however, despite the great efforts in improving models, calculations still yield unsatisfactory results in the prediction of the calculated lines of descent, especially in the presence of H_2O at elevated pressures. On the basis of experimental data of Almeev et al. (2006, 2007) the COMAGMAT model has been recently refined, allowing one to predict effect of H_2O on phase equilibria more correctly. In this work we demonstrate the application of the refined COMAGMAT model to constrain magma differentiation processes for calc-alkaline series of Klyuchevskoy-Bezymianny volcanoes and low-K tholeiitic series of Mutnovsky volcano.

Mutnovsky volcano. The new version of the COMAGMAT program was initially verified using results of our crystallization experiments on Mutnovsky basalt performed in hydrous conditions at 100 and 300 MPa (see Botcharnikov et al. this volume). Phase diagram constructed on the basis of our calculations and modeled liquid lines of descent are in general agreement with those produced in experiments. The existence of magma differentiation at shallow depths and the hydrous character of Mutnovsky magmas, already demonstrated experimentally, were also supported by our polybaric fractional crystallization calculations (a proxy of magma ascent).

Klyuchevskoy volcano. The high-magnesian (HMB) to high-alumina (HAB) basaltic suite of Klyuchevskoy volcano has been previously reproduced by 40% fractionation of Ol–Aug–Sp assemblages during ascent of the parental HMB magma over the pressure range of 19–7 kbar at 1350–1108C with 2 wt.% of H_2O in the initial melt and 3 wt.% of H_2O in the resultant HAB melt (Ariskin et al. 1995). Our new calculations demonstrate more shallower depths of initial magma generation (14-15 kbar, 1 wt.% H_2O in initial melt), their subsequent magma ascent (decompression with a pressure release rate of 0.3 kbar/% cryst.) and formation of typical HAB liquids at pressures ~ 4 kbar in the presence of about 1.5 wt.% H_2O. Despite a good agreement with natural liquid lines of descent, our data are not supported by recent studies of primitive melt inclusions from Klyuchevskoy HMB (Mironov 2009) where melt inclusion compositions are more rich in CaO and H_2O and depleted in SiO_2. Such discrepancy requires new experimental studies to reconcile whole rock and melt inclusion compositions in HMBs of Klyuchevskoy volcano. The experimental results would also have an important implication to the genesis of primitive

magmas in island arcs.

Bezymianny volcano. Previous petrological and geochemical studies point out on the presence of a large magma chamber beneath Bezymianny volcano, where parental HAB magmas can stagnate and differentiate at nearly isobaric conditions producing evolved andesites and dacites (*e.g.* Ozerov et. al 1997). Our new data demonstrate that Bezymianny andesitic and dacitic melts can not be produced by HAB crystallization at isobaric conditions. In particular, the predicted CaO depletion in residual melts related to the crystallization of clinopyroxene, is not as strong as observed in natural systems. According to our optimal model, the Bezymianny petrochemical trend can be reproduced (only up to the appearance of hornblende-bearing andesites) by polybaric crystallization of Klyuchevskoy HMB derivative magma (~7 wt.% MgO, ~16 wt% Al_2O_3, 1.6% wt. H_2O) in the course of subsequent magma ascent with a slower (in comparison to Klyuchevskoy) pressure release rate of 0.1 kbar/%cryst. Fractional crystallization occurs in a pressure interval of 5 to 0.5 kbar and at slightly oxidized conditions (along the NNO+1 oxygen buffer, NNO – nickel-nickel oxide). The silica enrichment trend of Bezymianny volcanics is explained by the early crystallization of magnetite in hydrous andesitic melts. At lower pressures, more evolved dacitic melts are close to H_2O-saturation and amphibole should appear on their liquidus, thus emphasizing the "calc-alkaline" affinity of Bezymianny lavas.

The approach used in our work combines (1) experimental determination of phase equilibria in natural magmas, (2) verification and "tuning" of thermodynamic models and (3) application of the improved models for predicting magma differentiation processes (fractional crystallization, decompressional crystallization). This approach also relies on an excellent geochemical and mineralogical characterization of the volcanic systems of interest. It demonstrates a high potential and can be applied to selected volcanoes during the next phase of KALMAR project.

References

Almeev R, Holtz F, Koepke J, Parat F (2006) Effect of small amount of H_2O on the liquidus of olivine, plagioclase and clinopyroxene: an experimental study at 200 and 500 MPa, EMPG-XI, 11-13th September, University of Bristol, UK

Almeev R, Holtz F, Koepke J, Parat F, Botcharnikov R (2007) The effect of H_2O on olivine crystallization in MORB: Experimental calibration at 200 MPa, Am. Mineral., 92(4), 670-674.

Ariskin AA, Barmina GS, Ozerov AY, Nielsen RL (1995) Genesis of high-alumina basalts from Klyuchevskoy volcano, Petrology, 3, 449-472

Botcharnikov R, Shishkina T, Almeev R, Holtz F, Portnyagin M. (2011) Evaluation of storage conditions and degassing processes for natural magmas: An effective combination of natural observations and experimental methods (this volume)

Mironov N (2009) The origin and evolution of magmas from Klyuchevskoy volcano, Kamchatka – the study of melt inclusions in olivine, PhD dissertation, Moscow (*in Russian*).

Ozerov A, Ariskin A, Kyle P, Bogoyavlenskaya G, Karpenko S (1997) Petrological-geochemical model for genetic relationships between basaltic and andesitic magmatism of Klyuchevskoy and Bezymianny volcanoes, Kamchatka, Petrology, 5(6), 550-569

Structure and regional stress of the Vulkanologov Massif (Western Bering Sea) based on swath bathymetric surveys

Boris Baranov[1], Reinhard Werner[2]

[1] IO RAS, P.P. Shirshov Institute of Oceanology RAS, Nakhimovsky prospekt 36, 117997 Moscow, Russia; email: bbaranov@ocean.ru
[2] IFM-GEOMAR, Leibniz Institute of Marine Sciences, Wischhofstrasse 1-3, 24148 Kiel, Germany

The most peculiar feature of the Western Bering Sea (Komandorsky Basin) floor is a huge volcanic massif located about 60 km to the north from the Komandorsky Islands. This structure called Vulkanologov Massif was discovered in 1984 during RV Vulkanolog Cruise (Seliverstov et al. 1986). It has diameter of about 40 km and height more then 3.5 km. Up to beginning of 90-th Vulkanologov Massif was investigated by different methods including bathymetric mapping with using of single-beam echosounder (Seliverstov 1998). For the first time the swath bathymetric surveys were conducted on this structure in autumn of 2009 during SO 201-2 Cruise. This cruise was carried on in the frame of German-Russian project KALMAR (**K**urile-Kamchatka and **Al**eutian **M**arginal Sea – Island **Ar**c System).

Swath bathymetric surveys give us an opportunity to clarify the main structural features of the Vulkanologov Massif area including its central part (Piip Volcano), Komandor Graben and Alpha Ridge (Fig. 1). So, real idea was obtained about distribution of the normal fault scarps, which locate in western and eastern parts of the Vulkanologov Massif and in the Komandor Graben. The strikes of the normal faults scarps suggest

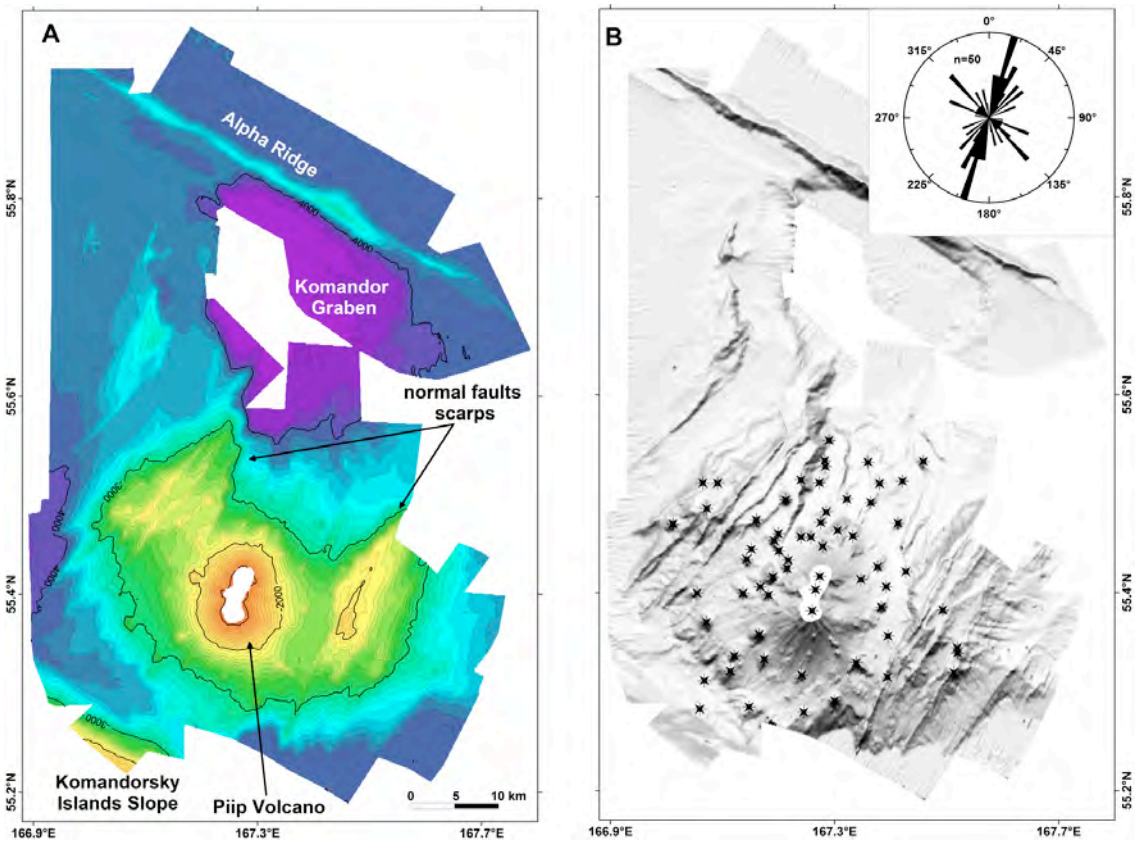

Fig. 1: Shaded bathymetry of the Vulkanologov Massif area located in rear part of the Komandorsky Islands, Western Bering Sea. Contour interval is 100 m (A); distribution of the flank cones (stars) and trends of the maximum horizontal compression (inset)(B).

dextral strike-slip movements along the fracture zones associated with Komandorsky Islands slope and Alpha Ridge.

In addition to many volcanic forms including flank cones, volcanic ridges and lava flows were detected in the Vulkanologov Massif. The flank cones are the most peculiar features among them. 57 cones locate in Vulkanologov Massif, besides about half of them (25 cones) are spaced at Piip volcano. The height of cones changes from 10 m up to 250 m and their diameters vary from 100 m up to 1,5 km. Main amount of the flank cones locates to the west from the Piip Volcano axis (Fig. 1B).

According to Nakamura (1977) the distribution of the flank cones will be elongated in the direction of the maximum horizontal compression (S_H) of the regional stress. To determine direction of the S_H we have used two parameters (Paulsen, Wilson, 2010): (1) flank cones alignments based on cone centers, and (2) flank cones alignments based on cone shapes. Two directions of the S_H were obtained, namely NW-SE and NNE-SSW (Fig. 1B, inset). First direction is weakly expressed and corresponds to direction of the maximum horizontal stress obtained on base of focal mechanism solutions (Heidbach et al. 2008). The second direction is determined by existence of feeder dikes, which trend parallel to the S_H direction and orthogonal to the minimum horizontal stress (S_H). S_H direction is roughly coincided with strike of normal faults scarps and governed by regional extension existing in this part of the Komandorsky Basin.

References

Heidbach O, Tingay M, Barth A, Reinecker J, Kurfeß D, Müller B (2008) The World Stress Map database release 2008 doi:10.1594/GFZ.WSM.Rel2008

Nakamura K (1977) Volcanoes as possible indicators of tectonic stress orientation – principle and proposal. Journal of Volcanology and Geothermal Research 2:1-16

Paulsen TS, Wilson TJ (2010) New criteria for systematic mapping and reliability assessment of monogenetic volcanic vent alignments and elongate volcanic vents for crustal stress analyses. Tectonophysics 482: 16–28

Seliverstov NI, Avdeiko GP, Ivanenko AN, Shkira VA, Khabunaya SA (1986) New submarine volcano in the western Aleutian Arc. Volcanology and Seismology 5: 3-16 (in Russian)

Seliverstov NI (1998) Seafloor structure offshore the Kamchatka Peninsula and geodynamics of the junction of the Kurile-Kamchatka/Aleutian islands arcs. Scientific World, Moscow: 16

Multi-beam investigations in the SO 201-2 Cruise: an overview

Boris Baranov[1], Reinhard Werner[2], Nikolay Tsukanov[1], Maxim Portnyagin[2] , Gene Yogodzinski[3]

[1] IO RAS, P.P. Shirshov Institute of Oceanology RAS, Nakhimovsky prospekt 36, 117997 Moscow, Russia; email: bbaranov@ocean.ru
[2] IFM-GEOMAR, Leibniz Institute of Marine Sciences, Wischhofstrasse 1-3, 24148 Kiel, Germany
[3] Department of Earth and Ocean Sciences, University of South Carolina, 701 Sumter Street, Columbia, SC 29208, USA

The investigation area in the SO 201-2 Cruise (KALMAR Project) embraced Kurile-Kamchatka/Aleutian junction area and Western Bering Sea. Multi-beam survey was performed in this area for the first time within study areas shown in Fig.1. Bathymetric maps were obtained for study areas B, 7 and E the most detailed.

Polygon B is located on continental and oceanic slopes of the Kurile-Kamchatka Trench in the point where Obruchev Rise subducts under Kamchatka Peninsula. Oceanic slope of the trench consists of several steps divided by scarps with heights from 500 to 1000 meters. The scarps strike parallel to the trench axis and correspond to normal faults which originate due to oceanic plate bending before its subduction into the trench. Peculiar morphologic features of the trench axial part permit to suppose that blocks of the Obruchev Rise begin to separate from oceanic plate; it causes migration of trench axis towards the ocean. Trench migration in its turn results in accretion of the oceanic blocks to the insular slope of the trench.

The structure of volcanic edifice (Vulkanologov Massif) located in the rear area of the Komandorsky Islands was investigated in detail within study area 7. Data obtained during bathymetric survey contributed a lot in understanding of structural pattern of this region. Great number of flank cones were found on the massif slopes; analysis of their distribution may be used for determination of dominant stresses system. Reliable distribution pattern for NE-striking normal faults which are widely spread on both eastern and western flanks of the massif was obtained. Earlier the normal faults were distinguished only on the eastern flank of the Vulkanologov Massif. Presence of EW-striking reverse faults were supposed for the western one (Seliverstov 1998); it contradicted general geodynamic situation observed for the Western Aleutian Arc.

Within study area E (Shirshov Ridge western slope) bathymetric survey was carried out in its southern, central and northern parts. It was found that structural pattern is one and the same for all these parts. Two systems of disjunctive dislocations were distinguished: NS-striking and NW-SE-striking faults. Faults of the first system correspond to steep scarps with height 350-500 m; they are faced to the west or east and limit tilted blocks formed due to extension and spreading in the Komandorsky Basin. Faults of the second system form graben-like structures cutting the main massif of the Shirshov Ridge. These structures obviously mark the terminations of transform fault zones; the last, as it was established on base of geophysical data, cross the Komandorskaya Basin from the Shirshov Ridge to the eastern slope of the Kamchatka Isthmus (Baranov et al. 1991; Seliverstov 1998). Separate areas of transform fault zones were mapped within study areas 3, 7, 5 and 12. All of them are represented by linear rises, striking in NW-SE direction. Structural pattern of the faults points on dextral displacements within study area 12.

Combined interpretation of bathymetric multi-beam data and available geophysical data will lead to better understanding of the tectonic pattern of the northern Kurile-Kamchatka Trench and the Western Bering Sea.

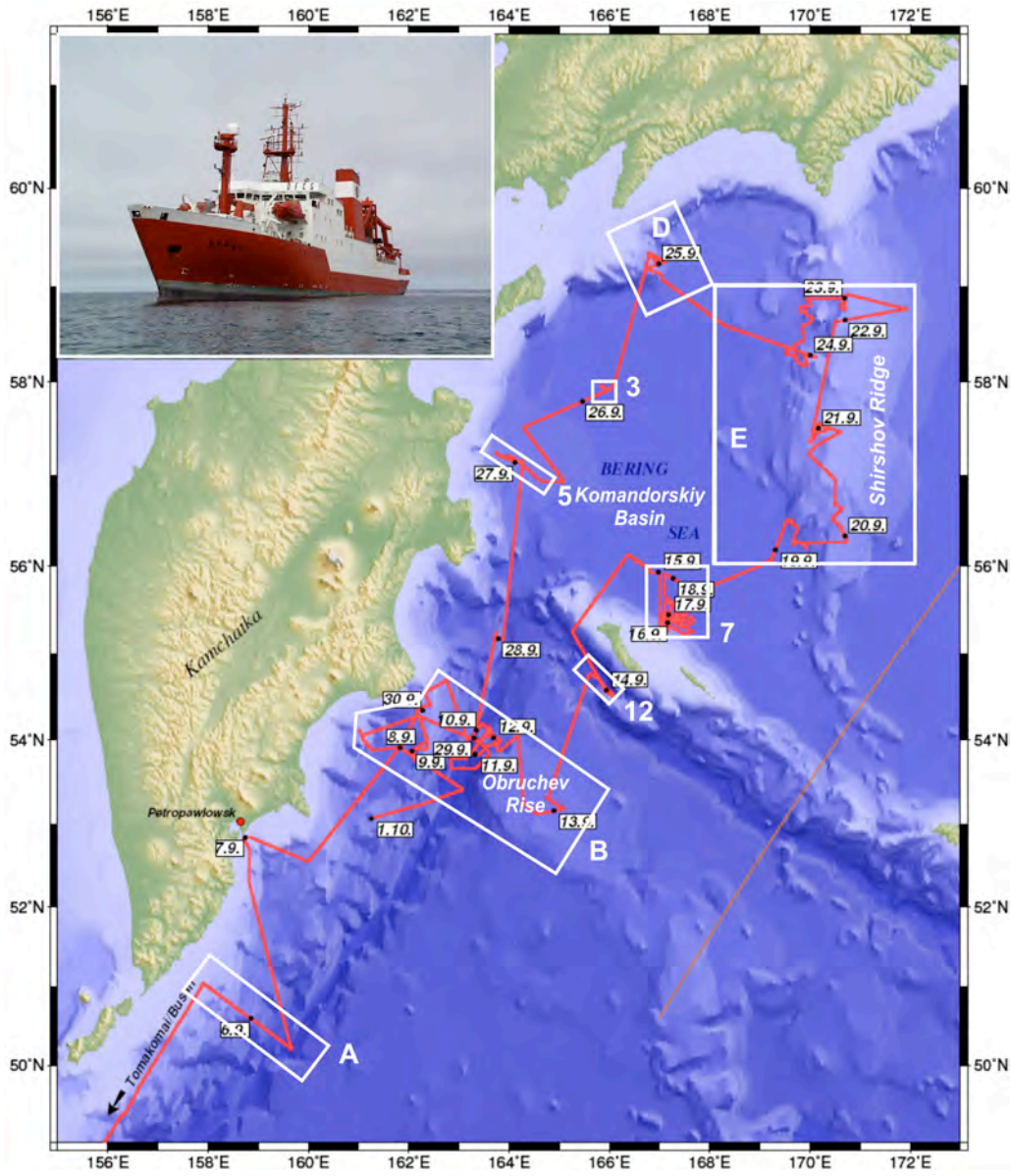

Fig. 1: Location of the study areas (white numbered rectanculars) in the SO 201-2 Cruise. Inset shows RV SONNE

References

Baranov BV, Seliverstov NI, Muravev AV, Muzurov EL (1991) The Komandorsky Basin as a product of spreading behind a transform plate boundary. Tectonophysics 199: 237-269

Seliverstov NI (1998) Seafloor structure offshore the Kamchatka Peninsula and geodynamics of the junction of the Kurile-Kamchatka/Aleutian islands arcs. Scientific World, Moscow: 164 (in Russian)

The Cretaceous Normal Superchron in the Northwest Pacific

Udo Barckhausen[1], Sina Muff[2], Christoph Gaedicke[1]

[1] BGR, Federal Institute for Geosciences and Natural Resources, Geozentrum Hannover, Stilleweg 2, 30655 Hannover, Germany; email: Udo.Barckhausen@bgr.de
[2] Institut für Geophysik der Universität Kiel, Otto-Hahn-Platz 1, 24118 Kiel, Germany

During cruise SO-201 KALMAR, a number of long magnetic profiles were acquired in the Northwest Pacific in an area where the oceanic crust was formed during the Cretaceous Normal Superchron (Chron 34, 118 Ma – 83 Ma; Cande, Kent 1995). For this time period there is also the name "Cretaceous Magnetic Quiet Zone" in use, a misleading term since the earth's magnetic field was not "quiet" during this time and the oceanic crust of the respective age shows significant magnetic anomalies. However, there is still no consensus among researchers whether or not magnetic anomalies within Chron 34 can be correlated and thus be used as time markers in oceanic crust (Dyment et al. 2009). Of all oceanic areas with crust dating from the Chron 34 time period, the Northwest Pacific is the least studied.

The magnetic profiles of cruise SO-201 and other suitable magnetic profiles were analyzed in order to find possible correlations of magnetic anomalies along assumed isochrones or perpendicular to the known fracture zones, resp. Since no obvious correlations could be established, the question was addressed with statistic methods. If magnetic anomalies were correlated along isochrones, then magnetic profiles should show different anomaly amplitudes and anomaly wavelengths depending on their direction with respect to the isochrones. We calculated mean values for these parameters for profiles running approximately parallel to the assumed isochrones as well as profiles running approximately perpendicular to them. No significant differences were found which would be indicative of correlations among the magnetic anomalies. Instead, crustal segments separated by fracture zones from each other show different characteristics in their magnetic anomalies while the anomalies themselves seem to be distributed randomly.

References

Cande SC, Kent DV (1995) Revised calibration of the geomagnetic polarity time- scale for the Late Cretaceous and Cenozoic. J. Geophys. Res. 100, 6093-6095

Dyment J, Gallet Y, Hoise E (2009) First complete high-resolution record of the Cretaceous Normal Superchron. Eos Trans. AGU 90 (52), Fall Meet. Suppl., Abstract GP31A-05

Evaluation of storage conditions and degassing processes for natural magmas: An effective combination of natural observations and experimental methods

Roman Botcharnikov[1], Tatiana Shishkina[1], Renat Almeev[1], Francois Holtz[1], Maxim Portnyagin[2]

[1] Institute of Mineralogy, Leibniz University Hannover, Callinstrasse 3, 30167 Hannover, Germany; email: r.botcharnikov@mineralogie.uni-hannover.de
[2] IFM-GEOMAR, Leibniz Institute of Marine Sciences, Wischhofstrasse 1-3, 24148 Kiel, Germany

Experimental simulation of magma crystallization and degassing processes is a powerful tool for the investigation of natural magmatic systems. It provides accurate information on the mechanisms and efficiency of magma crystallization, on the solubility behaviour and partitioning of volatiles and trace elements between magmatic phases. It also allows quantitative evaluation of physical and chemical properties of the magma (e.g., viscosity, density, vesicularity), and of the dependence of such properties on the main factors controlling magmatic processes, i.e., T, P, fO_2, system composition. The combination of experimental data, geochemical data and natural observations provide constraints on the pre-eruptive conditions, especially on the pressures (depths), temperatures and volatile contents in the magma chamber prior to volcanic eruption.

Modern experimental methods are designed for experimental studies in a wide range of pressures and temperatures typical for natural magmas in the magmatic reservoirs within the Earth's crust (i.e., up to 1-2 GPa and up to 1500°C). Specific types of experimental apparatus and techniques provide possibility to simulate magmatic conditions with controlled redox state of the system by varying hydrogen fugacity and volatile composition of the magma. The processes of magma evolution during ascent can be simulated by controlled decompression rate. The experiments on element and volatile diffusion as well as on magma rheology provide knowledge on kinetic aspects of magmatic processes.

Here we present one example of experimental study focused on the magmatic system of Mutnovsky volcano, Kamchatka. The recent data obtained within the framework of a pilot DFG-funded project on Mutnovsky volcano have a broad application and can be used to constrain a general genetic model for the formation of island arc tholeiitic series and will provide estimates on the budget and contribution of magmatic volatiles to the magmatic-hydrothermal volcanic systems.

1. Volatile solubility experiments were conducted in an internally heated pressure vessel (IHPV) at pressures of 50 to 500 MPa and temperature of 1250ºC. The solubility of H_2O in equilibrium with pure H_2O fluid increases from about 2.2 wt.% at 50 MPa to about 8.8 wt.% at 500 MPa. The concentration of CO_2 increases from about 200 to 3400 ppm in glasses which were in equilibrium with the most CO_2-rich fluids.

The obtained results enable a quantitative interpretation of volatile concentrations in glass inclusions to evaluate the magma storage conditions and degassing paths of natural island arc basaltic systems. The experimental database covers the entire range of volatile compositions reported in the literature for natural melt inclusions in olivine from low- to mid-K basalts, indicating that most melt inclusions were trapped or equilibrated at relatively shallow levels in magmatic systems (<15-20 km). The relatively low H_2O and CO_2 contents in the melt inclusions in olivines from Mutnovsky indicate that they were trapped from strongly degassed magma at shallow depths.

2. Phase relations of the Mutnovsky parental magma were investigated as a function of pressure, fO_2 and water activity (aH_2O). The experiments show that with decreasing temperature, the crystallization sequence in melts containing ~ 3 wt% H_2O is as follows: Mt → Mt + Pl → Mt + Pl + Ol → Mt + Pl + Ol + CPx→ Mt + Pl + Cpx + Opx, where Cpx and Opx are high and low-Ca pyroxene respectively. At higher water activities this crystallization sequence is complicated by

the presence of amphibole (Hbl) at temperatures below 1000°C. In the presence of Hbl, Cpx and Opx do not crystallize simultaneously. Magnetite does not crystallize in runs above 1050°C from melts with low H_2O content.

3. Study of natural samples from Mutnovsky volcano and information gained from the combination with experimental studies

Three major types of erupted basalts can be distinguished: CPx-Ol-Pl-, Ol-Plag- and rare OPx-CPx-Pl-bearing rocks, suggesting that parental melts probably evolved along Ol+Pl and Ol+Pl+Cpx low-pressure cotectics, similar to MORB-type magmas. However, in contrast to MORBs, Mutnovsky volcanics exhibit a pronounced FeO and TiO_2 depletion and SiO_2 enrichment, suggesting earlier Fe-Ti-oxide onset crystallization, which, in turn, can be achieved only in the presence of significant amounts of water at more oxidized conditions.

Glass inclusions in olivines (Fo_{75-80}) from tephra of Mutnovsky volcano have basaltic to andesitic compositions and overlap with the general petrochemical trend of Mutnovsky volcanic series, indicating that they are evolved derivates of the parental Mutnovsky melts.

The inclusions contain 1.7-2.7 wt.% H_2O and 0-180 ppm CO_2, indicating pressures of entrapment less than 110 MPa (less than 3 km) when magma was already significantly degassed. Moreover, values of H_2O analysed in melt inclusions are similar to the H_2O-contents in experimental residual glasses where Ol+Pl+CPx+Mt association was crystallized. In the glassy inclusions of Mutnovsky $S^{6+}/\Sigma S$ vary from 0.4 to 1, which corresponds to $\log fO_2$ from QFM+0.9 to QFM+1.7 (Jugo et al. 2010). These fO_2 values are in a good agreement with previous estimations of redox conditions for island arc magma systems.

Summary and magma storage conditions:

The combination of the natural and experimental observations gives us the possibility for evaluation of storage and pre-eruptive conditions for Mutnovsky magmas. We can expect a magma chamber below Mutnovsky volcano at depth not deeper than 9 km (300 MPa), in which H_2O-rich magma was stored at approximately 1025-1075°C and relatively oxidized redox conditions (QFM+0.9 to QFM+1.7) and in which the mineral association Ol+Pl+CPx+Mt was stable. The low water concentrations (and extremely low CO_2 concentrations) analyzed in glass inclusions in olivine can indicate that there is a shallow magma chamber (~ 100 MPa) in which olivine crystallized from an already partially degassed magma.

References

Jugo PJ, Wilke M, Botcharnikov RE (2010) Sulfur K-edge XANES analysis of natural and synthetic basaltic glasses: Implications for S speciation and S content as function of oxygen fugacity, Geochim. Cosmochim. Acta 74: 5926-5938

Shishkina T, Botcharnikov RE, Holtz F, Almeev RR, Portnyagin MV (2010) Solubility of H_2O and CO_2-bearing fluids in tholeiitic basalts at pressures up to 500 MPa Chemical Geology 277: 115-125

Spatial and temporal variability of an oxygen minimum zone in the marginal NW-Pacific during the last deglaciation to Holocene: indications from benthic foraminiferal and biogeochemical data

Natalia Bubenshchikova[1], Dirk Nürnberg[2], Ralf Tiedemann[3]

[1] IO RAS, P.P. Shirshov Institute of Oceanology, Nakhimovsky prospekt 36, 117997 Moscow, Russia; email: bubench@mail.ru
[2] IFM-GEOMAR, Leibniz Institute of Marine Sciences, Wischhofstrasse 1-3, 24148 Kiel, Germany
[3] AWI, Alfred Wegener Institute for Polar and Marine Research, Am Handelshafen12, 27568 Bremerhaven, Germany

Reduction of intermediate water ventilation and/ or intensification of oxygen minimum zone (OMZ) appear to have been widespread events during the Bølling-Allerød and Preboreal intervals not only in the Eastern Pacific but in the North Pacific (e.g. Crusius et al. 2004, McKay et al. 2005, Shibahara et al. 2007). This study present evidences on spatial and temporal variability of the OMZ intensity in the Okhotsk Sea during the last glacial Termination (T) I - Holocene inferred from benthic foraminiferal and biogeochemical data of four cores: LV28-2-4, LV28-40-5, LV28-43-5 and MD01-2415.

At present, the Okhotsk Sea contributes to ventilation of intermediate NW-Pacific via production of the oxygenated Okhotsk Sea Intermediate Water (OSIW: ~200-800 m). In the Okhotsk Sea, OMZ appears as a layer with oxygen contents 0.3-1.5 ml l^{-1} between ~800 and 1500 m water depths. The OMZ results from high primary productivity; predominant ventilation of the upper 500 m of OSIW; an inflow of the oxygen-depleted intermediate water from the North Pacific (core at ~800-1200 m with 0.6-1 ml l^{-1} of O_2), designated as Deep Pacific Water (DPW: ~800-1500 m) in the Okhotsk Sea; varying vertical mixing and regional topography.

The KOMEX cores LV28-2-4, LV28-40-5 and LV28-43-5 taken during the V28 cruise of the R/V *Akademik M.A.Lavrentyev* in 1998 cover 46, 78 and 52 ka, respectively (e.g. Bubenshchikova et al. 2010). The IMAGES core MD01-2415 collected during the WEPAMA 2001 cruise of the R/V *Marion Dufresne* represents the last 1.1 million years (Nürnberg and Tiedemann 2004). The shallower cores MD01-2415 and LV2-43-5 (~800 m water depth) from the northern and Kamchatka slope are located near the upper edge of the modern OMZ. The deeper cores LV28-2-4 and LV28-40-5 (~1300 m water depth) from the Sakhalin slope occur near the low OMZ edge.

In this study, foraminiferal data for the TI – Holocene of cores: LV28-2-4 (32 samples), LV28-43-5 (43 samples), LV28-40-5 (27 samples) and MD01-2415 (57 samples) were used only. To reconstruct variability of OMZ, we applied downcore distributions of the dominant (> 25%) species and the Dysoxic (0.1-0.3 ml l^{-1}), Suboxic (0.3-1.5 ml l^{-1}) and Oxic (1.5-6 ml l^{-1}) assemblages, which were obtained following the definition of Kaiho (1994) by grouping of all species of cores (see Bubenshchikova et al. 2010). Additional proxies included the sediment color* b, total organic carbon, calcium carbonate and biogenic opal data of cores under study.

A two-step intensification of the Okhotsk Sea OMZ during the Bølling-Allerød and Preboreal was reconstructed by increases of the Dysoxic and Suboxic C assemblages (mainly *Bolivina spissa, Brizalina subspinescens* and *Valvulineria sadonica*) in four cores (Figure 1A-B). Bottom water oxygenation near the core sites from 800-1300 water depths appears to have decreased by factor two or three in the Preboreal as compared to the present (1.0-1.3 ml l^{-1} O_2). In addition, spreading of the OMZ core likely existed in that time. As it follows from the percentages of the Dysoxic and Suboxic C assemblages in the Preboreal (Figure 1B), the shallower cores MD01-2415 and LV28-43-5 were likely located within the OMZ core with maximal oxygen depletion, while the deeper cores LV28-2-4 and LV28-40-5 were close to the low edge of the OMZ core.

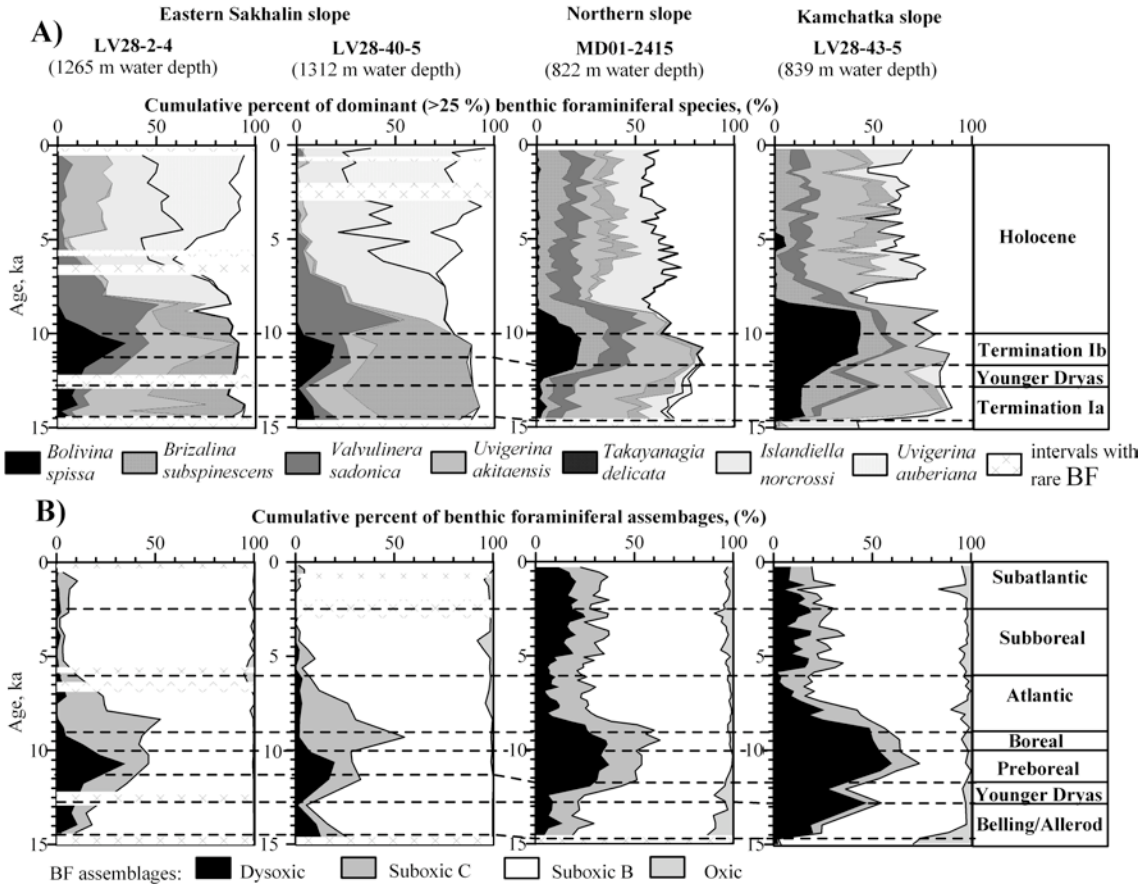

Fig. 1: Downcore distributions of: A) the dominant (> 25%) benthic foraminiferal species, and B) benthic foraminiferal assemblages indicative of the different bottom water oxygenation (%) during the Termination I – Holocene in cores LV-28-2-4, LV-28-40-5, MD01-2415 and LV28-43-5.

The intensification of OMZ was driven by the last deglacial warming and sea level rising. It was controlled by enhanced oxygen consumption due to decay of marine and terrestrial organic matter originated from maxima of marine productivity and terrestrial input from the submerged shelves (Seki et al. 2004). Other controlling factors were: retreat of the Okhotsk Sea ice cover; reduction of the OSIW production; enhanced inflow of the oxygen-depleted DPW because of the northward expansion of oxygen-poor "southern component intermediate water" from the subtropical and tropical Pacific (McKay et al. 2005, Shibahara et al. 2007); formation of a stable water column stratification.

During the Boreal and Atlantic, the OMZ weakened and its core contracted toward the present state in the Okhotsk Sea. It is evidenced by sharp declines of the Dysoxic and Suboxic C assemblages from 10 to 9 ka and from 9 to 6 ka, respectively, in the deeper cores LV28-2-4 and LV28-40-5 (Figure 1B). In the shallower cores MD012415 and LV28-43-5, the Dysoxic and Suboxic C assemblages show less steep decrease from 10 to 6 ka (Figure 1B) indicating less pronounced weakening of OMZ. Decrease of marine productivity took place in the Okhotsk Sea in the early Holocene because of decreasing terrestrial input from the submerged shelves (Seki et al. 2004). Thus, low oxygen consumption due to the decay of a decreasing amount of marine and terrestrial organic matter is suggested to be a main controlling factor of the weakening of OMZ in the Boreal and Atlantic.

During the Subboreal and Subatlantic, short-term intensifications of OMZ were recorded only in the shallower cores MD012415 and LV28-43-5 by increases of the Dysoxic and Suboxic C assemblages (Figure 1B). These intensifications are suggested to be governed mainly by the high productivity events originated from strengthening of upwelling

on the northern and Kamchatka slope and/ or from enhanced input of nutrients with fluvial discharge in response to changes in the terrestrial vegetation. In addition, a probable influence of decreases of the OSIW production on the short-term intensifications of OMZ is not excluded.

Our results indicate that intensification of OMZ in the Okhotsk Sea during the Bølling-Allerød and Preboreal correlates to that recorded in the North Pacific (Crusius et al. 2004, McKay et al. 2005, Shibahara et al. 2007).

References

Bubenshchikova N, Nürnberg D, Gorbarenko SA, Lembke-Jene L (2010) Variations of the Oxygen Minimum Zone of the Okhotsk Sea during the last 50 kyr as indicated by benthic foraminiferal and biogeochemical data. Okeanologiya 50 (1), 93-106

Crusius J, Pedersen TF, Kienast S, Keigwin L, Labeyrie L (2004) Influence of northwest Pacific Intermediate Water oxygen concentrations during the Bølling-Allerød interval (14.7-12.9 ka). Geology 32 (7), 633-636

Kaiho K, (1994) Benthic foraminiferal dissolved-oxygen index and dissolved-oxygen levels in the modern ocean. Geology 22, 719-722

McKay JL, Pedersen TF, Southon J (2005) Intensification of the oxygen minimum zone in the northeast Pacific off Vancouver Island during the last deglaciation: Ventilation and/or export production? Paleoceanography, 20, PA4002, doi:10.1029/2003PA000979, 2005

Nürnberg D, Tiedemann R (2004) Environmental change in the Sea of Okhotsk during the last 1.1 million years. Paleoceanography 19, PA4011, doi:10.1029/2004Pa001023

Seki O, Ikehara M, Kawamura K, Nakatsuka T, Ohnishi K, Wakatsuchi M, Narita H, Sakamoto T (2004) Reconstruction of paleoproductivity in the Sea of Okhotsk over the last 30 kyr. Paleoceanography 19, PA1016, doi:10.1029/2002Pa000808

Shibahara A, Ohkushi K, Kennett JP, Ikehara K (2007) Late Quaternary changes in intermediate water oxygenation and oxygen minimum zone, northern Japan: A benthic foraminiferal perspective. Paleoceanography, 22, PA3213, doi:10.1029/2005PA001234, 2007

Diatom stratigraphy and paleogeography of the Western Bering Sea over the past 170 ka

Marina Cherepanova [1], Sergey Gorbarenko [2], Mikhail Malakhov [3], Dirk Nürnberg [4]

[1] Institute of Biology and Soil Science FEB RAS, 159, Prospect 100-letiya, 690022 Vladivostok, Russia; email: cherepanova@ibss.dvo.ru
[2] V.I. Il'ichev Pacific Oceanological Institute FEB RAS, 43, Baltiyskaya Street, 690041 Vladivostok, Russia,
[3] NEISRI FEB RAS, Northeastern Integrated Scientific-Research Institute FEB RAS, Portovaya St. 16, 685000 Magadan, Russia
[4] IFM-GEOMAR, Leibniz Institute of Marine Sciences, Wischhofstrasse 1-3, 24148 Kiel, Germany

The diatoms of the Core SO201-2-85-KL sediments from West part of the Bering Sea have been studied. Diatom assemblages are presented by 120 taxa. The changes of abundance of the diatom valves in sediments, species diversity, composition of dominant species, and combinations of ecological groups of diatom along core sediments allow us to establish some biostratigrpahic units (Fig.) reflecting general paleoceanographic events of North Pacific region, and corresponding to 1–6 Marine Isotopic Stages (MIS).

Diatom assemblage in **Unit VI** (1812-1298 cm) is represented by rare diatom valves. There is a maximum of *Thalassiosira antarctica* and *Paralia sulcata* at this stratigraphic level. Unit 6 may represent the sea ice advanced conditions that marked the Illinois Glaciation and correlated with MIS 6. The frequency of the diatom valves increase to Unit 6 bottom, and *Th. antarctica* predominate among another diatoms. This interval may be considered as warmer 6.5 substage.

Unit V (1298-774 cm) is characterized by sufficient abundance of the diatom valves. Species *Th. antarctica* is dominance, and *Th. latimarginata* and *Rhizosolenia hebetata* f. *hiemalis* are subdominant. Pelagic species of the genus *Coscinodiscus* as well as *Thalassiothrix longissima* and *Neodenticula seminae* are found in this diatom association. It seems, that forming of diatom assemblage Unit 5 reflects sea-level increase during Pelukian Transgression and marks Sangamon Interglacial Period. This paleogeographic event is corresponded to MIS 5. It's important that very high diatom valves quantity in interval 1236-1298 cm is one of the biostratigraphic features of warmest substage MIS 5.5.

The diatom number is sharply declined in the sediments of **Unit IV** (774-590 cm). Only *Th. antarctica* has dominant status. Another diatoms species are represented by cold-water *Bacterosira fragilis*, *Th. hyalina*, *Th. nordenskioeldii*, *Th. kryophila*. Ice-species *Nitzschizia grunovii* and *N. cylindrus* appear near Unit 4 base, and mark the beginning of the Early Wisconsin Glaciation Age correlated with MIS 4.

Unit III (590-296 cm) represented by diatom assemblage with dominant nerithic species *Th. antarctica*, *Th. latimarginata* and sublittoral *Paralia sulcata*. The frequencies of the diatom valves are increased (ex g. *Actinopthyhus senarius* specifically). This unit may correspond to the interstage of the Middle Wisconsin and correlate with MIS 3.

The sharp decrease of the diatom abundance and diversity are main feature of the assemblage formed at **Unit II** (296-80 cm). It should be noted that maximum frequencies of *Th. antarctica* and *Paralia sulcata* are notable too. The sediments of this interval have the highest abundance cold-water species *Th. kryophila* and *Th. hyalina*. Some increase of shelf species *Diploneis smithii*, *D. interrupta*, *Delphineis surirella* as well as Pliocene species of the genus *Pyxidicula* are observed in this assemblage. Unit 2 reflects the Late Wisconsin glacial advance condition with low sea-level and corresponds to MIS 2.

The sediments of **Unit I** (80-0 cm) characterize as diatom ooze with very high diatom valves content and species diversity. The high abundance of *Th. antarctica*, *Th. latimarginata*, and species spores of the genus *Chaethoceros* is a principal specificity of diatom assemblage of this unit. Pelagic *Coscinodiscus oculus-iridis* and *Neodenticula seminae* commonly encountered in this sediment.

The diatom assemblages of determinate stratigraphic units show variations that

reflect changes in environmental conditions of the western Bering Sea over the last 170 ka with high resolution.

This work was supported by FEBRAS Projects 09-II-UO-08-003, 09-II-CO-07-003, 09-I-P15-02 and grand of CRDF - 10-05-92514-IC and RFBR 10-05-00160a and BMBF grant 03G0201A, 03G0672A.

Marine heat flow measurements offshore Kamchatka – results and interpretation

Georg Delisle[1], Michael Zeibig[1]

[1] BGR, Federal Institute for Geosciences and Natural Resources, Geozentrum Hannover, Stilleweg 2, 30655 Hannover, Germany; email: georg.delisle@bgr.de

Marine heat flow measurements on oceanic crust offshore Kamchatka had previously been carried out by Russian workers. Their results indicated anomalously high heat flow near the Meiji Seamount which represents an atypical condition for oceanic crust of Cretaceous age. This result gave rise to the speculation in the literature of rejuvenated volcanism in old crust. Our measurements were designed to verify the earlier results and to improve the delineation of the anomalous heat flow region

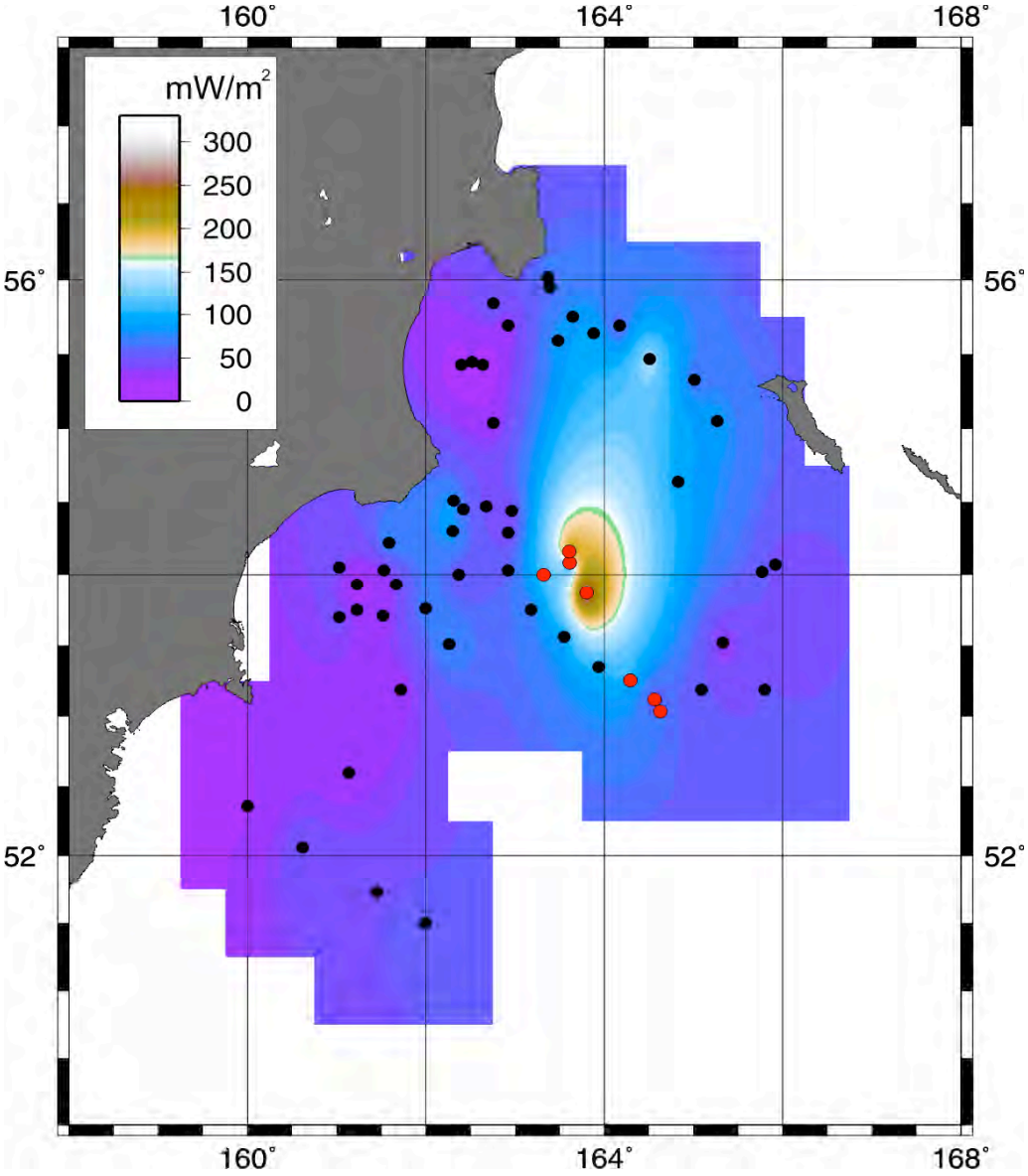

Fig. 1: Summary of all heat flow measurements in the investigated area. Measurements by KALMAR are indicated by red dots.

Seven heat flow measurements were carried out during KALMAR in two specific areas defined by the research permit issued by Russian authorities. Since initial sediment coring experiments by KALMAR had encountered hard ground (high percentage of volcanic particles in the sea bottom sediments) we chose to employ the BGR-hard ground heat flow probe, which is specifically designed for deployment in such unfavorable conditions. The probe measures the in-situ the thermal gradient in sea floor sediments and in a follow-up experiment their in-situ thermal conductivity.

Our points of measurement lie along an east-west profile along the towards the subduction trench descending oceanic plate. This area is affected by segmentation into a horst and graben structure which favors the development of pronounced fracture systems. The available seafloor topography shows in addition signs for slumping of sediments down both flanks of the Meiji Seamount.

At three stations an anomalous temperature distribution in the water column was noted. Instead of steadily decreasing water temperatures we found temperature inversions at a depth of 3800 to 3900 m and slightly higher temperatures at the sea floor. The cause of this inversion is unknown. The magnitude of the temperature inversion is too small to have a potentially significant impact on the marine heat flow distribution.

Our measurements resulted in highly linear temperature gradients and yielded in-situ thermal conductivities mostly in the expected range between 0.85 – 1 $Wm^{-1}K^{-1}$. We have verified the presence of a large positive heat flow anomaly at the western flank of Meiji Seamount (see Fig. 1). We interpret this anomaly as result of deep reaching vigorous natural convection of fluids in highly fractured oceanic crust. Sediment slumping might have uncovered warmer and deeper levels of the sediments - an effect which potentially might have added to the observed positive heat flow values. Noticeably the measurements near the flat top of the Meiji Seamount, where the sea floor topography gave us no indications of faulting, have resulted in (for this type and age of crust) "normal" heat flow values of 40 – 50 mWm^2.

References

Smirnov YB, Sugrobov VM (1979) Terrestrial heat flow in the Kurile-Kamchatka & Aleutian provinces – I Heat flow and tectonics. Volcanol. Seismol. 1: 59-73 (in Russian)

Smirnov YB, Sugrobov VM (1980) Terrestrial heat flow in the Kurile-Kamchatka & Aleutian provinces – II The map of measured and background heat flow. Volcanol. Seismol. 1: 16-31 (in Russian)

Smirnov YB, Sugrobov VM (1982) Terrestrial heat flow in the northwestern Pacific. Tectonophysics, Vol. 83, 1-2, 109-122

Sugrobov VM Yanovsky FA (1993) Terrestrial heat flow, estimation of deep temperature and seismicity of the Kamchatka region. Tectonophysics, Vol. 217,1-2, 43-53

Tuezov IK, Epaneshnikov VD, Gornov PYU (1991) Heat field of the lithosphere in northeast Asia and the northwestern sector of the Asia-Pacific transition zone. In: Cermak V, Rybach L (Eds) Terrestrial heat flow and the lithosphere structure. Springer-Verlag, Berlin: 238-263

Heavy mineral assemblages of the tephra layers found in sediments from the Bering Sea and the north-western Pacific Ocean

Alexander Derkachev[1], Nataliya Nikolaeva[1]

[1]POI FEB RAS, V.I. Ilichev Pacific Oceanological Institute FEB RAS, Baltiyskaya Street 43, 690041 Vladivostok, Russia; email: derkachev@poi.dvo.ru

Mineral composition of volcaniclastic material carries significant information about many sides of volcanic explosions (magma source, character of the melt magmatic differentiation, temperature and pressure in the magmatic camera and others). The investigation of mineral phases in the volcanic explosive products is a usual procedure in many works on volcanology and petrology of the igneous rocks.

But works concerning mineralogy of pyroclastic material especially in its distal distribution (tephra layers), are marked more rarely, and they are mainly directed to the decision of questions connected with both tephrostratigraphic correlation of deposits and estimation of tephra source (Geptner, Ponomareva, 1979; Braitseva et al. 1997; Derkachev et al. 2004; Jensen et al. 2008; Okumura 1991; Smith et al. 2002; Shan 1998 and others).

The tephra samples were selected from core SO201-2 taken during cruise on the R/V SO201-2 carried out in the framework of the Russian-German KALMAR Project. The investigation of mineral components from tephra layers was done in two steps: a) the estimation of heavy mineral assemblages; 2) the study of chemical composition for single mineral with the use of electron probe microanalysis (EPMA). Our presentation contains only information about features of the tephra layer mineral assemblages, not concerning mineral chemical composition.

Mineralogical analysis of the heavy fraction (density > 2.8 g/cm^3) was carried out under a polarizing microscope with the use of an immersion liquid. 61 samples from 35 tephra

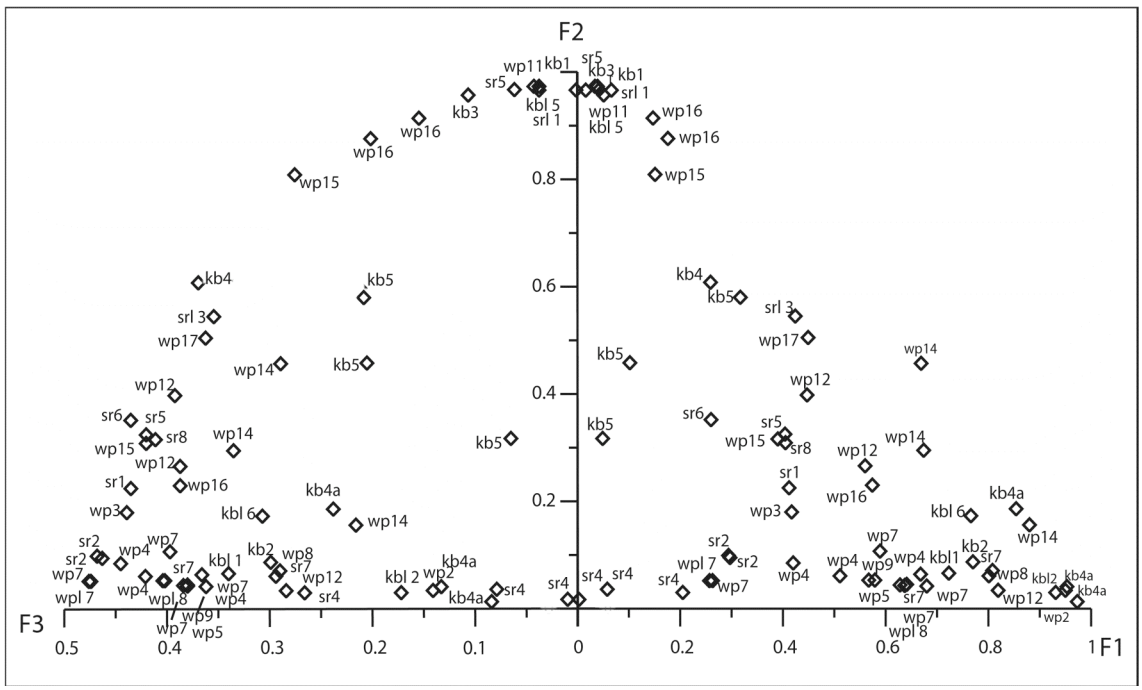

Fig. 1: Binary plot of factor loadings (F1-F2-F3) (on the basis of Q-factor analysis) for heavy mineral assemblages from tephra layers in Holocene-Pleistocene sediments of the Bering Sea and north-western Pacific Ocean. Notes: explanation is listed in the Table 1. Abbreviatures mean the index of tephra layers.
Table 1

Tab.1: Values of variables for highest factor loadings in Q-mode analysis of heavy mineral composition

Sample	*gor, cm*	*tephra*	*Cpx*	*Opx*	*Hb1*	*Hb2*	*Ep**	*Zr**	*Ap*	*Ol*	*Bi*	*faktor*
So201-9	*314-316*	KB4a	23.62	75.69	0.00	0.00	0.00	0.0	0.00	0.0	0.69	f1
So201-40	*114.5-116*	WP2	30.64	67.04	1.16	0.00	0.00	0.0	0.58	0.0	0.58	f1
So201-9	*359-360*	KB3	16.39	0.67	69.24	7.36	0.00	0.66	1.00	0.0	4.68	f2
So201-81	*833*	SR5	9.74	1.3	72.73	8.12	0.00	0.0	2.60	0.0	5.52	f2
So201-40	*613-613.5*	WP11	7.54	1.4	83.24	3.63	0.56	0.0	1.12	0.0	2.51	f2
So201-85	*83-85*	SR2	70.42	8.7	3.48	0.0	10.44	2.61	4.35	0.0	0.0	f3
So201-40	*455.5-457.5*	WP7	75.96	6.25	0.0	0.0	5.29	0.48	12.02	0.0	0.0	f3
So201-40	*881*	WPL7	85.45	7.27	0.0	0.0	1.82	0.0	3.64	1.82	0.0	f3
So201-77	*650-653*	SR4	1.67	0.0	1.67	0.0	0.0	0.0	0.0	96.66	0.0	f4
So201-85	*668*	SR4	14.29	2.38	2.38	0.0	0.0	0.0	0.0	80.95	0.0	f4
So201-9	*513-515*	KB5	10.96	1.37	23.29	1.37	0.0	0.0	0.0	0.0	63.01	f5
So201-9	*512-513*	KB5	24.42	1.16	24.42	3.49	3.49	1.16	1.16	1.16	39.54	f5

Notes: Abbreviations of minerals: Cpx - clinopyroxene, Opx - orthopyroxene, Hb1 - brown-green hornblende, Hb2 - brown and basaltic hornblende, Ep* - sum of epidote and chlorite, Zr* - sum of zircon, garnet, tourmaline, titanite, Ap - apatite, Ol - olivine, Bi - biotite.

layers estimated in the Holocene-Pleistocene deposits of the Bering Sea and the north-western Pacific Ocean were studied. The obtained data were subjected to the methods of multivariate statistics (correlation, cluster and factor analyses).

Some mineral assemblages were singled out on the relation between dark colour minerals (Fig. 1). Bi-pyroxene mineral assemblages with a small admixture of hornblende are characteristic for most of the studied tephra layers. Q-factor analysis showed that 99.5 % of all variability is explained by 5 factors. First three factors with the loads of 32.5, 18.8 and 39.9 % ascertain the significant part of total dispersion.

First factor characterizes predominantly orthopyroxene-clinopyroxene assemblage with the prevalence of orthopyroxene (up to 75 %; Table 1, Fig. 1). Apatite and olivine is present as a small admixture. Mineral assemblages with the sharp prevalence of clinopyroxene (up to 70-85 %) and almost complete absence of hornblende occur rarely, and they are determined by 3^{d} factor. On mineral composition, the WP7, WPL7, SR2, WP4 and partly SR4 tephra layers are their typical representatives.

Second factor defines mineral assemblages with a high content of hornblende (up to 83.2 %). Apatite and biotite occur as well (up to 5.5 %). The KB3, SR5, WP11, KB1 and KBL5 tephra layers are typical representatives of these assemblages. The close composition but with sharply increased content of biotite (up to 30-63 %) is characteristic for the KB5 tephra layer, and this mineral assemblage is singled out by 5th factor.

The SR4 tephra layer has exotic mineral composition. A high content of olivine (up to 53-96 %), and subordinated amount of clinopyroxene, rarely orthopyroxene is its specific feature. Chromite occurs as a small admixture. This assemblage is estimated by 4th factor.

On the basis of their mineral composition investigations, some tephra layers are well correlated in different sediment cores. Most certain correlation is marked for the KB3-SR5-WP11, and also for the SR2 and SR4 tephras. Such correlative regularity is confirmed by data on the geochemistry of

glass shards from these layers (Derkachev et al. this volume).

Besides, minerals-indicators which can characterize volcanic areas are estimated. These are hornblende, biotite and olivine. For the most studied tephra layers, the sources of the explosions are unknown. That is why data on heavy mineral assemblages may be used to estimate volcanic provinces (zones) in which eruptions of single volcanoes are imprinted in the chronicle of sedimentary sequence. For example, the presence of both hornblende and biotite in the KB5, KBL5 and KB1 tephra layers testifies certainly about an influence of back-arc volcanism of the Sredinny Kamchatka Ridge where volcanic rocks with similar mineral complex are distributed (Braitseva et al. 1997). In combination with data on geochemistry of glass shards, obtained results will allow to carry out an identification of the tephra layers more confidently.

References

Braitseva OA, Ponomareva VV, Sulerzhitsky LD, Melekestsev IV, Bailey J (1997) Holocene key-marker tephra layers in Kamchatka, Russia. Quaternary Res. 47: 125-139

Derkachev AN, Nikolaeva NA, Gorbarenko SA (2004) The peculiarities of supply and distribution of clastogenic material in the Sea of Okhotsk during Late Quaternary. Russian Journal of Pacific Geology 23 (1): 37-52

Geptner AR, Ponomareva VV (1979) The application of mineralogical analysis for correlation of the Shiveluch volcano tephra. Bull. Volcanolog. 56: 126-130

Jensen BJL, Froese DG, Preece SJ, Westgate JA, Stachel T (2008) Anextensive middle to late Pleistocene tephrochronologic record from east-central Alaska. Quaternary Science Reviews, 27: 411-427

Okumura K (1991) Quaternary tephra studies in the Hokkaido district, northern Japan. Quaternary Res. 30: 379–390

Shane P (1998) Correlation of rhyolitic pyroclastic eruptive units from the Taupo Volcanic Zone, New Zealand by Fe-Ti oxide compositional data. Bull. Volcanology. 60: 224–238

Smith VC, Shane P, Smith IEM (2002) Tephrostratigraphy and geochemical fingerprinting of the Mangaone Subgroup tephra beds, Okataina Volcanic Centre, New Zealand. New Zealand Journal of Geology & Geophysics 45: 207–219

Marker tephra layers in the Holocene-Pleistocene deposits of the Bering Sea and the north-western Pacific Ocean

Alexander Derkachev[1], Maxim Portnyagin[2], Vera Ponomareva[3], Sergey Gorbarenko[1], Mikhail Malakhov[4], Dirk Nürnberg[2], Jan-Rainer Riethdorf[2], Ralf Tiedemann[5], Christel van den Bogaard[2]

[1] POI FEB RAS, V.I. Ilichev Pacific Oceanological Institute FEB RAS, Baltiyskaya Street 43, 690041 Vladivostok, Russia; email: derkachev@poi.dvo.ru
[2] IFM-GEOMAR, Leibniz Institute of Marine Sciences, Wischhofstrasse 1-3, 24148 Kiel, Germany
[3] IVS FEB RAS, Institute of Volcanology and Seismology FEB RAS, Piip Boulevard 9, 683006 Petropavlovsk-Kamchatsky, Russia
[4] NEISRI FEB RAS, North-East Interdisciplinary Science Research Institute FEB RAS, Portovaya St. 16, 685000 Magadan, Russia
[5] AWI, Alfred Wegener Institute for Polar and Marine Research, Am Handelshafen12, 27570 Bremerhaven, Germany

The ash layers (tephra) are one of the reliable indicators of large explosive volcanic eruptions and they occur in the continental deposits as well as in the sedimentary cover of the adjoining sea basins. Besides, these layers are effective time markers under both stratigraphic study of sedimentary sequences and dating of past events which are often used under paleoclimatological and paleoceanological reconstructions. Lastly, catastrophic volcanic eruptions affect adversely on an environment, ecological situation and human activity. That is why it is necessary to forecast the future behaviour of concrete volcanoes and possible spatial distribution of unhealthy products of their activity. For these purposes, the study of separate tephra layers is required.

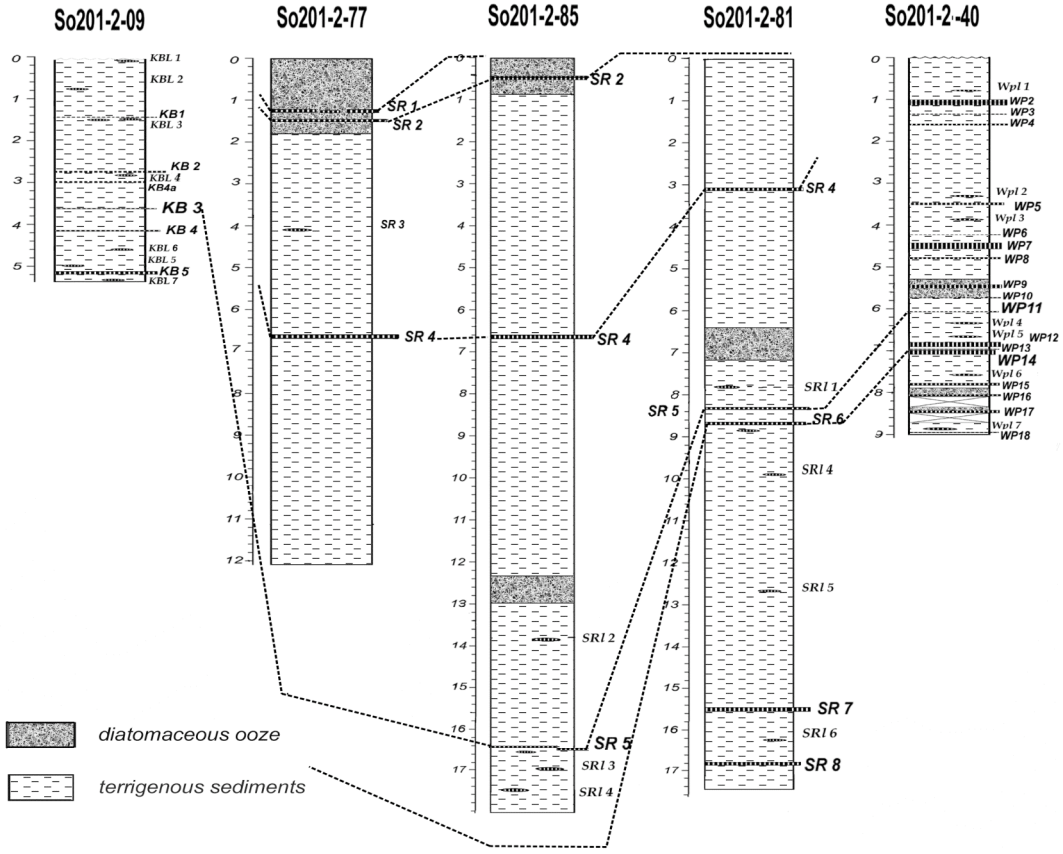

Fig. 1: Marker tephra layers on Holocene-Pleistocene deposits from Bering Sea and north-western Pacific Ocean.

In the framework of the Russian-German KALMAR Project, the R/V Sonne cruise SO201-2 was carried out in 2009. Five cores of bottom sediments were investigated within the western Bering Sea, in the Kronotsky Bay and on the Meiji Seamount (north-western Pacific Ocean). They have recovered the Holocene-Pleistocene deposits with numerous tephra layers of different thickness (Fig. 1). Cores from the Bering Sea contained 8 layers and 6 lenses, from the Kronotsky Bay - 6 layers and 7 lenses, from the Meiji Seamount - 18 layers and 7 lenses.

Main goals of the investigations performed by authors were the following: estimate the spatial-temporal distribution of tephra layers, identify the sources of explosive eruptions, fulfill the tephrostratigraphic correlation of sediment cores. The study of morphology for glass shards, heavy mineral assemblages (61 analyses), electron probe microanalysis (EPMA) of both glass shards (1550 analyses) and of mineral phenocrysts (1180 analyses) were made as a part of the combined research. Such detail investigations of the tephra layers from marine deposits in this region were not known from studies and microprobe. All chemical analyses were obtained at IFM-GEOMAR at the JEOL JXA 8200. Age determination for tephra layers was realized on the basis of age scale developed by authors. Here we report some pilot results from this investigation.

The chemical composition of volcanic glass shards between layers is different. On the TAS diagram, most of them are homogeneous and have rhyolitic compositions (Fig. 2). The glass shards of heterogeneous composition (andesite-basalt, andesite, dacite, trachyandesite-trachydacite) occur rarely. Studied tephra layers also vary on K_2O/SiO_2 ratio from low-K to high-K. It shows the diversity of supply sources.

Comparative analysis of glass shards on the chemical composition has allowed estimate the marker tephra layers which are traced in the Holocene-Pleistocene deposits of the Bering Sea and the north-western Pacific Ocean. They are presented with increasing age:

1) SR1 tephra is of a high alkalinity (trachyandesite-trachydacite); presumable age is about 8600 years, possible source is Plosky volcano.

2) SR2 tephra is characterized by high-K trachydacite composition and correlates with tephra from core GC11 taken on the Bowers Ridge (southern Bering Sea). Approximate age is about 10.5 kyr; probable source is one of the Aleutian Island Arc volcano.

3) SR4 tephra is characterized by high-K andesite-basaltic composition; glass shards are of black colour and have inclusions of olivine and rarely chromite. Presumable age is 64-65 kyr. Exact source is unknown; possibly it is one from the Klyuchevskaya volcanic group.

4) SR5 tephra is correlated with WP11 tephra (core SO201-2-40, Meiji Seamount) and KB3 tephra (core SO201-2-09, Kronotsky Bay). In chemical composition, it relates to low-K rhyolites. Amphiboles including basaltic, are dominating phenocrysts. The age of this tephra is about 160-165 kyr. Its source is not determined.

5) SR6 tephra is correlated with WP14 tephra from core So201-2-81 in chemical composition. It relates to medium-K rhyolites. Presumable age of it is about 180-185 kyr. The source of volcanics is unknown.

SR1-SR6 tephras described above were estimated in Holocene-Pleistocene section within the western Bering Sea (Fig. 1).

Some other tephra layers from core So201-40 also have correlative importance. These are WP3, WP4, WP6, WP8 and WP15 tephras which are correlated with tephra from cores taken on the Detroit Seamount (cores GC32, GC36, MD01-2416 and ODP 883). Among them, WP3 and WP4 tephras are of definite interest because they are well compared with deposits of the pyroclastic flows from the Gorely volcano (Kamchatka). Its eruption happened at about 37-40 kyr. Data obtained by us confirm this age.

Results obtained by us have allowed essentially refine information about large Holocene-Pleistocene eruptions of the Kamchatka volcanoes. This new self-consistent database of high-quality analyses will be a basis for further development of tephrochronological scale for the Bering Sea and the north-western Pacific Ocean.

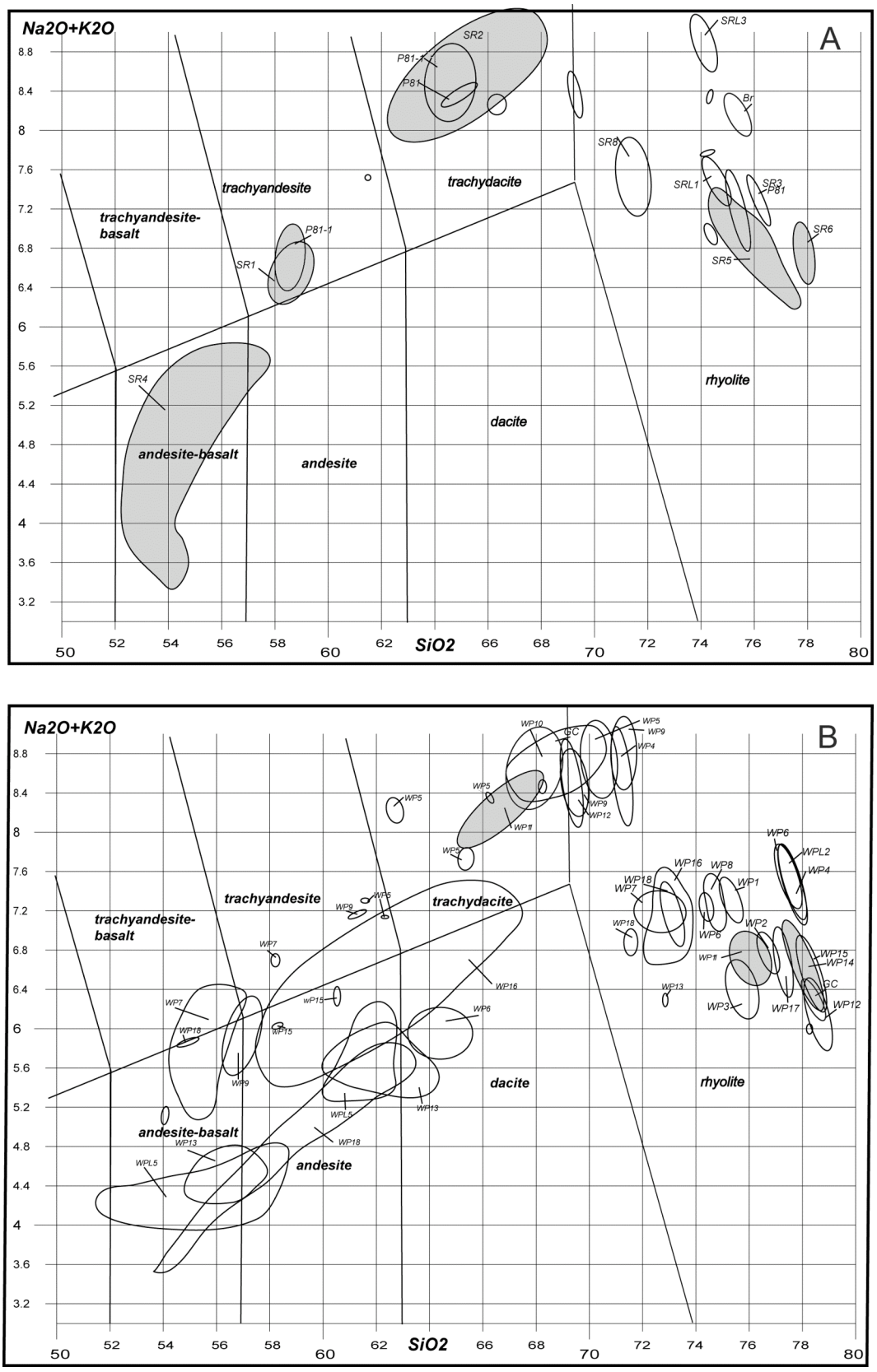

Fig. 2: Total alkali-silica diagram (TAS, Le Bas et al. 1986) of glass shards for chemical discrimination on tephra layers from Bering Sea (A) and Meiji Seamount (B) sediments.

Holocene Palaeoenvironment on Kamchatka

Bernhard Diekmann[1], Annette Bleibtreu[2], Bernhard Chapligin[1], Verena de Hoog[2], Oleg Dirksen[3], Veronika Dirksen[3], Ulrike Hoff[1], Hans-Wolfgang Hubberten[1], Conrad Kopsch[1], Hanno Meyer[1], Larisa Nazarova[1], Christel van den Bogaard[4]

[1] AWI, Alfred Wegener Institute for Polar and Marine Research, Telegrafenberg A43, 14473 Potsdam, Germany; email: Bernhard.Diekmann@awi.de
[2] University of Potsdam, Institute of Earth- and Environmental Science, Karl-Liebknecht-Str. 24-25, 14467 Potsdam-Golm, Germany
[3] IVS FEB RAS, Institute of Volcanology and Seismology FEB RAS, Piip Boulevard 9, 683006 Petropavlovsk-Kamchatsky, Russia
[4] IFM-GEOMAR, Leibniz Institute of Marine Sciences, Wischhofstrasse 1-3, 24148 Kiel, Germany

Palaeoclimatic processes in the northwestern Pacific realm are not well understood so far. Here we present results on the reconstruction of the Holocene terrestrial palaeoenvironment on Kamchatka, inferred from lake-sediment records and peat sections. The study followed a multi-proxy approach, using sedimentological data and fossil bioindicators, such as diatoms, pollen, and chironomids (Dirksen et al. this volume, Dirksen, Diekmann this volume; Hoff 2010, Hoff et al. submitted this volume). Chronostratigraphy of the studied records was achieved through radiocarbon dating and tephrostratigraphy.

The sediment core with the oldest sediments was retrieved from Lake Sokoch, an up to six metre deep lake of proglacial origin, situated at the treeline in the Ganalsky Ridge of southern central Kamchatka (53°15,13'N, 157°45.49' E, 495 m a.s.l.). The pollen record documents local vegetation history of the Holocene (Dirksen, Dirksen 2008; Dirksen, Diekmann this volume). Forests with both birch and alder trees associated with ferns indicate humid and relatively warm conditions in the mid-Holocene between 6.9 and 4.5 ka BP. A decrease in tree density and alder and ferns document late Holocene climate deterioration and establishment of more continental conditions afterwards. A relatively warm and dry spell with an advance of birch forests interrupted general cooling between 2.2 and 1.7 ka BP, while the last millennium was characterized by cool and relatively wet conditions. This pattern of vegetation change is consistent with vegetation dynamics observed along the Pacific coast of Kamchatka (Dirksen, Uspenskaia 2005). At Lake Sokoch, climate changes also affected limnoecology, as the moist stages showed the highest intensity of biological productivity in a fully water-filled lake basin, indicated by high amounts of fossil diatoms and organic remnants of green algae. Fossil diatom assemblages point to lake-level fluctuations and changes in the trophic status of the lake trough time in response to environmental changes (Hoff 2010, Hoff et al. this volume). In the surrounding Sredniaya Avacha, mid-Holocene climate change is also documented by repeated glacial advances after 4.3 ka BP (Savoskul 1999).

Lacustrine sediment records of mid- to late Holocene age were also recovered from the up to 30 m deep Two-Yurts Lake, which occupies a former proglacial basin at the eastern flank of the Central Kamchatka Mountain Chain, the Sredinny Ridge (56°49.6'N, 160°06.9'E, 275 m a.s.l.). As in the Lake Sokoch record, pollen data again give evidence of a decrease in humidity after 4.5 ka BP. Palaeotemperature signals inferred from fossil midge remains (chironomids) indicate summer cooling at the same time, followed by climate amelioration between 3.4 and 1.1 ka BP, cool conditions during the last millennium, and warming during recent times. Stable-oxygene isotope data in silica shells of fossil diatoms, in turn, point to prolonged late Holocene cooling. They moreover reveal a period of modified lake-water sources between 4.4 and 3.6 ka BP, which likely can be explained with the storage of winter precipitation in glacial ice of the mountainous hinterland. This glacial local event thus is consistent with mid-Holocene climate deterioration. Limnoecological changes went along with climate change, as indicated by fossil diatom assemblages (Hoff 2010, Hoff et al. this

volume). Thus, the warmer intervals, particularly between 3.0 and 1.0 ka BP show higher concentrations of planktonic diatoms that prefer thermally stratified lake water, pointing to an earlier ice-out and a longer and warmer growing season. In another small lake nearby Two-Yurts Lake, diatom signals of a warmer interval in the late Holocene are confined to the time interval between 2.5 and 1.2 ka BP (Hoff 2010, Hoff et al. submitted).

In summary, our findings give evidence of longterm climate changes that suggest the existence of a warm and humid early Holocene climate optimum between roughly 9.0 and 4.5 ka BP, followed by climate deterioration of the neoglacial epoch in concert with summer cooling, glacial advances, and enhanced continentality. Two strong cooling episodes punctuated late Holocene climate development between 4.5 and 3.5 ka BP and during the last millennium, marking the prelude of neoglacial cooling and the Little Ice Age. This general development of Holocene climate on Kamchatka is in line with environmental changes in the neighbouring Sea of Okhotsk, where the pattern of sea-ice dynamics is consistent with early Holocene warmth and Neoglacial climate cooling (e.g. Itaki, Ikehara 2004; Wang, Wang 2008). While the marine records from the Sea of Okhotsk mainly reflect winter conditions, our findings show that summer climate on Kamchatka shows a similar trend of temporal change. Meteorological observations and ice-core data from the second half of the last century show that both summer and winter climate on Kamchatka is controlled by the complex interplay of the Pacific Decadal Oscillation and the Arctic Oscillation that both control the influence of maritime or continental air masses and the intensity of rain- or snow-bringing cyclones (Matoba et al. 2011). From our findings, we may state, that the influence of summer cyclones, bringing warm and moist air from southern sources, on Kamchatka was stronger prior to the Neoglacial.

References

Dirksen V, Dirksen O. (2008) Late Pleistocene to Holocene climate changes on Kamchatka, Russian Far East, inferred from pollen records. Geophysical Research Abstracts 10:EGU2008-A-10287

Dirksen VG, Uspenskaia ON (2005) Holocene climate and vegetation changes in Eastern Kamchatka based on pollen, macrofossil and tephra records. Geophysical Research Abstracts 7:EGU05-A-01435

Hoff U (2010) Freshwater diatoms as indicators for Holocene environmental and climate changes on Kamchatka, Russia. PhD thesis, University of Potsdam, 95 pp.

Hoff U, Dirksen O, Dirksen V, Herzschuh U, Hubberten H-W, Meyer H, van den Bogaard C, Diekmann B (submitted) Late Holocene diatom assemblage in a lake sediment record of central Kamchatka, Russia. Paleolimnology

Itaki T, Ikehara K (2004) Middle to late Holocene changes of the Okhotsk Sea Intermediate Water and their relation to atmospheric circulation. Geophysical Research Letters 31: L24309

Matoba S, Shiraiwa T, Tsushima A, Sasaki H, Muravyev YD (2011) Records of sea-ice extent and air temperatures at the Sea of Okhotsk from an ice core of Mount Ichinsky, Kamchatka. Annals of Glaciology 52: 44-50

Savoskul OS (1999) Holocene Glacier Advances in the Headwaters of Sredniaya Avacha, Kamchatka, Russia. Quaternary Research 52: 14-26

Wang WL, Wang LC (2008) Reconstruction of oceanographic changes based on the diatom records of the central Okhotsk Sea over the last 500000 Years. Terrestrial Atmospheric and Oceanic Sciences 19: 403-411

Holocene terraces and landslide events in northern and southern Kamchatka: evidence of sharp tectonic and volcanic unrest at 2800-2900 ^{14}C BP

Oleg Dirksen[1], Christel van den Bogaard[2], Tohru Danhara[3], Bernhard Diekmann[4]

[1] IVS FEB RAS, Institute of Volcanology and Seismology FEB RAS, Piip Boulevard 9, 683006 Petropavlovsk-Kamchatsky, Russia; email: dirksen@kscnet.ru
[2] IFM-GEOMAR, Leibniz Institute of Marine Sciences, Wischhofstrasse 1-3, 24148 Kiel, Germany
[3] Kyoto Fission Track Co. Ltd., Kyoto, Japan
[4] AWI, Alfred Wegener Institute for Polar and Marine Research, Telegrafenberg A43, 14473 Potsdam

Tephrochronological investigations conducted under the umbrella of KALMAR project have allowed us to determine the age of the lake and river terraces as well as date the paleolandslides, i.e. the events which trace the tectonic activity, at northern (Two-Yurts lake) and southern (Three sister river) parts of Kamchatka. We also correlated the results with previously obtained data on other parts of Kamchatka to get a regional time-schedule of tectonic activity.

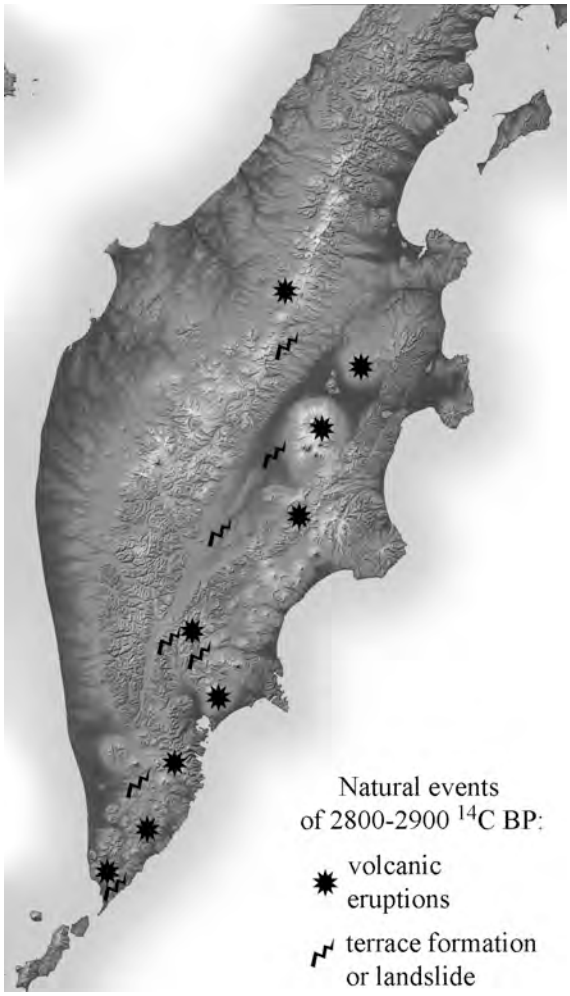

Detail study of distal tephras around Two-Yurts lake established the main marker ash layers in this area. These are the ashes of different Kamchatka volcanoes: Shiveluch, 900, 1400, 1750, 2800, 4700, 4800 and 8300 ^{14}C BP; Ksudach, 1800 ^{14}C BP, Avachinsky, ca 2000 ^{14}C BP, Klyuchevskoy 2850 ^{14}C BP, and Khangar, 6900 ^{14}C BP. The main ash markers for Three Sister river are the tephras of Ksudach (1000 ^{14}C BP), Khodutka (2500 ^{14}C BP), Dikii Greben (4500 ^{14}C BP) volcanoes and Kuril lake caldera (7600 ^{14}C BP). We used these local tephrastratigraphical scales to reconstruct the timing of landscape change, in particular to date the formation of lake and river terraces and the landslide events. Both features can be regarded as indicators of increased tectonic activity.

The oldest Holocene lake terrace found near Two-Yurts lake is approx. 3 m high above the present day level of the lake. The age of the terrace is about 2900-3000 ^{14}C BP. Two younger terraces of 0.5 m and 1 m height reveal an age of about 1000 and less than 900 ^{14}C BP. We also found several Holocene landslides which probably were the results of strong earthquakes which, in turn, could also testify for tectonic activity. The ages of landslides were estimated as ca. 4000, 2900 and 2000-2100 ^{14}C BP. At the southernmost tip of Kamchatka, at Three sister river valley, we found two terraces, which have ages of 8000 and 2800-2900 ^{14}C yrs, respectively.

At the junction of Levaya Avacha and Vershinskaya rivers we discovered six river terraces. They are either 1, 1.5, 2, 4, 7.5 and 11 m above the recent holm. The ages of these terraces are about 600, 2000, 2900, 7500 and 9000 ^{14}C BP, respectively. At Savan river we have dated seven terraces. The age of three older terraces range from

10000 to 8300 ^{14}C BP. The other four are 4300, 2900, 2600 and 1000 ^{14}C years old.

Thus, two main stages of tectonic activity can be distinguished for the most part of the peninsula: Early Holocene (8000 – 10000 ^{14}C BP) and Late Holocene (2900 – 600 ^{14}C BP) separated by a mid-Holocene tectonic repose period (3000 – 8000 ^{14}C BP). These periods of unrest are characterized by numerous tectonic movements that resulted in sequences of river and lake terraces and landslides. The most dramatic event was the beginning of the Late Holocene stage. According to our data, the sharp increase of tectonic activity occurred at 2800 – 2900 ^{14}C BP at southern, eastern and northern parts of Kamchatka. Tectonic movements ca 2900-3000 ^{14}C BP were detected for the Central Kamchatka Depression (Pevzner et al. 2006). It was also the time of sharp increase of volcanic activity. Several large monogenetic volcanoes erupted 2800-2900 ^{14}C BP in many parts of the peninsula (e.g. Dirksen and Melekestsev 1999, e.g. Dirksen et al. 2003). Strong eruptions of stratovolcanoes also occurred at that time (Bazanova et al. 2005, e.g. Ponomareva et al. 2007). Thus, we suppose, that the time of 2800-2900 ^{14}C BP could be regarded as a time of whole-Kamchatka sharp and sudden increase of tectonic and volcanic activity.

The study was supported by BMBF grant 03G0640A as well as DFG and RFBR grants.

References

Bazanova LI, Braitseva OA, Dirksen OV, Sulerzhitsky LD, Danhara T (2005) Ashfalls from the largest Holocene eruptions along the Ust'-Bol'sheretsk - Petropavlovsk-Kamchatsky traverse: sources, chronology, recurrence. Volcanol. and Seismol., (6), 30–46, (In Russian)

Dirksen OV, Melekestsev IV (1999) Chronology, evolution and morphology of plateau basalt eruptive centers in Avacha River area, Kamchatka, Russia, Volcanol and Seismol., 21(1), 1–28

Dirksen O, Bazanova L, Portnyagin M (2003) Chronology of the volcanic activity in the northern part of Sredinny Range (Sedanka lava field) in the Holocene, in Volcanism and geodynamics, Materials of the II Russian symposium on volcanology and paleovolcanology, Ekaterinburg, 871–874

Pevzner MM, Ponomareva VV, Sulerzhitsky LD (2006), Holocene soil-pyroclastic successions of the Central Kamchatka depression: ages, structure, depositional features, Volcanol. and Seismol., (1), 24–38, (In Russian)

Ponomareva VV, Kyle PR, Pevzner MM, Sulerzhitsky LD, Hartman M (2007) Holocene eruptive history of Shiveluch volcano. Kamchatka Peninsula. In: Eichelberger J, Gordeev E, Kasahara M. Izbekov P, Lees J (Eds) "Volcanism and Subduction: The Kamchatka Region", American Geophysical Union Geophysical Monograph Series, Volume 172: 263-282

New Holocene pollen record from Sokoch Lake, southern Kamchatka, and its paleoclimatic implications

Veronika Dirksen[1], Bernhard Diekmann[2]

[1] IVS FEB RAS, Institute of Volcanology and Seismology FEB RAS, Piip Boulevard 9, 683006 Petropavlovsk-Kamchatsky, Russia; email: dirksenvg@kscnet.ru
[2] AWI, Alfred Wegener Institute for Polar and Marine Research, Telegrafenberg A43, 14473 Potsdam, Germany

Lacustrine sediment core from the Sokoch Lake, southern Kamchatka, were studied by pollen and microfossil analysis. The record obtained covers the past ca. 9400 years and thus represents almost the whole Holocene. Seven radiocarbon dates provided a reliable chronology of the record; all ages are given in calibrated years BP. Based on changes in pollen assemblages reflecting vegetation dynamics around the Sokoch Lake, eight zones were recognized; changes in local spores and microfossils (mainly algal remains) abundance documented well an evolution of lake ecosystem giving additional paleoenvironmental information.

The Sokoch Lake basin is surrounded with terminal moraines that suggest its origin as a result of glacial retreat. The initial lake stage between ca. 9400 and 8900 yrs BP, however, reflect not properly cold conditions. At that time, alder and birch bushes dominated around the lake; tree alder is common in forest pointing to very wet, maritime climate. This is in good agreement with previous findings from peats at the Pacific coast as well as the Two-Yurts Lake record at the Central Kamchatka. The next zone (ca. 8900-7700 yrs BP) shows a trend to warmer conditions resulting in an afforestation peak, which fits well to the first coming of stone birch to the Pacific coast recorded there between ca. 8900-7400 yrs BP. The following two zones reflect relatively warm conditions most likely related to the Holocene thermal maximum. The period ca. 7700-5900 yrs BP was rather warm and wet: tree alder is still abundant in surrounding forest. Since ca. 5900 yrs BP alder forest retreats abruptly and never comes back again that suggests a turn to drier and more continental climate conditions. At the same time, stone birch forest reaches another maximum, which can be compared with forest advance recorded at the Pacific coast at ca. 5800-4500 yrs BP. Changes in local environment may also suggest climate amelioration between ca. 7700-4600 yrs BP. The concentration of green algae increased, and several spore taxa, which could be regarded as facultative thermophilous, were frequent at this interval.

Upper part of the record shows the climate deterioration and continuous increase in continentality. The zone ca. 4600-3250 yrs BP indicates rather cold and wet conditions, when forest strongly retreated while shrubs, grasslands and peat bogs progressed. This cooling event correlates well with other records from Kamchatka and can be attributed to the Neoglacial time. The next period (ca. 3250-2300 yrs BP) was drier and still cool; the Sokoch Lake became shallower and started to fill up. Between ca. 2300-1500 yrs BP, forest around the lake advanced again in response to warmer conditions. Remarkable abundance of white birch in forest, according to its ecology, points to enhanced continentality and seasonal contrast during that period. The latest interval after ca. 1500 yrs BP, except the uppermost sample, shows that the diverse shrub formations returned and widely spread indicating cooler and wetter conditions. It seems that there are offsets in the age of climatic events since the Neoglacial period recorded at the Sokoch Lake sediments and the Two Yurts Lake, as well as other sites wherever in Kamchatka. Most likely, such a discrepancy arose from increased heterogeneity of spatial patterns within the peninsula in response to enhanced climate continentality. Nevertheless, the Sokoch Lake record well documents the Holocene climate change on Kamchatka and thus can be regarded as one of key records for the region.

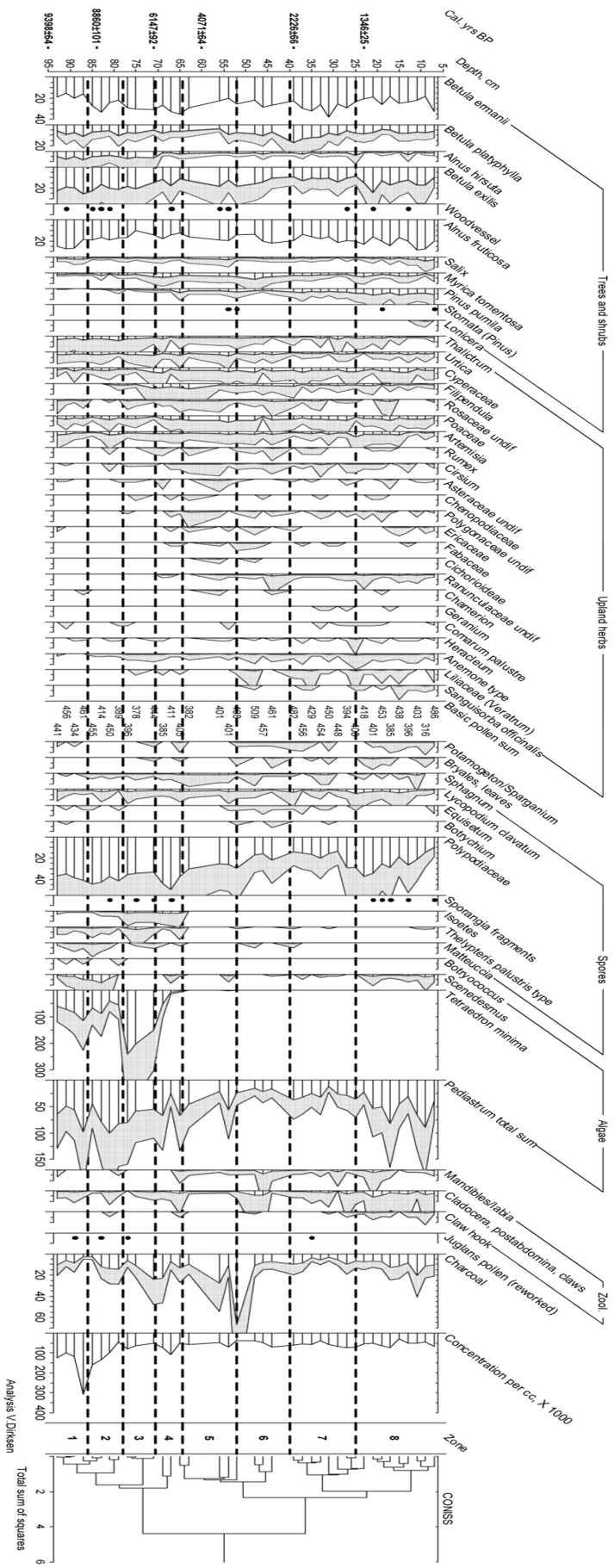
Sokoch Lake
pollen & microfossil diagram
selected taxa
Cal. yrs BP
Depth, cm
Betula ermanii
Betula platyphylla
Alnus hirsuta
Betula exilis
Woodvessel
Alnus fruticosa
Salix
Myrica tomentosa
Pinus pumila
Stomata (Pinus)
Lonicera
Thalictrum
Urtica
Cyperaceae
Filipendula
Rosaceae undif
Poaceae
Artemisia
Rumex
Cirsium
Asteraceae undif
Chenopodiaceae
Polygonaceae undif
Ericaceae
Fabaceae
Cichorioideae
Ranunculaceae undif
Chamerion
Geranium
Comarum palustre
Heracleum
Anemone type
Liliaceae (Veratrum)
Sanguisorba officinalis
Basic pollen sum
Potamogeton/Sparganium
Bryales, leaves
Sphagnum
Lycopodium clavatum
Equisetum
Botrychium
Polypodiaceae
Sporangia fragments
Isoetes
Thelypteris palustris type
Maltaeucia
Botryococcus
Scenedesmus
Tetraedron minima
Pediastrum total sum
Mandibles/labia
Cladocera, postabdomina, claws
Claw hook
Juglans pollen (reworked)
Charcoal
Concentration per cc. X 1000
Trees and shrubs
Upland herbs
Spores
Algae
Zool.
Zone
CONISS
Total sum of squares
Analysis V.Dirksen

Hydrography of the NW Pacific off Kamchatka and of the SW Bering Sea

Wolf-Christian Dullo[1], Sergey Shapovalov[2]

1 IFM-GEOMAR, Leibniz Institute of Marine Sciences, Wischhofstrasse 1-3, 24148 Kiel, Germany; email: cdullo@ifm-geomar.de
2 IO RAS, P.P. Shirshov Institute of Oceanology RAS, Nakhimovsky prospekt 36, 117997 Moscow, Russia

The surface hydrography of the subarctic North Pacific is characterized by a counterclockwise regime of the involved currents. The Subarctic Current flows from W to E almost along the latitude of 40° N. Off the American continent it divides into the southward flowing California Current and into the northward flowing Alaska Current. The Alaska Current develops into the Alaska Stream running along the Aleutian Islands from E to W. Waters exiting the Bering Sea through the Kamchatka Strait merge with the Alaskan Stream to form the East Kamchatka Current, flowing in a southward direction and later mixing with waters coming from the Sea of Ochotsk to form the still southward flowing Oyashio Current. Somewhere around 40° N off Japan the Oyashio converges with the Kuroshio Current to constitute the Subarctic Current (1). This simple current regime is more complex, since it involves two separate gyres, the Alaskan Gyre and the Western subarctic Gyre, and the Northwestern Subtropical Gyre and the Northeastern subtropical Gyre respectively.

The vertical structure of the water mass distribution is characterized by the upper mixed layer, by a cold intermediate layer of low salinity water, a warmer intermediate layer, and a deep water from surface to bottom. A very strong thermocline in concert with a distinct halocline separates the surface mixed water from the cold intermediate water. This water is formed in the Bering Sea during winter time. The Bering Sea is a source region for the Western Subarctic Pacific Water (WSPW), which plays a major role in the circulation of the western subarctic Pacific. The Western Subarctic Pacific Water is characterized by a marked stratification with cold upper layers in winter and a remarkable dichothermal layer around 100 m depth during summer. Beneath the cold low-salinity WSPW lies a mesothermal layer which is a major feature of the waters off Kamchatka. This layer consists of warm (~3.5–3.8ºC) water at a depth range between 200 - 600 m. The source of the mesothermal water in the western Sub-Arctic Gyre and the Alaskan Stream is the warm and saline water of the Kuroshio located south and east of Japan. Below the mesothermal layer there is the domain of the North Pacific Deep Water (NPDW). Properties of the water in the Pacific are set by their very distant sources in the Antarctic and the North Atlantic, with modification through diapycnal processes, oxygen consumption as well as nutrient regeneration, and by the complicated basin geometry.

Preliminary results of hydrographic measurements

Hydrographic measurements of temperature, salinity, and oxygen collected during the SO201-2 cruise in the NW Pacific and the Bering Sea were used to characterize the distribution of temperature, salinity, typical water masses, and their spatial variability in the region. The position of the stations responds to the original aim of the project, and some valuable information on the water column can be extracted.

The general pattern in all stations shows a rapid decrease in sea surface temperature within the upper 50 m of the water column followed by a slight increase below 150 m and 210 m respectively down to 200 and 290 m which marks the constant thermocline. Below, temperature decreases reaching values around 1.47°C in the deepest station (SO201-2-32CTD: 4282 m) off Kamchatka (Fig. 1). Salinity in contrast, increases rapidly in the sea surface water of the upper 50 m, followed by slightly constant values down to 150 m and 210 m, respectively. The distinct increase below marks the halocline, which parallels the thermocline. Highest salinity values within the deep water were recorded around 34.69 PSU off Kamchatka (SO201-2-32CTD: 4282 m).

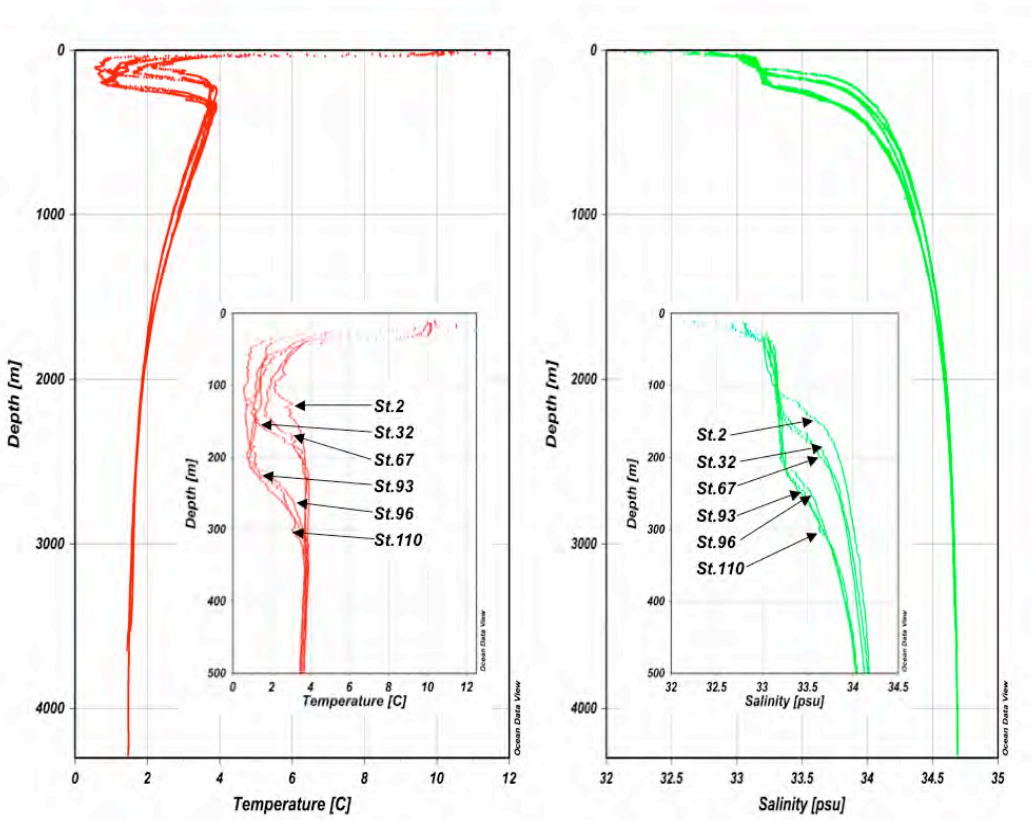

Fig. 1: Temperature and salinity profiles. The insets display the upper 500 m enlarged.

The deeper position of the thermocline and the halocline shown in figure 1. is observed in the northern stations (93, 96, 110) of the Komandorsky Basin running over the Shirshov-Ridge, while the shallower thermocline and halocline occurs in the southern Komandorsky Basin (Station 67) and in the stations off Kamchatka (2, 32: Fig. 1).

The high temperatures and low salinity values of the uppermost, and almost homogenous 20 m we ascribe the seasonal effect of the summer warming and in relation to this to higher rates of precipitation, runoff, and ice-melting. The pronounced cooling in the sea surface water masses reflects winter water, which is the source for WSPW. Coldest temperatures were recorded in station SO201-2-110 at 109 m showing 0.57°C. The winterwater mainly forms in the northern Bering Sea, which is nicely seen in Figure 5.1.3. The Stations 93, 96, and 110 are characterized by a distinct T-minimum which is less pronounced in station 67 due to advection of Pacific Water mainly through the Near Strait and less through the Kamchatka Strait (Takahashi 2005). The signature of the winterwater within the two Pacific stations (2, 32) originate from the advection of Bering Sea Water through the Kamchatka Strait. Fig. 2. summarizes the observed watermasses.

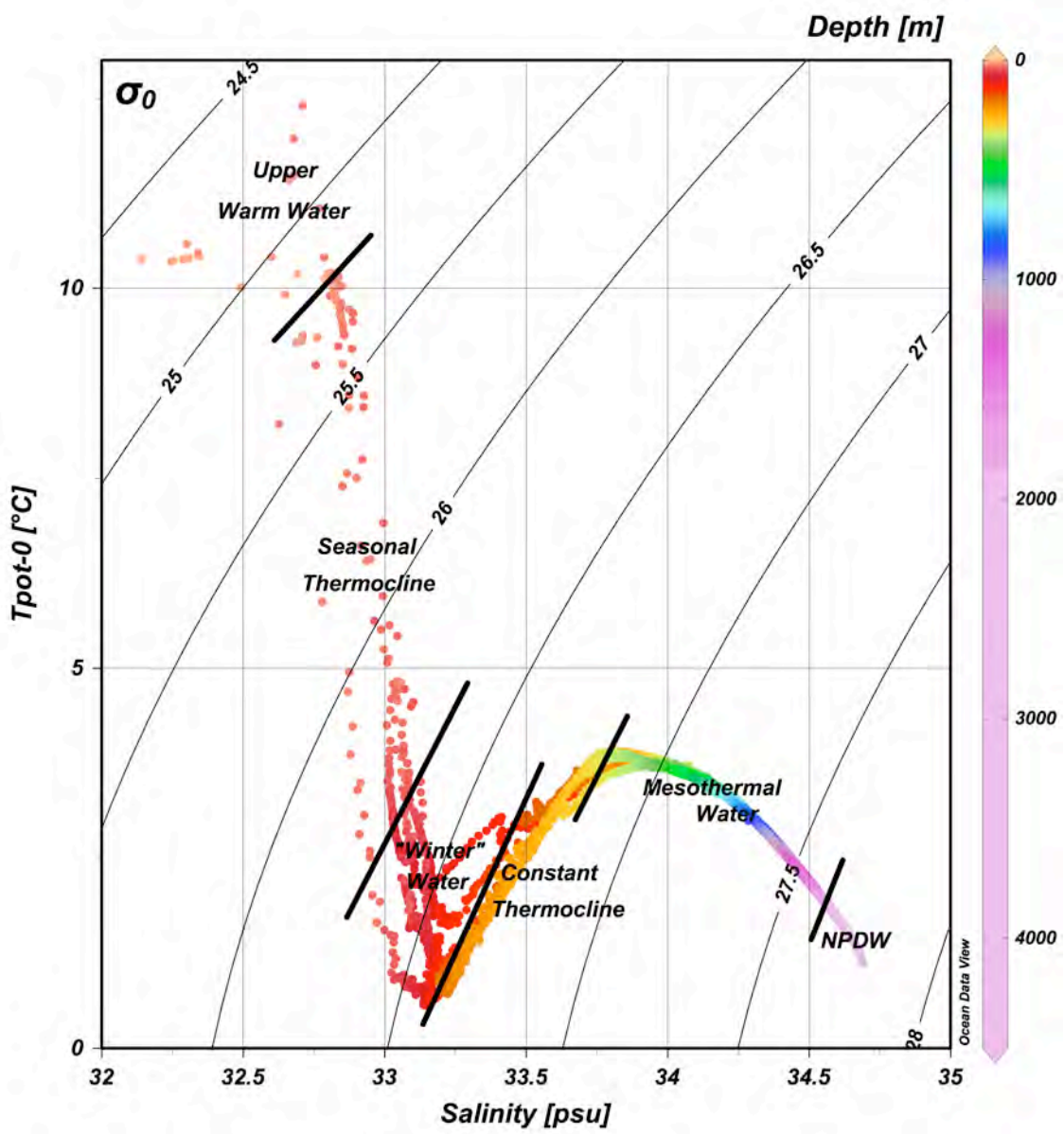

Fig. 2: T-S plot showing the different water masses.

The Krusenstern Fault, NW Pacific: A Reactivated Cretaceous Transform Fault?

Ralf Freitag[1], Christoph Gaedicke[1], Nikolay Tsukanov[2], Udo Barckhausen[1], Dieter Franke[1], Ingo Heyde[1], Stefan Ladage[1], Rüdiger Lutz[1], Michael Schnabel[1]

[1] BGR, Federal Institute for Geosciences and Natural Resources, Geozentrum Hannover, Stilleweg 2, 30655 Hannover, Germany; *corresponding author: ralf.freitag@bgr.de
[2] IO RAS, P.P. Shirshov Institute of Oceanology RAS, Nakhimovsky prospekt 36, 117997 Moscow, Russia

Since Lower Cretaceous times, the Pacific Plate converges against the active margin of Asia. During subduction, the upper plate is strongly deformed by shortening and exhumation. Since the Paleocene, numerous allochthonous terranes were accreted to Kamchatka as part of the Eurasian Plate. At latest Kronotsky-Shipunsky terrane, an island arc of Upper Cretaceous to Eocene age accreted in the Upper Miocene about 9 Ma ago. Recently, the Meiji-Rise, the northwestern most part of the Emperor Seamount Chain approaches the subduction zone. The Meiji-Rise is Upper Cretaceous in age (81-85 Ma) and is elevated about 2500 m above the surrounding seafloor. Meiji is bordered by a system of dextral strike-slip faults of the Aleutian trench in the NE and by a former transform fault in the SW: the Krusenstern Fault (Fig. 1).

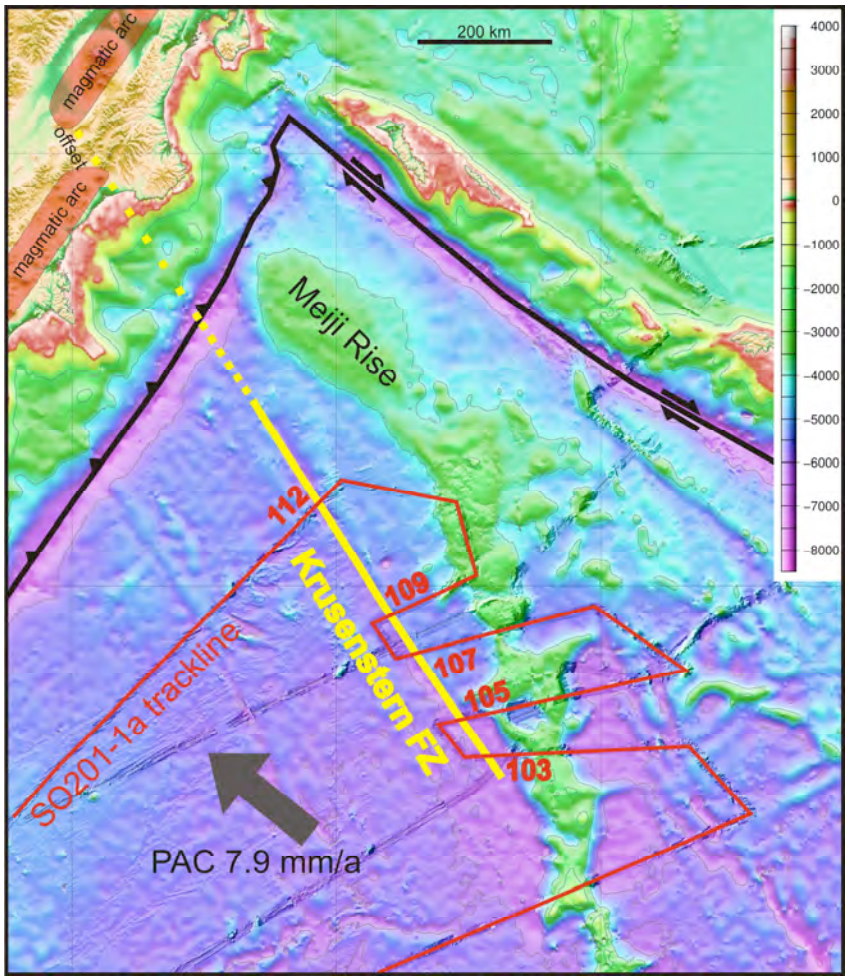

Fig. 1: The Meiji-Rise is bordered by the Aleutian trench in the north and by the Krusenstern Fracture Zone in the south. The imaginary onshore continuation of this zone crosses the fore-arc directly at the magmatic arc offset. Note the enormous difference in depth between the Meiji rise (2500 m) and the abyssal plane south to the fracture zone (5500 m).

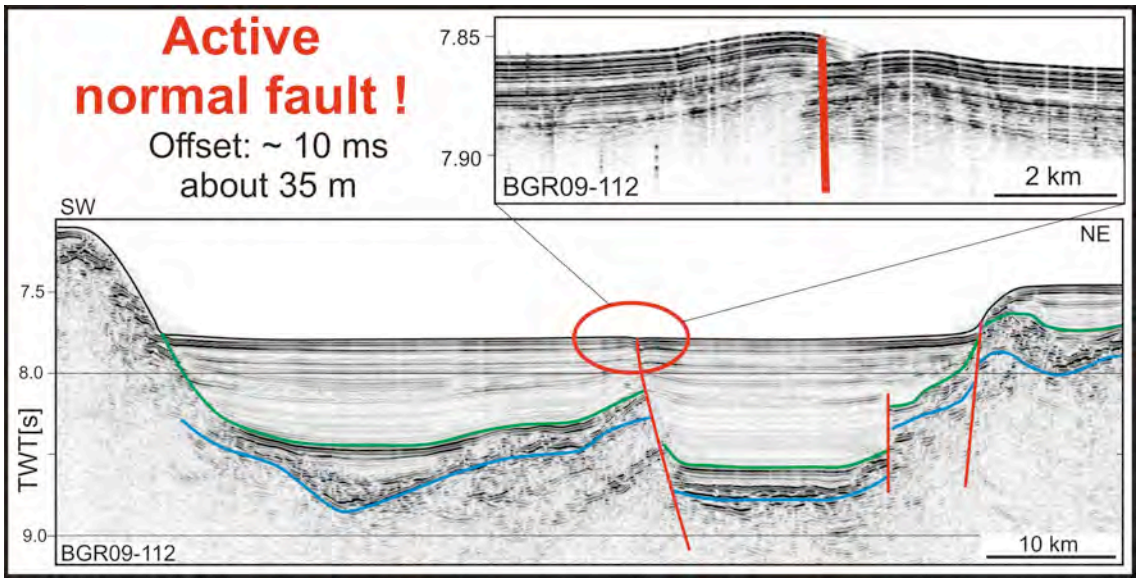

Fig. 2: Multi-channel seismic profile (lower) crossing the Krusenstern fracture zone. The mapped fault plane cuts through the uppermost sediments and reaches the seafloor. On the sediment echo-sounder data (upper), the shift of the surface strata is clearly visible.

The Krusenstern Fault was crossed several times during the RV Sonne cruise SO201-1a and was mapped with geophysical methods. It comprises only minor asymmetries and vertical displacement in the SE and is covered completely by sediments. The displacement and morphological expression of the fault increase rapidly towards the NW. In profile BGR09-107, the SW shoulder of the asymmetric transform fault is already about 1000 m above the surrounding seafloor. In this profile, a relay ramp was mapped pointing to a former dextral plate movement along the fault.

Further in the NW (profile BGR09-109), the displacement increases rapidly while the rough morphology is covered by young deep sea sediments. On the northwestern most profile, the recent activity of the Krusenstern Fault is proofed by echo sounder data: The surface sediments are shifted about 35 m and from MCS it is visible that it is a deep-seated crustal fault (Fig. 2). The Krusenstern fault is a crustal normal fault dipping towards NE, which means the NE area of the Meiji Seamount is structural lower. It is not clear from our data wether there is a strike slip component along the fault.

Because no magnetic anomalies are detectable on the oceanic crust, one can only speculate about the age of the Krusenstern Fault. The acute angle of the fault and the longitudinal shape of the Meiji seamount make a synchronous evolution unlikely. The fact, that the fault seems to be covered by another seamount south of Tenji points to a pre-Emperor age. Some authors interpret the fault as a transform fault of the mid-ocean ridge between the Pacific Plate and the Kula Plate during the Cretaceous Long Normal Superchron.

The reactivation of the Krusenstern Fault may be the result of the subduction and accretion of the Meiji seamount at the Kamchatka margin. The Meiji Seamount is elevated about 2500 m relative to the surrounding seafloor, the crust is much thicker. As the linear extension of the trench does not change, this area must subduct faster in the north of Krusenstern Fault, where the Meiji Seamount is located. The Krusenstern Fault is compensating this different vertical movement in the vicinity of the trench. The sharp bend of the magmatic arc onshore Kamchatka lies in the direct continuation of the Krusenstern Fault. For larger earthquakes, the Krusenstern Fault may act as a segment boundary.

Surface uplift and rock exhumation of morphotectonic blocks at the active fore-arc of Kamchatka, Russia

Ralf Freitag[1,2], Dorthe Pflanz[1,5], Christoph Gaedicke[2], Nikolay Tsukanov[3], Boris Baranov[3], Matthias Krbetschek[4]

[1] University Jena, Institute of Earth Sciences, Structural Geology Group, Burgweg 11, 07749 Jena, Germany; email: ralf.freitag@bgr.de
[2] BGR, Federal Institute for Geosciences and Natural Resources, Geozentrum Hannover, Stilleweg 2, 30655 Hannover, Germany
[3] IO RAS, P.P. Shirshov Institute of Oceanology RAS, Nakhimovsky prospekt 36, 117997 Moscow, Russia
[4] Saxonian Academy of Sciences in Leipzig, Research Center Geochronolgy Quaternary, Institute of Applied Physics, TU Bergakademie Freiberg, Leipziger Str. 23, 09596 Freiberg, Germany
[5] Present Address: National Taiwan University, Dept. of Geosciences, No.1. Sec. 4th, Roosevelt Rd., Taipei 10617, Taiwan

It is widely recognized, that the unusual right-angle junction between the Kamchatka arc and the Aleutian arc (Fig. 1) plays a key role in understanding the recent tectonics of the NW-Pacific region. Most authors agree that the junction right off the Cape Kamchatka Peninsula (CKP) is a collision zone between the two arcs, caused mainly by the westward motion of the Western Aleutian Margin.

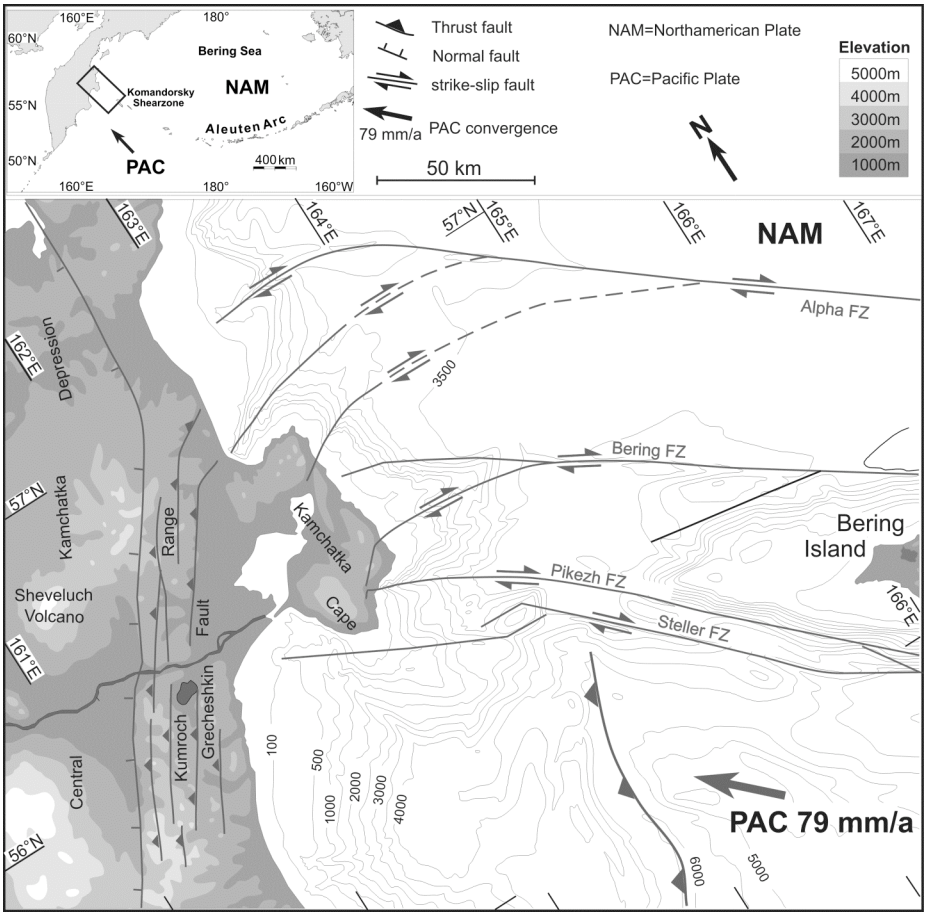

Fig. 1: Structural sketch of the junction area between the Kamchatka and Aleutian Arc right off the Kamchatka Cape peninsula. Stain partitioning occurs in the Komandorsky shearzone. Some of the strike-slip faults (i.e. Pikezh) continue on-shore and bend to the S forming horse-tail structures. Therefore, they also cut through the Upper Plate. The convergence of the Lower Plate as well as the exhumation increases from N to S, as the distinct segments converge with different velocities.

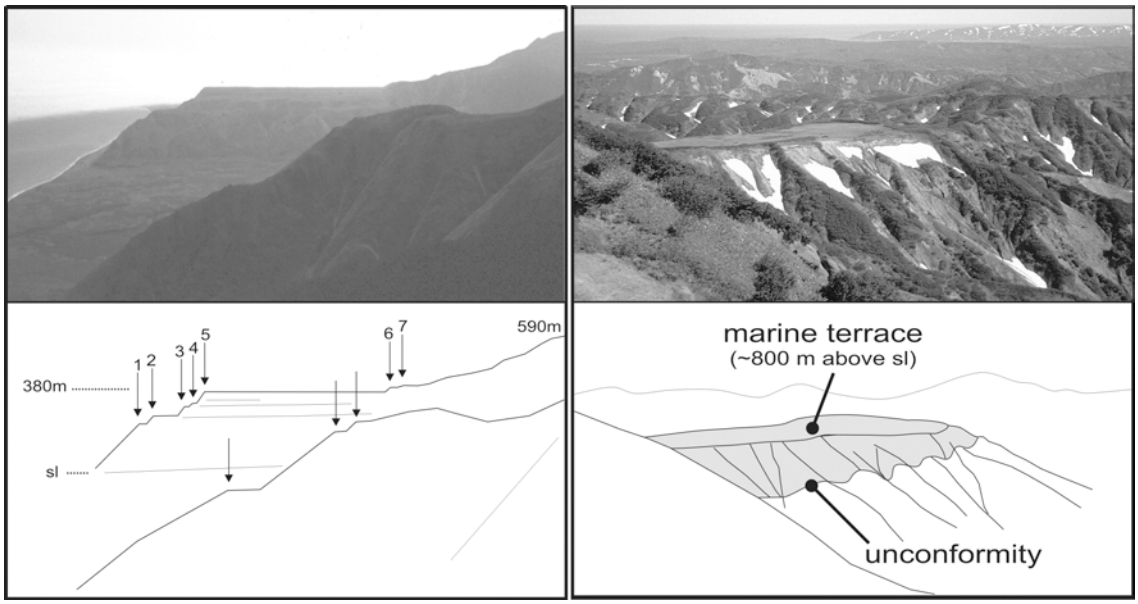

Fig. 2: Examples of high uplifted marine terraces along Kamchatka Cape Peninsula shoreline

To prove the concept of discrete morphotectonic blocks and segmentation for the fore arc, structural investigations, remote sensing applications as well as dating of exhumed rocks and young marine and alluvial deposits where carried out.

Since Mesozoic times, the continental crust at the active margin of Kamchatka grows by accretion of allochthonous terranes. This growth is documented in the differential exhumation of morphotectonic blocks along the Kamchatka trench. Due to this exhumation and uplift, as well as sea-level changes, numerous alluvial and marine terraces formed along the shorelines of Kamchatka (Fig. 2). The absolute radiometric age determination of those terraces allows us to document the relative vertical movement and the absolute uplift rates of the active blocks in high time-resolution.

Strain partitioning between the Pacific Plate and the North American Plate is compensated along dextral strike-slip faults in the Komandorsky Shear-zone (Fig. 1). The strike-slip faults segments the Lower Plate, the discrete segments converge with increasing velocity from N to S against Kamchatka. The most active faults cut the Upper Plate and are exposed onshore.

Results from our subproject TP1 in the framework of the integrated German-Russian research project KALMAR (*K*urile-Kamchatka and *AL*eutean *MAR*ginal Sea-Island Arc Systems: Geodynamic and Climate Interaction in Space and Time, grant number BMBF 03G0640C) are the following: The mean exhumation rate along the Kamchatka margin varies from about 0.2 up to 1.1 mm/yr. The exhumation rates are linked to morphotectonic blocks and exhumation is partially separated along discrete trench-orthogonal active faults. These active faults can be structurally mapped onshore Kamchatka and they seam to be related to pre-existing features of the incoming Pacific Plate.

OSL-ages of the terraces resting on top of the morphotectonic blocks point to recent uplift rates varying from about 2.8 mm/yr up to about 7.5 mm/yr in specific areas during Holocene times. The OSL-ages are generally in a good agreement with the results from dating using the method of cosmogenic nuclides. A good correlation between lower plate convergence, fore-arc geometry, exhumation, elevation and age of marine and alluvial terraces was found.

The recent morphology results from the interplay of subduction, accretion, collision, and uplift as well as sea-level changes, erosion and climate. We present the first radiometric quantitative results about transport, sedimentation, age and uplift of marine terraces on Eastern Kamchatka by OSL-dating. The dated terraces proof the concept of morphotectonic blocks on Kamchatka Cape Peninsula

Exhumation and surface uplift at the Kamchatka-Aleutian triple junction area – Results from KALMAR neotectonics group (TP1)

Ralf Freitag[1], Dorthe Pflanz[2], Nikolay Tsukanov[3], Christoph Gaedicke[1], Matthias Krbetschek[4], Boris Baranov[3], Nikolay Seliverstov[5]

[1] BGR, Federal Institute for Geosciences and Natural Resources, Geozentrum Hannover, Stilleweg 2, 30655 Hannover, Germany: email: ralf.freitag@bgr.de
[2] National Taiwan University, Dept. of Geosciences, No.1. Sec. 4th, Roosevelt Rd., Taipei 10617, Taiwan
[3] IO RAS, P.P. Shirshov Institute of Oceanology RAS, Nakhimovsky prospekt 36, 117997 Moscow, Russia
[4] Saxonian Academy of Sciences in Leipzig, Research Center Geochronolgy Quaternary, Institute of Applied Physics, TU Bergakademie Freiberg, Leipziger Str. 23, 09596 Freiberg, Germany
[5] IVS FEB RAS, Institute of Volcanology and Seismology FEB RAS, Piip Boulevard 9, 683006 Petropavlovsk-Kamchatsky, Russia

Along the active margin of Kamchatka, lower plate material is transferred to the upper plate since the Lower Cretaceous Period. This has led to the growth of continental crust. Key processes for the continental growth are the amalgamation of island arcs and the evolution of the orogenic wedge built up by frontal accretion and underplating. The geometry of this wedge was episodically disturbed by the collision and accretion of oceanic plateaus since the Upper Cretaceous period. The most recent growth e.g. was the collision of the Kronotsky-Shipunsky terrane, a paleo-island arc, about 9 Ma ago. The associated vertical movements of the upper plate have led to exhumation of rocks and surface uplift. This exhumation and uplift has been quantified by

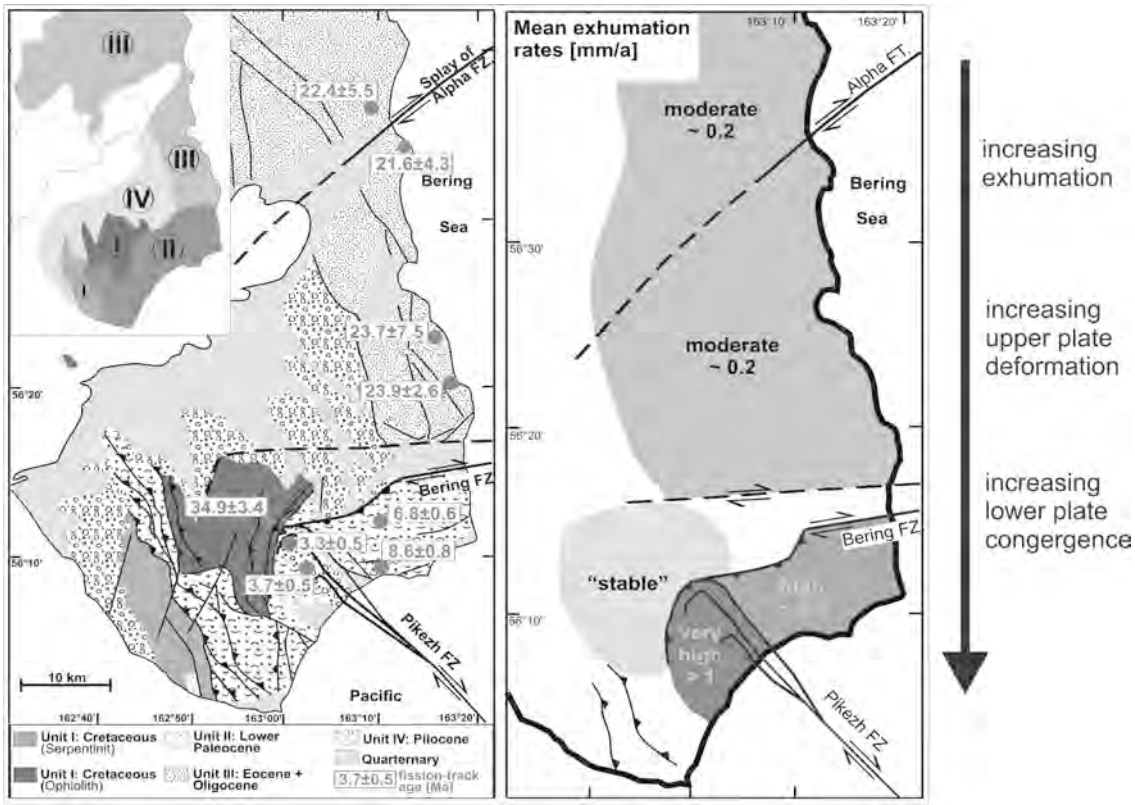

Fig. 1: Apatite fission track ages and mean exhumation rates on the Kamchatka Cap peninsula. The active faults (red) are the onshore continuation of lower plate faults. Exhumation, deformation and lover plate convergence increases from North to South.

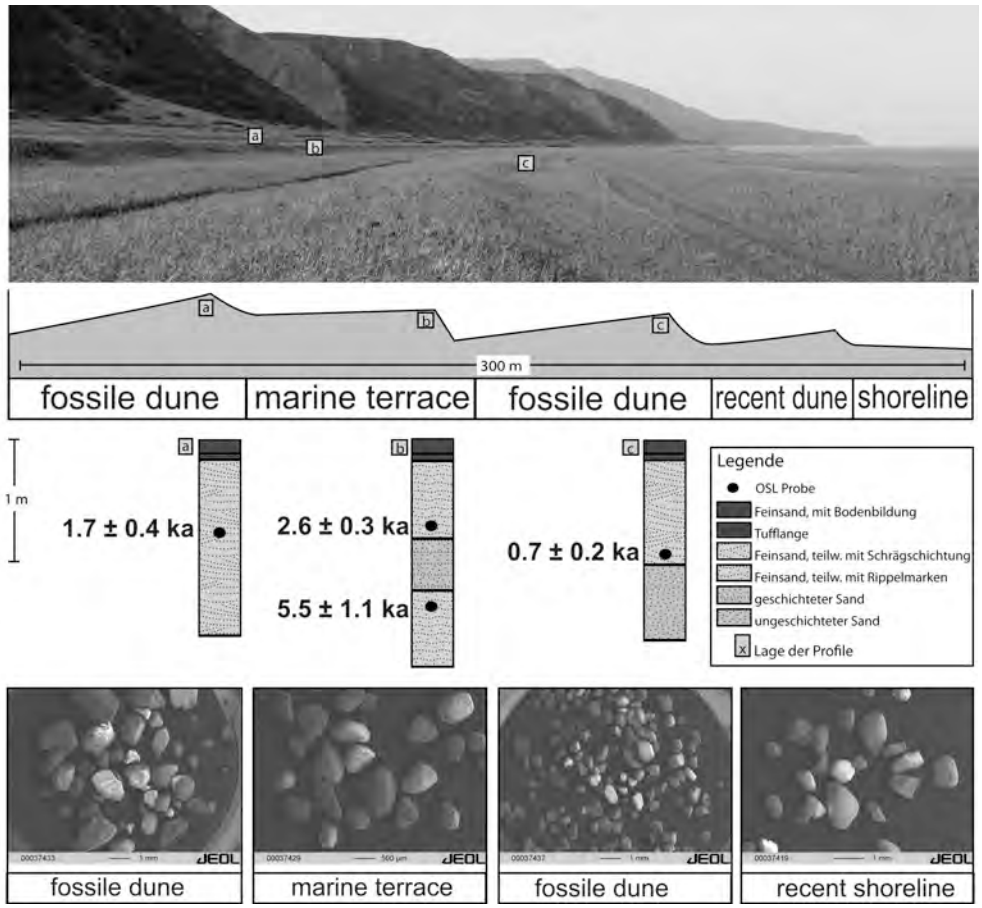

Fig. 2: Photo of a typical profile of terraces near the shoreline and a interpreting line drawing (top). Schematic cross sections through the dunes and terrace (middle) and REM photographs of the corresponding OSL-samples.

thermochronological methods (fission-track dating, FTD) and radiometric dating of terrace sediments (optical stimulated luminescence, OSL).

The recent surface shape and relief at the active Kamchatka margin is a result of the complex interplay of geodynamic processes like accretion, collision, exhumation and surface uplift on the one hand, and subaerial processes like erosion, sea level changes or glaciations on the other hand. This work presents newly acquired exhumation data and the first quantitative results about transport, sedimentation, age and uplift of terrace sediments at the Kamchatka-Aleutian triple junction by radiometric dating using the method of OSL.

We calculated surface uplift rates from OSL ages: 3.7–7.5 mm/yr on the Kamchatka Cape Peninsula, 2.2–3.5 mm/yr for the Kumroch Range and 2.5–3.7 mm/yr on Kronotsky Peninsula. The exhumation rates revealed from FTD varies from 0.2-1.1 mm/yr on Kamchatka Cape, 0.4-1.1 mm/yr along the Kamchatka River and from 0.15-0.8 mm/yr on Kronotsky, respectively.

Marine terraces serve as a reference for the sea level changes at the time of their deposition. Modern methods of remote sensing analysis are a key tool for three-dimensional mapping of terraces and to classify them in terms of generation, properties and elevation. The combination of remote sensing analysis methods and the radiometric dating by OSL provides excellent constraint for the interpretation of neotectonics in the coastal cordilliera of Kamchatka. The distribution and uplift of the dated terraces proves the concept of morphotectonic blocks. The revealed uplift rates as well as the exhumation rates are in good agreement with data from other circum-pacific active margins.

SO201 Leg 1a KALMAR – Geophysical Measurements in the North-west Pacific: An Overview

Christoph Gaedicke[1], Udo Barckhausen[1], Dieter Franke[1], Ralf Freitag[1], Ingo Heyde[1], Stefan Ladage[1], Rüdiger Lutz[1], Nikolay Tsukanov[2], Thomas Pletsch[1], Evgeny Sukhoveev[3], Hauke Thöle[1]

[1] BGR Federal Institute for Geosciences and Natural Resources, Geozentrum Hannover, Stilleweg 2, 30655 Hannover, Germany; email: christoph.gaedicke@bgr.de
[2] IO RAS, P.P. Shirshov Institute of Oceanology RAS, Nakhimovsky prospekt 36, 117997 Moscow, Russia
[3] POI FEB RAS, V.I. Ilichev Pacific Oceanological Institute FEB RAS, Baltiyskaya Street 43, 690041 Vladivostok, Russia

The RV Sonne-KALMAR cruise SO201 Leg 1a was carried out from 16th May until 9th June 2009. The cruise began and ended in Yokohama, Japan. During the cruise, marine geophysical measurements were carried out, using multichannel reflection seismics (MCS), magnetics and gravimetry. Simultaneously, the hull mounted swath bathymetric and sediment echo-sounding systems were operated. During the expedition, 11 MCS profiles with a total of 2,714 km were acquired. Additionally, 3,180 km were recorded using only potential field methods (Fig. 1). The focus on MCS profiles laid on the examinations of the northern section of the Emperor Seamount chain. The structure and the architecture of the seamounts and of the surrounding sediments were recorded. On the oceanic crust, fracture zones were surveyed that strike at an acute angle towards the chain of the extinct volcanoes. For sediment correlation purposes, ODP drillhole 882 on the Wayne Seamount was crossed. A 431 km long profile parallel to the Kamchatka deep sea trench was used to determine the sedimentary cover of the oceanic crust and to reconstruct two fracture zones that probably influence the deformation of the forearc of Kamchatka. Based on the seismic profiles and on the recorded bathymetry, 36 sampling points were defined, where crystalline rocks of the oceanic crust and of the submarine volcanoes crop out at the seafloor. Samples were taken during SO201 Leg 1b. Four seismic sequences are distinguished (Fig. 2).

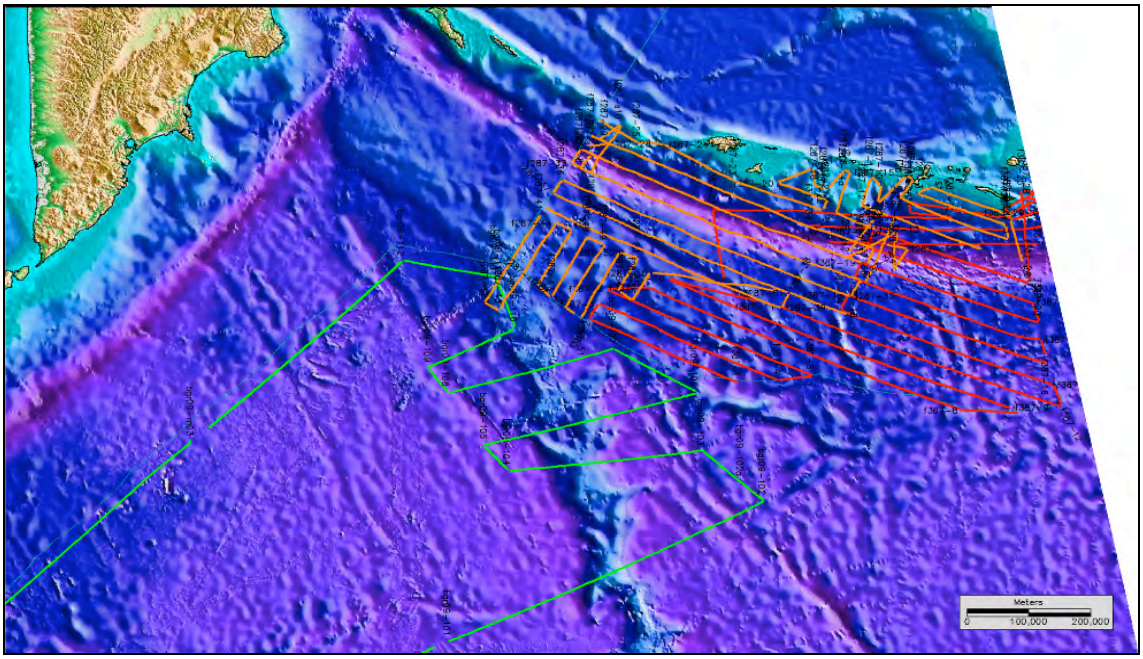

Fig. 1: Geophysical profiles of the expedition SO-201 Leg 1a KALMAR (green). Additional data available in the project are shown (red/orange: USGS, single channel seismics). The highlighted green line shows the position of profile BGR09-103 (Fig. 2).

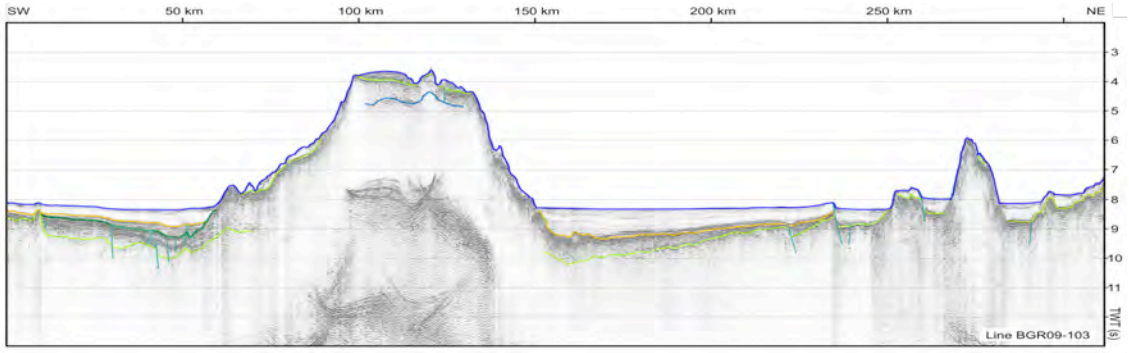

Fig. 2: Reflection seismic profile BGR09-103 over the Jimmu Seamount. The flexure of the oceanic crust around the Jimmu Seamount is very well recognizable. The plateau on the seamount is covered by contourites.

The lowermost sequence is formed by the oceanic acoustic basement. Around the seamounts, it is covered by a wedge-shaped sequence characterized by strong amplitudes. We interpret this sequence to consist basalt flows in connection with the formation of the seamounts. The following overlying sequence of continuous reflectors is built up by erosion products of the seamounts that were dumped around the seamounts during the erosive, subaerial phase. The youngest sequence consists of hemipelagic/pelagic well stratified sediments, levelling the flexure of the oceanic lithosphere.

During the research cruise, continuous gravity measurements were carried out using BGR's own KSS31M marine gravimeter system. A chain of gravity maxima up to 300 mGal high and between 30 to 70 km wide striking north-northwest – south-southeast is related to the Emperor Seamounts. On both sides, the maxima are accompanied by gravity minima of 80 to 100 km width. They reflect the flexure of the lithosphere caused by the additional mass of the volcanic load. The stiffness of the lithosphere plate leads to a regional isostatic compensation, causing an increase of the water depth of about 500 m on both sides of the seamount chain. We calculate 2D density models on base of gravity and MCS data. The models show that the seamounts have roots of about 1.5 to 2 times their height and that the sediment basins reach thicknesses of 1,5 to 3 km on their margins.

The oceanic crust of the Pacific plate off Kamchatka and the northern Kuril Islands was most likely formed during the so-called Cretaceous Normal Superchron, a time between 118 Ma and 83 Ma where no magnetic field reversals took place. Therefore, the age of the crust can not be determined by classic methods using the earth magnetic field reversals recorded in the magnetic anomalies. Nevertheless, in the magnetic data from the profiles of cruise SO201 significant differences of the anomalies appear between the individual crustal segments separated by fracture zones. A new approach to age determination for oceanic crust of this age range tries to correlate changes in the paleointensity of the earth's magnetic field during the Cretaceous Normal Superchron (e. g. Dyment et al. 2009). In the framework of a bachelor's thesis at Hannover University we currently examine the different possibilities to use the magnetic data of cruise SO201 for a further characterization of the subducting crust off Kamchatka. For this purpose, also applicable magnetic profiles from the Geodas data archive are being reprocessed and incorporated.

References

Dyment J, Gallet Y, Hoise E (2009) First complete high-resolution record of the Cretaceous Normal Superchron, Eos Trans. AGU, 90 (52), Fall Meet. Suppl., Abstract GP31A-05

Evolution of the Late Pleistocene Old Shiveluch Volcano, Kamchatka

Natalia Gorbach[1], Maxim Portnyagin[2,3]

[1] IVS FEB RAS, Institute of Volcanology and Seismology FEB RAS, Piip Boulevard 9, 683006 Petropavlovsk-Kamchatsky, Russia; email: n_gorbach@mail.ru
[2] IFM-GEOMAR, Leibniz Institute of Marine Sciences, Wischhofstrasse 1-3, 24148 Kiel, Germany
[3] GEOKHI RAS, V.I.Vernadsky Institute of Geochemistry and Analytical Chemistry RAS, Kosygin St. 19, 119991 Moscow, Russia

Shiveluch volcanic massif, which covers an area of 1000 km^2 and has a volume of erupted products close to 1000 km^3, has a long and complex eruptive history. Its edifice includes the Late Pleistocene polygenic stratovolcano Old Shiveluch, which was partially destroyed by collapse crater, and Young Shiveluch eruptive center, which has been active through the Holocene (Melekestsev et al. 1991). The Shiveluch edifice hosts also a number of satellite lava domes of different age, such as the Late Pleistocene Semkorok domes in the southeast foot and the Holocene Karan domes on the western slopes of the Old Shiveluch. The southwestern sector of Old Shiveluch (also known as Baidarny Spur) is believed to comprise many monogenetic volcanic centers (Volynets et al. 1997).

Whereas data on geology, petrology and geochemistry of Young Shiveluch are relatively abundant (Volynets et al. 1997, Ponomareva et al. 2007, Portnyagin et al. 2007), details about the Late Pleistocene Old Shiveluch activity are poorly known (Menyayilov 1955, Melekestsev et al. 1991). Here we present results of the study undertaken within the KALMAR project which is aimed at filling the gap in knowledge of the whole-rock major, trace elements and phenocrysts composition of Old Shiveluch rocks series and genetic relationships between different rock types.

Old Shiveluch volcanic edifice is built up by coarse agglomerate tuffs related to the initial extrusive and explosive activity and overlying lava complex. Formation of the lava complex was associated with at least 4 eruptive centers, whose position was reconstructed along the rim of the collapse crater. Three main type of rock were distinguished in the Old Shiveluch volcanic edifice: magnesian andesites, high-Mg basaltic andesites and high-Al basaltic andesites (listed according to decreasing of erupted volume).

The magnesian andesites (SiO_2=57.3-63.8, TiO_2=0.47-0.83, Al_2O_3=16.5-17.6, MgO=2.8-4.8, K_2O=1.2-1.7 (wt.%), Cr=45-90, Ni=5-32 (ppm), Mg#=52.5-57.0 mol. %.) predominate in the initial agglomerate tuffs and compose the Main Summit lava section. The high-Al basaltic andesites (SiO_2=53.5-55.7, TiO_2=0.84-0.99, Al_2O_3=16.6-17.5, MgO=4.4-5.9, K_2O=0.87-1.18 (wt. %), Cr=35-99, Ni=2-26 (ppm), Mg#=52.1-56.1 mol%) compose lava flows in the western sector of Old Shiveluch and eruptive centers and dykes within the Baidarny Spur. Small volume high-Mg basaltic andesites (SiO_2=53.9-55.0, TiO_2=0.76-0.86, Al_2O_3=15.1-16.49, MgO=6.12-7.52, K_2O=1.18-1.27 (wt.%), Cr=175-315, Ni=2-26 (ppm), Mg#=58.8-63.7 mol. %.) were found at the boundary between the initial pyroclastic deposits and lava complex of Old Shiveluch

Our data on petrography, mineralogy and geochemistry suggest that all studied rocks are likely genetically related. These rocks form single trends of increasing concentrations of incompatible lithophile elements (e.g. Ba, K, Th) and decreasing concentrations of compatible trace elements (e.g. Cr, Ni) with decreasing MgO that suggests the dominant role of fractional crystallization at creating of the petrographic diversity of the Old Shiveluch rocks. Similar REE patterns and trace elements ratios (e.g. Zr/Y, La/Yb, Ba/Th, Ba/La, Th/La, Th/Yb) of high-Mg and high-Al basaltic andesites also indicate their origin from a common parental melt. The presence of several phenocrysts generations of olivine, clinopyroxene and amphibole indicates, however, a long and multi-stage crystallization history of the magmas at different crustal levels. The presence of high-

Mg and high-Al basaltic andesites in the Old Shiveluch is therefore more likely related to different conditions of magma evolution rather than to two different slabs, shallow and deep, subducting beneath Shiveluch (Ferlito 2011). These alternative hypotheses can be tested with the help of experimental studies simulating crystallization of Shiveluch magmas at different conditions.

This research was supported by the KALMAR project (BMBF grant 03G0640A), which funded geochemical and mineralogical investigations and the Grants of the Far East Division Russian Academy of Sciences (##07-III-D-08-095 and 09-III-A-08-422).

References

Ferlito C (2011) Bimodal geochemical evolution at Shiveluch stratovolcano, Kamchatka, Russia: Consequence of a complex subduction at the junction of the Kuril Kamchatka and Aleutian island arcs. Earth-Science Reviews 105(1-2): 49-69

Melekestsev IV, Volynets ON, Ermakov VA, Kirsanova TP, Masurenkov Yu.P (1991) Shiveluch volcano. In: Fedotov S. A., Masurenkov Yu. P. (Eds.) Active volcanoes of Kamchatka. 1, Nauka Press, Moscow: 84-92

Menyailov AA (1955) Shiveluch Volcano, its geologic structure, composition and eruptions. Trudi Laboratorii Vulkanologii, 9, 264 pp (in Russian)

Ponomareva VV, Kyle P, Pevzner MM, Sulerzhitsky LD, Hartman M (2007) Holocene Eruptive History of Shiveluch Volcano, Kamchatka Peninsula, Russia. In: Volcanism and Subduction: The Kamchatka region. Eichelberger J., Gordeev E., Izbekov P., Lees J. (Eds), AGU Geophysical Monograph, 172: 263-282 Portnyagin MV, Bindeman IN, Hoernle K, Hauff F (2007) Geochemistry of primitive lavas of the Central Kamchatka Depression: magma genesis at the edge of the Pasific Plate // Volcanism and Subduction: The Kamchatka region. Eichelberger J., Gordeev E., Izbekov P., Lees J. (Eds). AGU Geophysical Monograph 172: 203-244

Volynets ON, Ponomareva VV, Babansky AD (1997) Magnesian Basalts of Shiveluch Andesite Volcano, Kamchatka, Petrology (Engl. Transl.) 5/2: 183–196

Marine geophysical measurements in the northernmost part of the Emperor Seamount Chain in the Northwest Pacific

Ingo Heyde[1], Dieter Franke[1], Ralf Freitag[1], Christoph Gaedicke[1], Nikolay Tsukanov[2]

[1] BGR, Federal Institute for Geosciences and Natural Resources, Geozentrum Hannover, Stilleweg 2, 30655 Hannover, Germany, email: ingo.heyde@bgr.de
[2] IO RAS, P.P. Shirshov Institute of Oceanology RAS, Nakhimovsky prospekt 36, 117997 Moscow, Russia

In spring 2009 the research cruise SO-201 Leg 1a was carried out with RV SONNE in the framework of the KALMAR project which is funded by the German Ministry of Education and Research. During the cruise marine geophysical data were acquired including multi-channel seismic (MCS), magnetic and gravimetry. In addition the shipboard systems swath and sediment echo sounder were used. The main survey area was located in the northernmost part of the Emperor Seamount Chain were 11 profiles with a total length of 2283 km were acquired. The data give evidence of the structural build-up of the seamounts and the adjacent sediments. The focus of the contribution lies on the presentation and the interpretation of the gravity data.

The shipboard free-air gravity anomalies were compared with two free-air gravity data sets derived from satellite altimetry (version 18.1 from Sandwell and Smith (2005) and DNSC08 from Andersen et al. (2008)). The comparison resulted in the usage of the DNSC08 data set in areas where no shipboard data are available. A combined map of the free-air gravity anomalies was compiled (Fig. 1).

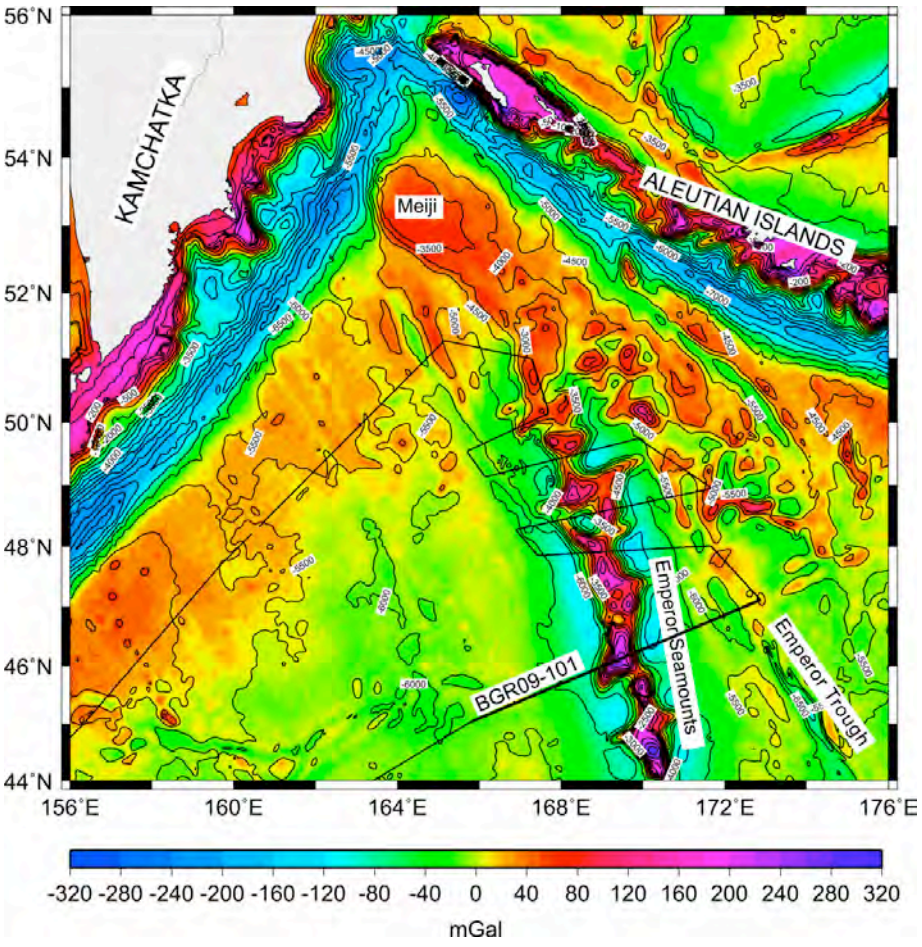

Fig. 1: Free-air gravity anomaly map. The underlying grid was compiled by merging shipboard and DNSC08 gravity data derived from satellite altimetry. The map is underlain by the DNSC08 bathymetry.

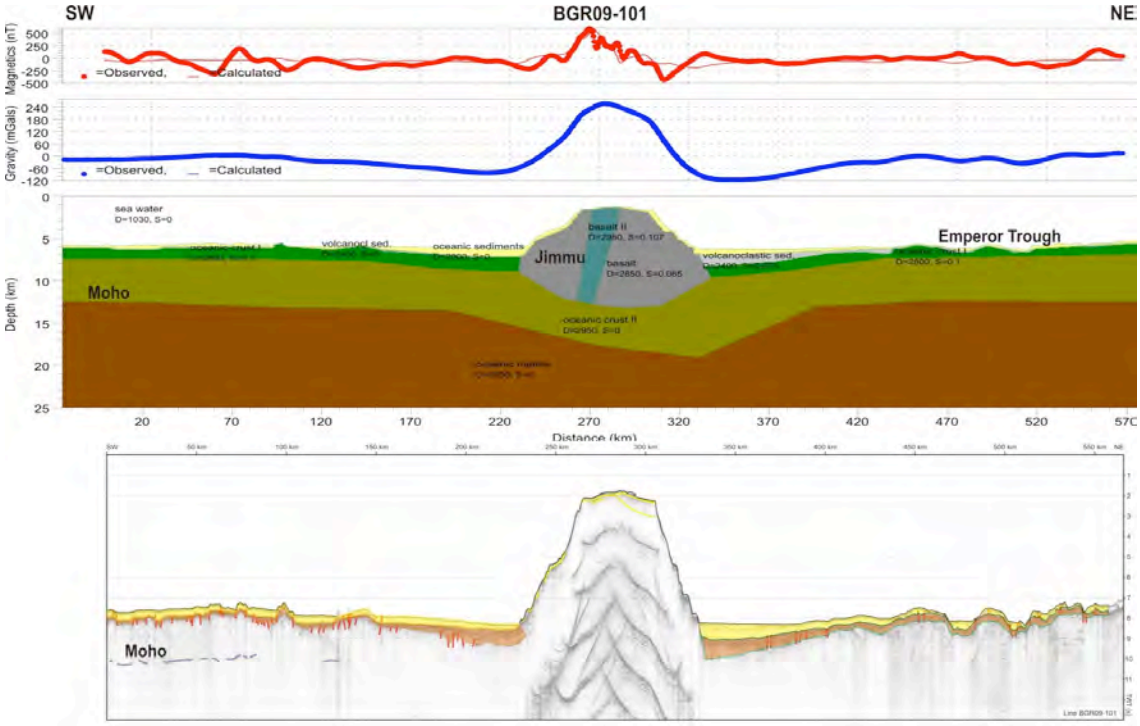

Fig. 2: 2D density/susceptibility model explaining the gravity and magnetic anomalies along BGR09-101 (above) and the corresponding MCS section (below). Density values in kg/m³, susceptibilities in SI units.

The Emperor Seamounts with an elevation of up to 5000 m are reflected in a chain of free-air gravity maxima of up to 300 m Gals with a width of 30 to 70 km. The NNW-SSE striking maxima are adjoined on both sides by gravity minima with a width of 80 to 100 km resulting from the flexure of the rigid lithosphere due to the additional volcanic load. To the East another elongated gravity minimum reflects the Emperor Trough which represents a fault zone on the oceanic crust striking in an acute angle to the seamount chain. To the North the seamount chain passes on to the broad Meiji Plateau. Maps of the Bouguer gravity anomalies and the isostatic residual anomalies were calculated showing further features.

Based on the gravity data along several profiles density models were developed taking into account the stacked and time-migrated MCS data. Fig. 2 shows the model along the southernmost profile BGR09-101. The models show that the seamounts have roots with thicknesses about two times of their respective elevation. The roots are mostly asymmetric with a deeper part in the East. The seamount tops have an almost flat morphology that appears to be erosional. The sediment basins bordering the seamounts show a thickness of 1.5 to 3 km. According to the MCS data three sequences could be distinguished. The lowermost represents basaltic flows associated with the formation of the seamounts. The following hanging sequence of continuous reflectors reflects the erosional debris deposited during the erosive subaerial period. The youngest sequence consists of pelagic sediments which increase in thickness towards the seamounts and compensate thus partly for the bathymetric depression due to the flexure of the oceanic lithosphere.

References

Andersen OB, Knudsen P, Berry P, Kenyon S (2008) The DNSC08 ocean wide altimetry derived gravity field. Presented EGU-2008, Vienna, Austria, April 2008

Sandwell DT, Smith WHF (2005) Retracking ERS-1 altimeter waveforms for optimal gravity field recovery, Geophys. J. Int., 163, 79–89

Fossil diatom assemblages in mid- to late Holocene lake sediments of central Kamchatka, Russia

Ulrike Hoff[1, 2], Bernhard Diekmann[1]

[1] AWI, Alfred Wegener Institute for Polar and Marine Research, Telegrafenberg A43, 14473 Potsdam, Germany
[2] Present Address: Hessisches Landesmuseum Darmstadt (HLMD), Friedensplatz 1, 64283 Darmstadt, Germany; email: U-Hoff@web.de

The German-Russian joint venture project KALMAR aims to assess the climate controlling features of the Kurile-Kamchatka-Aleutean-Sea-Island-Arc and its adjacent regions by palaeoenvironmental reconstructions *inter alia*. One aspect of KALMAR was the reconstruction of climate-related past terrestrial environmental changes from faunal and floral remains in lake sediments.

A characterization and in particular an interpretation of fossil diatom assemblages as well as the diatom geochemistry ($\delta^{18}O_{diatom}$) in those sediment cores are two aspects we focused on during the run time of our palaeolimnological subproject, subproject 5. This combination of taxonomical and geochemical methods was applied for the first time on lake-sediment records from Kamchatka (Hoff 2010).

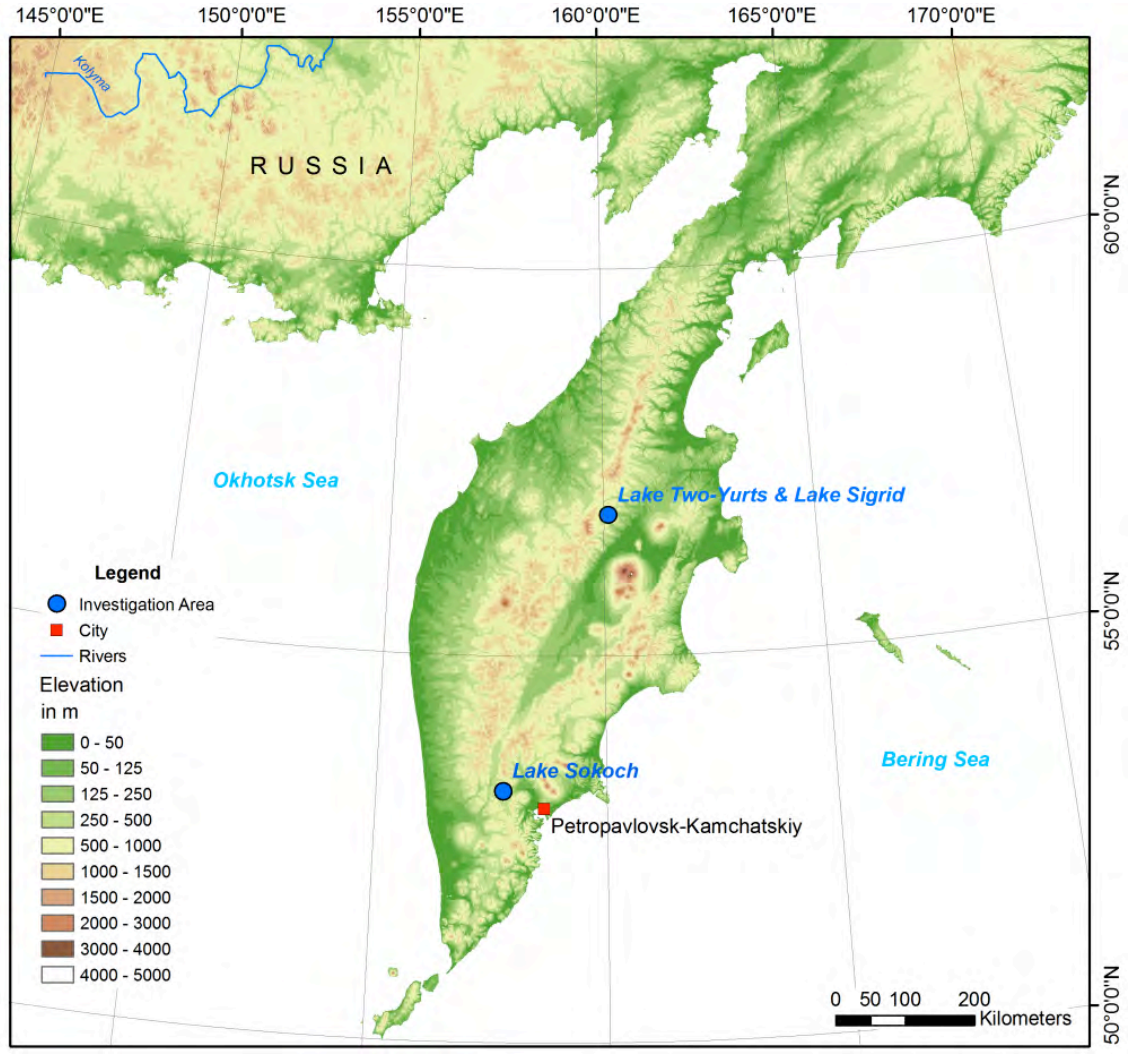

Fig. 1: Location of the three studied lakes on Kamchatka Peninsula.

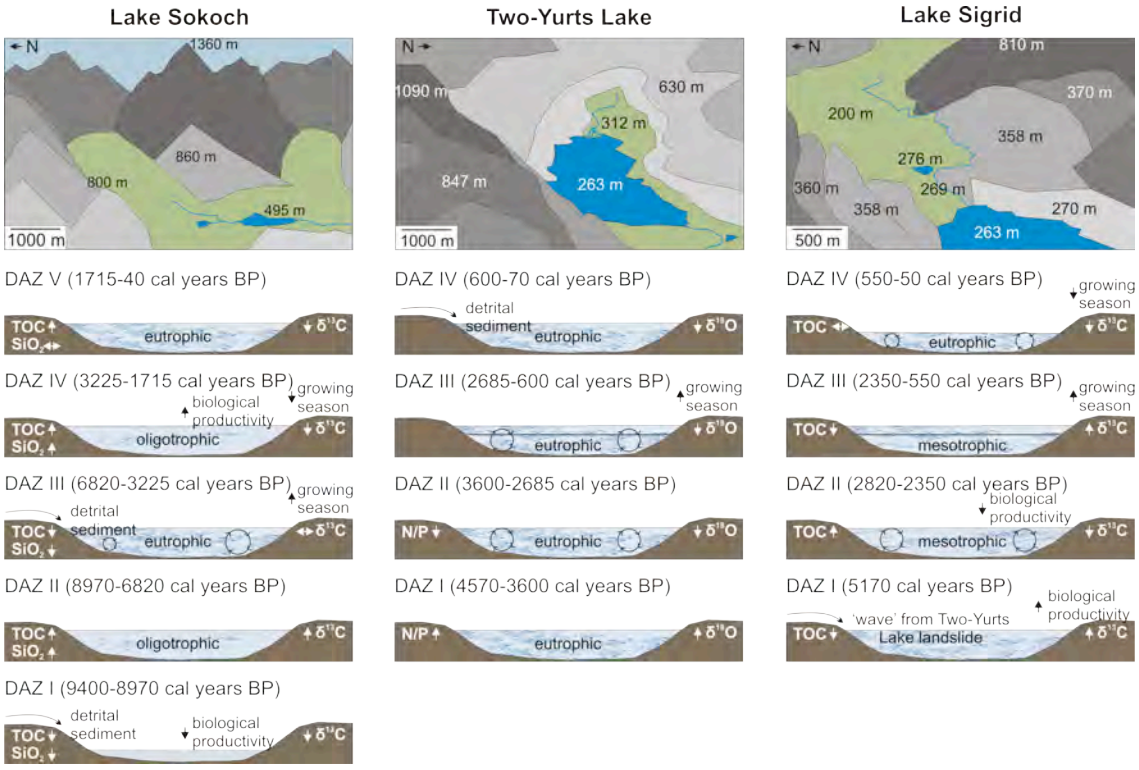

Fig. 2: Temporal variations of limnoecological conditions in three lakes of Kamchatka, as inferred from fossil diatom assemblages.

Within the study, a total of three lakes (Fig. 1) were selected to cover different environmental boundary conditions. They comprised a hydrologically closed seepage lake (Lake Sigrid) at a moderate elevation of about 280 m above sea level next to an open through-flow lake (Two-Yurts Lake) in central Kamchatka. The third study site was an open through-flow lake at an elevation of almost 500 m above sea level (Lake Sokoch) in south Kamchatka.

In total, a number of 133 diatom taxa were identified within the fossil records, whereof one taxon could be identified as an up-to-now unknown species. It is referred to as *Fragilaria flexura* sp. nov. U. HOFF ET LANGE-BERTALOT (Hoff et al. 2011).

Fossil diatom assemblages differ between the study sites and also through time in all investigated records. They reflect changes in partly climate-driven limnoecological boundary conditions, such as stratification of the water column, turbulence, water temperature and the geochemical character of the host water, trophy, or the amount of available nutrients (Fig. 2).

Two-Yurts Lake reveals highest biological productivity, due to a steady input of nutrients and diluted silica by its inflows, additionally supported by frequent occurring strong turbulences, enabling for a reworking and hence recycling of deposited nutrients/silica from the lake bottom surface sediments. Dominating species are *Aulacoseira subarctica* (O. MÜLLER) Haworth (indicator for strong turbulences) and *Stephanodiscus minutulus* (KÜTZING) CLEVE & MÖLLER (indicator for an increasing eutrophication). A trend towards colder conditions in the younger section is suggested by $\delta^{18}O_{diatom}$ values in the sediment cores from Two-Yurts Lake.

The closed seepage Lake Sigrid in turn reveals lowest numbers of diatoms per gram sediment (biological productivity) most likely due to its lacking inflows. Important taxa indicating changing conditions within the stratification as well as the lakes temperature are *Aulacoseira subarctica*, *Discostella pseudostelligera* (HUSTEDT) HOUK & KLEE, *Staurosira venter* (EHRENBERG) CLEVE & MÖLLER, *Achnanthidium minutissimum* (KÜTZING) D.B. CAERNECKI and *Psammothidium*

helveticum (HUSTEDT) L. BUKHTYAROVA & F.E. ROUND (Hoff et al. submitted). Whereas the increase of *P. helveticum* indicates an interval of decreasing temperatures, corresponding well to the Little Ice Age period of the Holocene history of Kamchatka.

Lake Sokoch shows a medium intense biological productivity, most likely caused by minor nutrient and diluted silica input into the lake and a geographical setting which is less exposed to fall winds than Two-Yurts Lake is. This lake is dominated by *Staurosira mutabilis* (W. SMITH) Grunow, *Staurosira venter* (EHRENBERG) CLEVE & MÖLLER, *Staurosira brevistriata* (GRUNOW) GRUNOW and *Staurosira harrisonii* (RAPER) GRUNOW, indicating quite constant limnological conditions through time. Nonetheless, the record includes an interval with more warm-living diatoms, reflecting the regional mid-Holocene climate optimum. The climate optimum was also inferred from the pollen records of Lake Sokoch and other sites on Kamchatka (Dirksen, Uspenskaia 2005; Dirksen this volume) and regional glaciation history in the wider area around Lake Sokoch (Savoskul 1999).

References

Dirksen VG, Uspenskaia ON (2005) Holocene climate and vegetation changes in Eastern Kamchatka based in pollen, macrofossil and tephra records. Geophysical Research Abstracts 7: EGU05-A-01435

Hoff U (2010) Freshwater diatoms as indicators for Holocene environmental- and climate changes on Kamchatka, Russia. PhD-Thesis University of Potsdam, Potsdam

Hoff U, Lange-Bertalot H, Diekmann B (2011) *Fragilaria flexura* sp. nov. (Bacillariophyceae) – A new freshwater diatom from a meso- to oligotrophic mountain lake on the Kamchatka-Peninsula, Russia. Nova Hedwigia (in press)

Hoff U, Dirksen O, Dirksen V, Herzschuh U, Hubberten HW, Meyer H, van den Bogaard C, Diekmann B (submitted) Late Holocene diatom assemblage in a lake-sediment record of central Kamchatka, Russia (submitted to the Journal of Palaeolimnology)

Savoskul OS (1999) Holocene Glacier Advances in the Headwaters of Sredniaya Avacha, Kamchatka, Russia. Quaternary Research 52: 14-26

Postglacial paleoceanography of the NW Pacific: an overview

Elena Ivanova[1], Ekaterina Ovsepyan[1]

[1] IO RAS, P.P. Shirshov Institute of Oceanology RAS, Nakhimovsky prospekt 36, 117997 Moscow, Russia; email: e_v_ivanova@ocean.ru

By now, only a few sediment cores are studied with millennial resolution from the subarctic north-western Pacific and Bering Sea, thus paleoceanographic reconstructions from the region are limited. Much more is done in the Sea of Okhotsk. The major problems with distinguishing the succession and timing of the regional paleoceanographic events result from (1) extensive dissolution of carbonate and siliceous microfossils, (2) poorly expressed oxygen isotope variability in the region as compared to the global stack LR04, and (3) uncertainty in reservoir age changes through time. These problems hamper the progress in regional paleoceanograhic studies and in assessment of the North Atlantic-North Pacific seesaw.

Only a few paleoceanographic works appeared after the synthesis provided by Takahashi (2005) and by papers in the same volume of the Deep-Sea Research (II, 52, 2005). Herein we summarize the existing knowledge on the regional stratigraphy (using the age-models from cited publications) and on paleoceanographic events during the last 20 kyr. supplemented by the recent findings from the KALMAR project (Riethdorf et al. 2010, Ovsepyan et al. 2010). As the available data on sea-surface temperatures (e.g. Gebhardt et al. 2008, Max et al. 2010) are quite controversial, we mainly consider changes in productivity and bottom-water ventilation during the early deglaciation, Bølling-Allerød (B/A) interglacial and associated melt-water pulse (MWP) 1a, Younger Dryas (YD), early and late Holocene.

In the NW Pacific, the early deglaciation is characterized by rather low productivity (inferred from low chlorine, biogenic opal and $CaCO_3$ values), very high sedimentation rates and IRD discharge (Gebhardt et al. 2008). In the western Bering Sea core SO201-2-85KL (water depth 968 m), we found that the maximum of planktic foraminiferal (PF) abundance occurred just after the LGM, i.e. preceded the well-established regional $CaCO_3$ spike associated to the B/A warming and MWP 1a. The spike in PF abundance record and the concurrent high value of *G. bulloides* seem to document the first prominent productivity change during the Termination I in the Western Bering Sea. They possibly reflect a decrease in winter sea-ice extent after the LGM and longer ice-free season. However, the lateral extent and timing of this event needs further investigation. Meanwhile, it coincides with the interval of relatively weak intermediate water ventilation on the Shirshov Ridge.

The end of early deglaciation is marked by an occurrence of alkenones and shift in diatom assemblages pointing to the seasonal sea ice over the Umnak Plateau, southern Bering Sea (Caissie et al. 2010). The late deglaciation is broadly characterized by laminated intervals of variable thickness and duration (e.g. Dullo et al. 2009) with diverse and productive diatom assemblages and increased coccolithophorid production (Caissie et al. 2010). During B/A, the high-productivity event is established by planktic and benthic foraminiferal data, carbon isotopes, $CaCO_3$ and TOC content in several locations including the Shirshov Ridge (Ovsepyan et al. 2010 and this volume; Riethdorf et al. 2010), Bowers Ridge (e.g. Gorbarenko et al. 2005, 2010), Sea of Okhotsk (e.g. Bubenshchikova et al. 2010) and subarctic northwest Pacific (Crusius et al. 2004, Gebhardt et al. 2008). This maximum most likely coincided with a melt-water pulse MWP 1a and with relatively weak to moderate intermediate water ventilation on the Shirshov Ridge, at several locations in the Sea of Okhotsk and northwest Pacific. The PF abundance on the Bowers Ridge reached the maximum value at that time unlike the Shirshov Ridge (Core SO201-2-85-KL). In the NW Pacific cores RAMA 44 and CH84-14 (Crusius et al. 2004), and MD01-2416 (Gebhardt et al. 2008), the high productivity is manifested by a maximum of biogenic opal concentration. In the latter core, it is preceded by the chlorins maximum during the early

deglaciation, just after the youngest IRD spike (Gebhardt et al. 2008). Origin of the high-productivity event at B/A interstadial is still illusive.

On the contrary, YD cooling is generally characterized by a low productivity but stronger intermediate water ventilation (Crusius et al. 2004, Bubenshchikova et al. 2010, Ovsepyan et al. this volume). The sharp increase in productivity and weakening of ventilation are associated to MWP 1b at the Preboreal warming. However, PF and BF are less abundant than at MWP 1b, especially on the Bowers Ridge (Gorbarenko et al. 2005). The productivity of calcareous microfossils was still rather high during the early Holocene, as follows from high abundance of benthic foraminifers dominated by *Bolivina seminuda and Bulimina exilis*, and high percentage of planktic *G. bulloides* on the Shirshov Ridge (Ovsepyan et al. 2010 and this volume), from the high $CaCO_3$ content on the Bowers Ridge (Gorbarenko et al. 2005), and from benthic assemblages in the Sea of Okhotsk (Bubenshchikova et al. 2010).

On the Shirshov Ridge, western Bering Sea, the strong decline in $CaCO_3$ content and pronounced increase in abundance of siliceous microfossils occur at the end of termination I (Ovsepyan et al. 2010 and this volume, Cherepanova et al. this volume), i.e. later than in the subarctic northwest Pacific. Planktic and benthic foraminifers are very scarce in the late Holocene sediments as a result of the switch from calcareous to siliceous microfossils accumulation. On the contrary, the diatoms pointing to ice free and high productivity conditions, as well as radiolarians, are very abundant during MIS 1 across the region (e.g. Caisie et al. 2010, Cherepanova et al. this volume).

Described succession of paleoceanographic changes from the last glacial termination into the Holocene largely results from the sea level rise and retreat of the sea ice coverage followed by the corresponding changes in the surface circulation, water exchange between the seas and Pacific through the straits, stratification and availability of nutrients in the euphotic zone.

This work was supported by grants OSL-10-14, OSL-11-11 and the Program 'Basic problems in Oceanology' by the Russian Academy of Sciences and by the KALMAR project BMBF grant 03G0201A.

References

Bubenshchikova NV, Nürnberg D, Gorbarenko SA, Lembke-Jene L (2010) Variations of the oxygen minimum zone of the Okhotsk Sea during the last 50 ka as indicated by benthic foraminiferal and biogeochemical data. Oceanology, 50 (1): 93-106 (in Russian)

Caissie BE, Brigham-Grette J, Lawrence KT, Herbert TD, Cook MS (2010) Last Glacial Maximum to Holocene sea surface conditions at Umnak Plateau, Bering Sea, as inferred from diatom, alkenone, and stable isotope records. Paleoceanography, 25, PA1206, doi:10.1029/2008PA001671

Cherepanova MV, Gorbarenko SA, Malakhov MI , Nürnberg D (this volume) Diatom stratigraphy and paleogeography of the Western Bering Sea over the past 170 ka

Crusius J, Pedersen T, Kienast S, Keigwin L, Labeyrie L (2004) Influence of northwest Pacific productivity on North Pacific Intermediate Water oxygen concentrations during the Bølling-Allerød interval (14.7-12.9 ka). Geology, 32 (7): 633-636

Dullo WC, Baranov B, van den Bogaard C (Eds.) (2009) FS Sonne Fahrtbericht / Cruise Report SO201-2 KALMAR: Kurile-Kamchatka and ALeutian MARginal Sea-Island Arc Systems: Geodynamic and Climate Interaction in Space and Time, Busan/Korea - Tomakomai/Japan, 30.08. - 08.10.2009 [Fahrtbericht]. In: IFM-GEOMAR Report, 35. IFM-GEOMAR, Kiel

Gebhardt H, Sarnthein M, Grootes PM, Kiefer T, Kühn H, Schmieder F, Röhl U (2008) Paleonutrient and productivity records from the subarctic North Pacific for Pleistocene glacial terminations I to V. Paleoceanography, 23, PA4212, doi:10.1029/2007PA001513

Gorbarenko SA, Basov IA, Chekhovskaya MP, Southon J, Khusid TA, Artemova AV (2005) Orbital and millennium scale environmental changes in the southern

Bering Sea during the last glacial-Holocene: Geochemical and paleontological evidence. Deep-Sea Research, II (52): 2174–2185

Gorbarenko SA, Wang P, Wang R, Cheng X (2010) Orbital and suborbital environmental changes in the southern Bering Sea during the last 50 kyr.. Palaeogeography, Palaeoclimatology, Palaeoecology 286: 97–106

Max L, Riethdorf JR, Nürnberg D. Tiedemann R (2010) Late Pleistocene to Holocene variations of sea surface conditions and intermediate water ventilation in the western Bering Sea Abstracts of the ICP 10, La Jolla, USA

Ovsepyan E, Ivanova E, Max L, Riethdorf JR, Tiedemann R, Nürnberg D (2010) Reconstruction of bottom water ventilation and export production based on benthic foraminiferal assemblages from the

Ovsepyan E, Ivanova E, Murdmaa I, Alekseeva T, Bosin A (this volume) Glacial – interglacial environmental changes on the Shirshov Ridge, Western Bering Sea: micropaleontological and sedimentary records from Core SO 201-2-85KL.

Riethdorf JR, Max L, Nürnberg D. Tiedemann R (2010). Sea surface temperature, marine productivity and terrigenous fluxes in the western Bering Sea during the last 150 kyr. Abstracts of the ICP 10, La Jolla, USA.

Takahashi K. (2005) The Bering Sea and paleoceanography. Deep Sea Research II (52): 2080-2091.

Diatoms in the Late Quaternary sediments of sediment core SO201-2-101-KL, Shirshov Ridge, the northwestern Bering Sea

Galina Kazarina[1], Maria Smirnova[1]

[1] IO RAS, P.P. Shirshov Institute of Oceanology RAS, Nakhimovsky prospekt 36, 117997 Moscow, Russia; email: manbka@mail.ru

Fossil diatoms have been studied in the sediment core SO201-2-101-KL, obtained from a depth of 607 m on the northern part of the Shirshov Ridge within the Russian-German project KALMAR. Laboratory processing of sediments and the implementation of diatom analysis were carried out according to the method adopted in the Shirshov Institute of Oceanology. Fixed amount of sediment was poured over by a small amount of natrium pyrophosphate and then boiled in the hydrogen peroxide, thus the sediment was disintegrated and exempt from possible organic impurities. Then it was washed out repeatedly in the distilled water. Measured volume of the obtaining suspension was placed under a coverslip, and fixed by Mountex. Micropaleontological slides have been studied under the transmitted light microscope Zeiss. We calculated at least 300 diatoms and made species identification.

Diatoms are present in significant numbers only in the upper 47 cm of the core. Diatoms almost absent lower in the profile, but occur in minor amounts in two short intervals (at 151-167 and 211-227 cm of core depth). Diatom flora mainly consists of boreal and arctic-boreal species dominated by *Thalassiosira gravida, Neodenticula seminae, Thalassionema nitzschioides*, and in less significant quantities of *Paralia sulcata*.

Based on the percentage of dominant species, the results of diatom analysis are interpreted as follows. There are two relatively warm and productive time intervals identified by increasing content of *Neodenticula seminae* within the upper 47 cm. Between them, we record a short episode with a relatively high content (17 %) of the shallow-water and coastal sublittoral species *Paralia sulcata* preceded by the complete absence of diatoms at 26-32 cm of core depth.

Based on the preliminary age model (Max et al. 2010 – pers. comm.), the uppermost peak in diatom abundances could correspond with the Preboreal warming, and lower peak with the Bølling/Allerød one. An occurrence of diatoms at core levels of 156-157, 166-167 and 211-217 cm might be due to changes in local depositional environments (reducing the supply of terrigenous material and associated enrichment of sediments by the biogenic silica) and/or with episodes of short-term improvement of conditions for the production of diatoms.

Living and dead benthic foraminifera in the Bering Sea

Sergei Korsun[1], Tatiana Khusid[1]

[1] IO RAS, P.P. Shirshov Institute of Oceanology RAS, Nakhimovsky prospekt 36, 117997 Moscow, Russia; email: s_korsun @ ocean.ru

Living benthic foraminifera from the Bering Sea are reported for the first time. We aim to trace the difference between the living and dead assemblages.

We examined living and dead foraminifera in six samples of surface sediments collected with a multicorer during SO201-2 Cruise in October 2009, including five samples (972 through 3920 m water depth) along the Shirshov Ridge in the Bering Sea and one sample (2640 mwd) in the NW Pacific south of the Komandor Islands. The samples (one slice 0-1 cm per station) were preserved with 2 g/l Rose Bengal stained 96% alcohol immediately upon retrieval. The lab processing included wet sieving on a 125-µm screen and drying. All the sampling locations are bathed by the Intermediate water gradually transiting below c. 3000 mwd into the North Pacific Deep Water and are characterized by temperatures decreasing from 3 to 1.5°C and salinities increasing from 34.3 to 34.7‰.

A total of 60 arenaceous and calcareous taxa were identified. The taxonomic diversity does not change much with water depth and ranges between 10 and 18 species per sample for both living and dead fauna.

At the two shallower stations, both living and dead assemblages were dominated by calcareous taxa with *Uvigerina peregrina* being most abundant. Planktonic foraminifera occurred here and were absent at greater water depths. The presence of planktonic foraminifera and the similarity between the living and dead faunas indicates that dissolution of calcareous foraminiferal shells is insignificant at depths <c.1300 m and that the dead assemblage inherits essentially the composition of the living assemblage.

At the two samples from intermediate water depths (c. 1300-2300 m), living foraminifera were as numerous as at the shallow stations (tens to a few hundreds individuals per 10 cm^3) and calcareous taxa accounted for 70-90% of the assemblage, whereas the dead assemblage consisted largely of arenaceous shells. Calcareous foraminifera still calcify successfully. The discrepancy between living and dead assemblages is due to rapid postmortem dissolution of the calcareous shells.

At the two deeper stations (c. 2300-4000 mwd), living foraminifera were scarce (15-20 specimens per 10 cm^3) and were dominated (~90%) by arenaceous taxa. Nearly all dead shells belonged to arenaceous foraminifera. The living foraminiferal assemblage is expectedly deprimated at these food-deficient depths; its calcareous constituent is even further depleted because the water is undersaturated severely with respect to $CaCO_3$. Consequently, the dead foraminiferal assemblage is composed of slowly but surely accumulating arenaceous shells.

Thus there is a remarkable dissimilarity between the living and dead assemblages at intermediate depths (c. 1300-2300 m). The degree of calcite undersaturation here is moderate and does not prevent foraminiferal biomineralization. However, after death and the decay of the cytoplasm, the empty shell gets exposed to the corrosive water and the calcite dissolves rapidly.

Active fault study in the Kamchatsky Peninsula, Kamchatka-Aleutian junction: in search for collision

Andrey Kozhurin[1], Tatiana Pinegina[2]

[1] Geological Institute, RAS, Pyzhevsky per. 7, 119017 Moscow, Russia; email: kozhurin@ginras.ru
[2] IVS FEB RAS, Institute of Volcanology and Seismology FEB RAS, Piip Boulevard 9, 683006 Petropavlovsk-Kamchatsky, Russia; email: tsunami@kscnet.ru

The idea of collisional interaction between the Kamchatka and the Aleutian island arcs rests on current plate boundaries configuration and vectors of plate relative movements. The western Aleutians are thought to be driven northwest by transcurrent movement of the subducting Pacific plate and to collide with Kamchatka in the area of the Kamchatsky Peninsula. The portion of the Aleutians affected by frictional force is limited in the NW by the Kamchatsky Straight, south of which the transform fault (edge of the Pacific Plate) plunges beneath Kamchatka. The Kamchatsky Peninsula, in this setting, can experience just a push of the Komandorsky Islands block.

Geist and Scholl (1994) placed the collisional contact between the Komandorsky segment of the Aleutians and Kamchatka immediately east of the Kamchatsky Peninsula, at the foot of the underwater. First Gaedicke et al. (2000), then Freitag et al. (2001) and recently Baranov et al. (2010) interpreted some of active faults of the SW of the Peninsula to be onshore extensions of the western Aleutians longitudinal faults. Basically, this means 1) placing the collisional contact further west, within the SE of the Kamchatsky Peninsula, 2) combining the part of the Peninsula embraced by these active faults into one rigid block with the Komandorsky Islands block, and 3) denying any independent movements of the peninsula block. Kozhurin (2007), instead, left the contact in the bottom in the west of the Kamchatsky Straight, and based on a simple model of several longitudinal blocks of western Aleutians moving northwest with rates decreasing south let the peninsula block move freely, probably rotating clock-wise.

Among the active faults of the Peninsula, there are two major faults: major, in a sense, that they cut off the Kamchatsky Peninsula from the Kamchatka mainland thus making the Peninsula to be a real separate block. Both were shown earlier as inferred faults by Kozhurin (2007), and were later, in 2008-2010, studied (Fig. 1).

One of the faults stretches N-S along the foot of the Kumroch Range steeper east-facing slope (north of approximately 56.45°N). Plan-view sinuous geometry, trenching and GPR data brought together, clearly demonstrate thrust movements on the shallow west-dipping fault plane. The strike-slip component in this motion, most likely small, seems probable, but still no evidences for it have been found. The fault seems terminating at ~56.45°N, replaced there probably by the fault # 3 with opposite (NW) vergence. The second of the two major faults starts close to the northern termination of the thrust fault and striking WNW reaches the Bering Sea shoreline and then most likely extends eastward into the Pokaty Canyon. The dominating component of movements along this fault is right-lateral (5-6 m of one-event dextral offsets were observed in the field). Paleoseismic study of the fault revealed that lateral movements occur in a highly transpressional environment.

The two faults form a structural combination, which strongly suggests active northwestward motion of the Peninsula block and its thrusting under the Kumroch Range. Yet the exact direction of the advance of the Kamchatsky Peninsula block cannot be determined unless the ratio between the strike-slip and thrust or reverse components is known.

There are at least three faults inside the peninsula block that most likely continue underwater, some distance down the continental slope, probably down to its base. These are faults ## 4, 5 and 6 in the SE of the Peninsula. Presently, the only way to decide whether these faults are direct extensions of the western Aleutians longitudinal faults is to compare kinematics of the offshore and

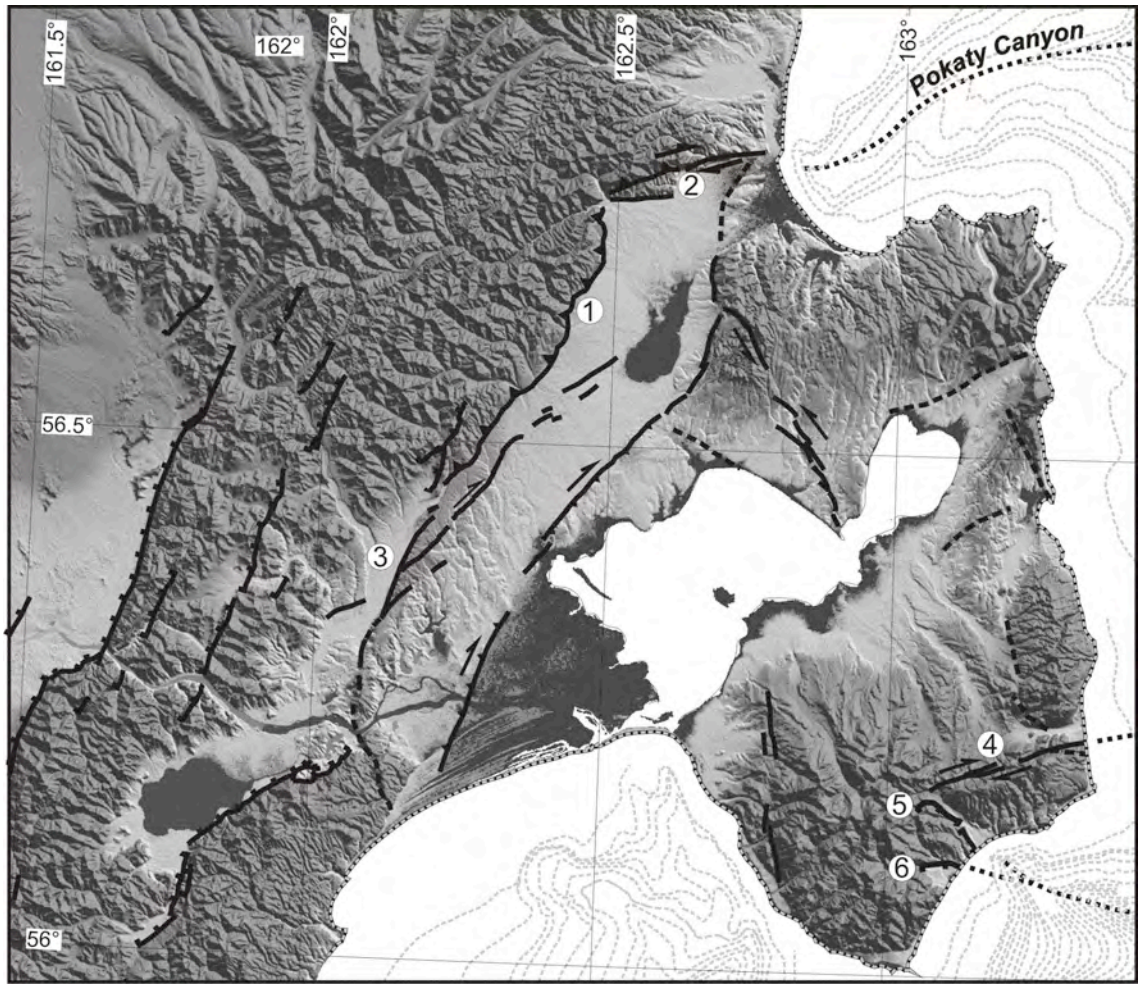

Fig. 1: Active faults in the Kamchatsky Peninsula, Kamchatka. Solid lines are for proved faults, dashed lines are for inferred faults. Arrows, ticks and teeth indicate strike-slip, normal and reverse/thrust components of movements. Dotted lines indicate probable position of underwater extensions of onshore faults. Numbers in circles are faults described in text.

onshore faults.

The fault # 4 is a purely strike-slip (right-lateral) fault. The vertical (reverse?) component of movements is negligibly small. The fault strike is notably oblique to the Bering Fault Zone of the Western Aleutians, and the absence of significant reverse or thrust component seems to contradict the model of direct onshore extension of the Bering Fault zone. Two other faults (5 and 6) of the NW strike display mostly normal motions and no signs of significant strike-slip offsets, neither left-lateral nor right-lateral, and thus cannot be linked easily to the underwater Pikezh Fault zone, which must be dominantly right-lateral. Thus it seems that the available data on the peninsula active faults kinematics do not much favor therefore the model, in which direct structural links between the Kamchatsky Peninsula block and the Komandorsky Islands block exist.

Based on the above, we conclude that active faulting in the Kamchatky Peninsula may be interpreted as reflecting collision of the western Aleutians with Kamchatka, but collision soft, when one of the colliding counterparts is not a single block but a set of several still able to move to some degree independently from each other.

References

Baranov B, Gaedicke C, Freitag R, Dozorova K (2010) Active faults of south-eastern Kamchatsky Peninsula and Komandorsky shear zone. Bulletin of Kamchatka regional association "Educational-scientific center". Earth Sciences 16: 66-77

Freitag R, Gaedicke C, Baranov B, Tsukanov N (2001) Collisional processes at the junction of the Aleutian-Kamchatka arcs: new evidence from fission track analysis and field observations. Terra Nova 13: 433-442

Gaedicke C, Baranov B, Seliverstov N, Alexeiev D, Tsukanov N, Freitag R (2000) Structure of an active arc-continent collision area: the Aleutian–Kamchatka junction. Tectonophysics 325: 63–85

Geist EL, Scholl DW (1994) Large-scale deformation related to the collision of the Aleutian Arc with Kamchatka. Tectonics 13: 538-560

Kozhurin AI (2007) Active Faulting in the Kamchatsky Peninsula, Kamchatka-Aleutian Junction. In: Eichelberger J, Gordeev E, Izbekov P, Lees J (eds) Volcanism and Subduction: The Kamchatka Region. American Geophysical Union, Washington, DC: 263-282

Parental melts of Avachinskiy volcano (Kamchatka) inferred from data on melt inclusions

Stepan Krasheninnikov[1], Maxim Portnyagin[1, 2]

[1] GEOKHI RAS, V.I.Vernadsky Institute of Geochemistry and Analytical Chemistry RAS, Kosygin St. 19, 119991 Moscow, Russia; email: spkrasheninnikov@mail.ru
[2] IFM-GEOMAR, Leibniz Institute of Marine Sciences, Wischhofstrasse 1-3, 24148 Kiel, Germany

Several recent studies of melt inclusions in island-arc rocks revealed a strong bimodality of the melt compositions at the predominance of basic and silicic melts and the scarcity of intermediate melts with SiO_2=59-66 wt% (e.g. Naumov et al. 1997; Reubi, Blundy 2009). These observations were used to interpret the origin of island-arc andesites by magma mingling, crustal assimilation and crystal accumulation rather than by fractional crystallization of basaltic magmas.

In this work we addressed the question about the origin of andesitic magmas in island-arc setting by systematic study of melt inclusions in minerals from Avachinskiy volcano in Kamchatka.

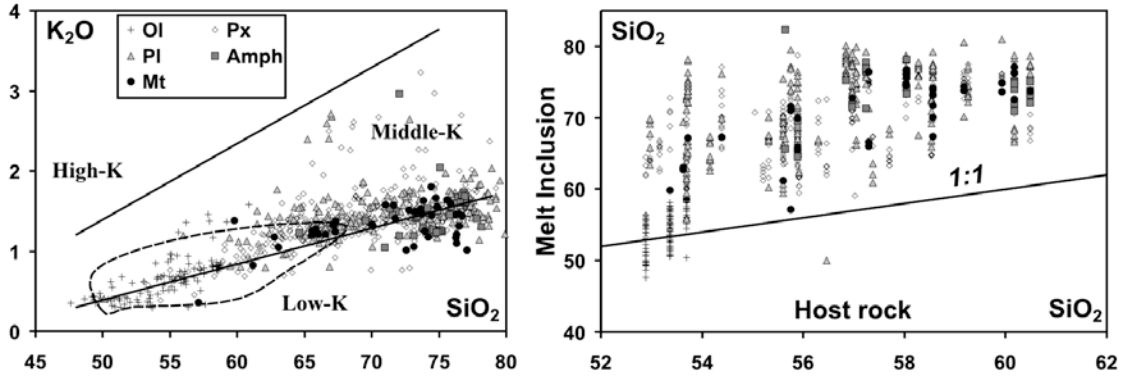

Fig. 1: Composition of melt inclusions in minerals and their host rocks. (a) Covariation of SiO_2 and K_2O in melt inclusions. The range of whole rock compositions (dashed curve) is after Bindeman et al. (2004). (b) Comparison of SiO_2 content in melt inclusions and host rocks

We studied melt inclusions in 6 different mineral phases from 61 tephra samples which represent 40 Holocene eruptions of this volcano including: 1) early phase of rare and voluminous andesitic eruptions (7.25-3.5 ky BP) and 2) later phase of frequent eruptions of basaltic andesites associated with the construction of the Young Cone (3.5 ky BP to present) (Braitseva 1998). We use the data to reconstruct the evolutional path of Avachinskiy melts prior eruptions and the changes in the magma feeding system beneath this volcano which occurred during the last ~7,000 years.

In the course of this study we analyzed ~500 melt inclusions in Ol (60 an.), Cpx and Opx (300 an.), Amph (60 an.), Pl (30 an.) and Mt (40 an.). All analyses were performed with the help of JEOL JXA 8200 wave-length dispersive electron microprobe at the IFM-GEOMAR (Kiel, Germany). The melt inclusions span a large range of compositions from basalts to rhyolites (Fig. 1). Both melt inclusion and host rock compositions plot predominantly along the line dividing low- and middle-K island-arc series. The trends of major elements are continuous, and no apparent bimodality is observed in the data set (Fig. 1a). Much of the major element variability can be explained by fractional crystallization from parental basaltic melts. The most primitive crystallizing assemblage is represented by Ol and Cr-Sp. Judging from decreasing CaO content in primitive melts, Cpx also joinded Ol at very early stages of crystallization. Plag appears on liquidus at ~53 wt% SiO_2, Mt and Ilm started to at ~57 wt%. Significant change of crystallizing assemblage occurred at ~60-62 wt% of SiO_2, when Opx replaced Ol, and Amph and Ap

become stable. Paragenesis of OPx, CPx, Amph, Pl, Mt, Ilm and Ap dominated the following evolution of melts toward strongly acid compositions with 78-80 wt% SiO_2.

Studied melt inclusions are rich in volatile components. Judging from low totals of microprobe analyses the amount of H_2O in parental basaltic melts was at least 2-3 wt% and increased up to 5-6 wt% in more silicic melts. SO_3 content was as high as 0.9 wt% in basaltic melts and decreased rapidly with increasing SiO_2. Cl concentrations in mafic melts were ~0.07 wt% and increased to ~0.20-0.25 wt% at SiO_2~70 wt% and then decreased in more evolved melts, probably, due to separation of Cl-rich hydrous fluid from evolved magmas.

In comparison with host rocks, melt inclusions tend to have more silicic compositions, and this difference tend to increase with increasing SiO_2 content in the host rocks (Fig. 1b). For example, olivine-hosted melt inclusions from rare basalts of Avachinskiy volcano have SiO_2 similar or slightly higher than host rocks. Melt inclusions in basaltic andesites (SiO_2=53-57 wt %) of the later stage of volcano formation (<3500 ky BP) range from andesitic to rhyolitic. Melt inclusions in andesites (SiO_2=57-63 wt %) of the earlier stage (3500-7250 ky BP) are mostly rhyolitic. Because the composition of melt inclusions is shifted to more silicic compared to their host rocks, nearly all Avachinskiy rocks should be affected by processes of crystal accumulation and do not correspond in composition to their parental melts.

Magma mixing of less and more evolved magmas also played an important role in the origin of Avachinskiy rocks and could plausibly occur during periodic replenishment of magma chamber with more primitive melts. Some studied silicic melt inclusions in CPX and Amph have relatively K-rich compositions and cannot be related to parental basaltic melts by simple crystallization process. These melts are considered to be exotic and can be formed by localized melting of hydrothermally altered wall rocks beneath volcano.

In summary, the new data on composition of melt inclusions allowed us to reconstruct the entire spectrum of parental melts for Avachinskiy volcano. Unlike other island-arc volcanoes, Avachinskiy melts do not display clear bimodality of SiO_2 content. Melts of intermediate compositions are relatively abundant and found in minerals from basaltic andesites. Melt inclusions in different minerals form coherent trends of major elements, which can be well explained by fractional crystallization. Our new data suggest that magma mixing and accumulation of minerals in evolved melts are important processes to generate island-arc andesites. The bimodality of island arc melts reported in previous several works can, however, originate from unrepresentative sampling.

This work was supported by the German-Russian KALMAR project (BMBF 03G0640A) and RFBR (#09-05-01234 and 10-05-00147).

References

Naumov BV, Kovalenko VI, Babansky AD, Tolstykh ML (1997) Genesis of andesites: evidence from studies of melt inclusions in minerals. Petrology, 5: 586-596

Reubi O, Blundy J (2009) A dearth of intermediate melts at subduction zone volcanoes and the petrogenesis of arc andesites. Nature, 461(7268): 1269-1273.

Braitseva OA, Bazanova LI, Melekestsev IV, Sulerzhitskiy LD (1998) Large Holocene eruptions of Avacha volcano, Kamchatka (7250-3700 ^{14}C years B.P.). Volcanology and Seismology 20(1): 1-27

Bindeman IN, Ponomareva VV, Bailey JC, Valley JW (2004) Volcanic arc of Kamchatka: a province with high- $d^{18}O$ magma sources and large-scale $^{18}O/^{16}O$ depletion of the upper crust. Geochim. Cosmochim. Acta 68: 841-865

Petrology and geochemistry of mantle rocks from the Stalemate Fracture Zone (NW Pacific)

Elisaveta Krasnova[1], Maxim Portnyagin[1,2], Sergei Silantiev[1], Reinhard Werner[2], Folkmar Hauf[2], Kaj Hoernle[2]

[1] GEOKHI RAS, V.I.Vernadsky Institute of Geochemistry and Analytical Chemistry RAS, Kosygin St. 19, 119991 Moscow, Russia; email: eakrasnova@gmail.com
[2] IFM-GEOMAR, Leibniz Institute of Marine Sciences, Wischhofstrasse 1-3, 24148 Kiel, Germany

The Stalemate Fracture Zone (FZ) is a 500 km long SE-NW trending transverse ridge between the northernmost Emperor Seamounts and the Aleutian Trench which originated by flexural uplift of Cretaceous oceanic lithosphere along a transform fault at the Kula-Pacific plate boundary (Lonsdale 1988). Sampling at the Stalemate FZ and the fossil Kula-Pacific Rift valley was carried out during the R/V SONNE cruise SO201 Leg 1b. A broad spectrum of rocks including serpentinites (DR37), gabbro (DR7,40), dolerites (DR7) and lavas (DR38,41) were obtained. These rocks are thought to represent a complete section of oceanic lithosphere formed at the fossil Kula-Pacific spreading center. Here we report first results on the composition and origin of serpentinites dredged from the Stalemate FZ at the station DR37 (Fig. 1a).

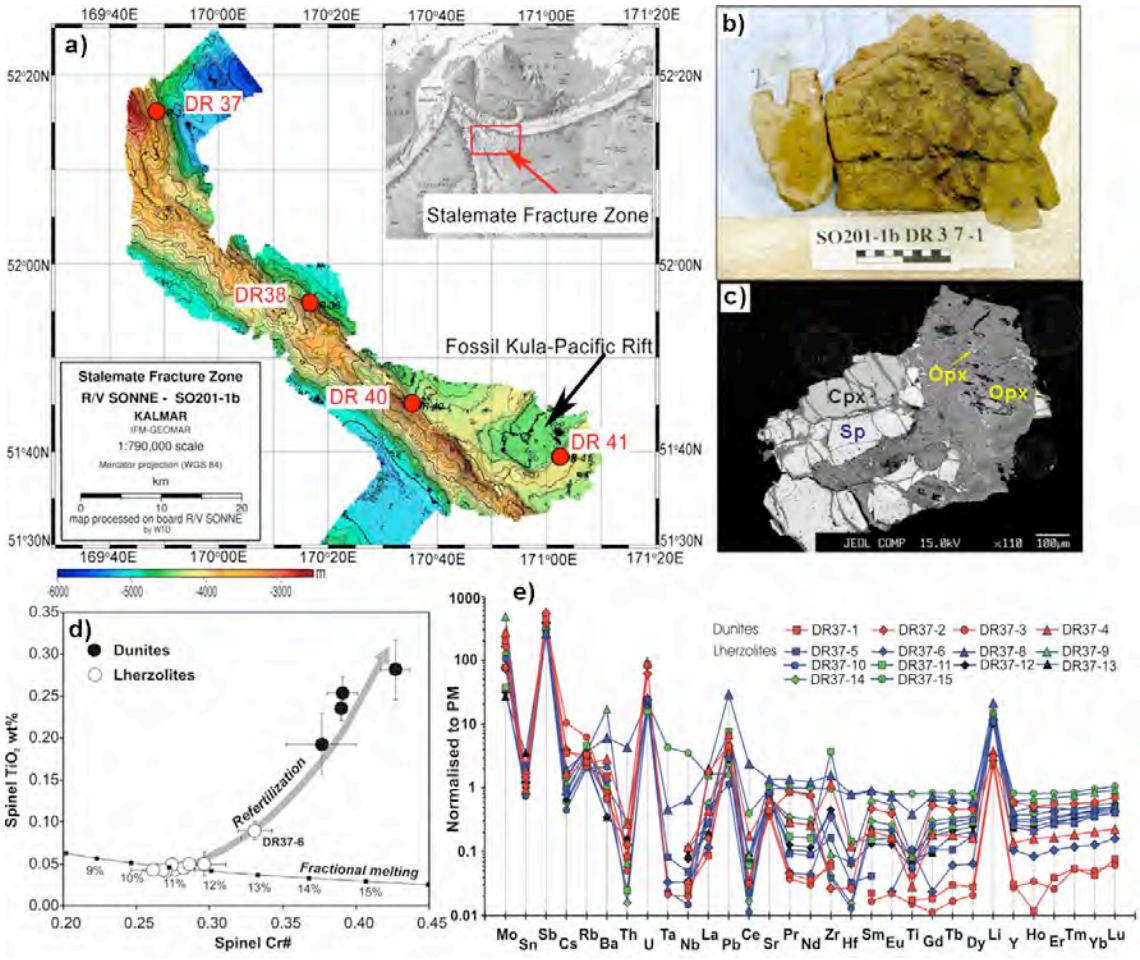

Fig. 1: Major results of study of the Stalemate F.Z. peridotites. (a) Overview map of the northern part of the Stalemate F.Z. and SO201-KALMAR Leg 1b dredge locations; (b) on-board photo of typical peridotite; (c) BSE photograph of relics of minerals in serpentinite studied by EMPA; (d) composition of spinel in lherzolites and dunites from the Stalemate F.Z.; (e) Primitive mantle-normalized trace element patterns of bulk-rock peridotites. The composition of primitive mantle is after McDonough & Sun (1995).

According to on-board description and petrographic investigations we distinguished two major groups of samples: (1) pyroxene-rich lherzolites and (2) pyroxene-poor dunites. All studied rocks were serpentinized to 80-100%. In order to reconstruct initial compositions of the studied peridotites, relics of primary minerals (spinel, clinopyroxene and orthopyroxene) were analyzed by electron probe JEOL 8200 at IFM-GEOMAR (Fig. 1b). We found that the compositions of the primary minerals change systematically from lherzolites to dunites. Spinel in lherzolites has higher Mg#, NiO, lower Cr#, Fe^{3+}# and TiO_2 (Mg#=0.65-0.68, NiO=0.26-0.34%, Cr#=0.26-0.33, Fe^{3+}#=0.021-0.030, TiO_2=0.04-0.09 wt%) than spinel in dunites (Mg#=0.56-0.64, Cr#=0.38-0.43, TiO_2=0.19-0.28 wt%, NiO=0.19-0.26%, Fe^{3+}#=0.027-0.043). Clinopyroxene in lherzolites is moderately Mg- and Ni-rich, Ti- and Na-poor and has lower Cr# (Mg#=91.7-92.4, Cr#=0.12-0.16, TiO_2=0.06-0.15 wt%, Na_2O=0.19-0.41 wt%, NiO=0.06-0.09 wt%) compared to clinopyroxenes analyzed in a sample of dunite DR37-3 (Mg#=93.7, Cr#=0.16, TiO_2=0.23 wt%, Na_2O=0.85 wt%, NiO=0.06 wt%). Orthopyroxene preserved in lherzolites has narrow compositional range (Mg#=90.3-90.9, Cr#=0.10-0.12, TiO_2=0.02-0.05 wt%, Na_2O=0.01-0.025 wt%, NiO=0.12-0.17 wt%). In general, the mineral compositions form continuous trends with end-members represented by lherzolite DR37-13, on the one side, and dunite DR37-3, on the other side. Minerals from lherzolite DR37-6 have transitional compositions between those in predominant lherzolites and dunites (Fig. 1c).

The continuous array of mineral compositions suggests close genetic relationships between the lherzolites and dunites. Compositions of minerals in lherzolites are similar to those from the Mid-Atlantic Ridge (e.g. Dick et al. 1984) and suggestive that the lherzolites are mantle residues after melt extraction at mid-ocean rift, possibly, at the Kula-Pacific Rift. As illustrated in Fig. 1c, the spinel composition in lherzolites corresponds to 10-12% of fractional melting. Compositions of spinel and pyroxene from dunites deviate strongly from the expected trend of partial mantle melting and require alternative explanation.

A possible model to explain the occurrence of dunites in close association with residual lherzolites in the Stalemate FZ could be reactive interaction of shallow residual mantle with deeper Ti- and Cr-rich melts. This process should lead to dissolution of pyroxenes in lherzolites and is thought to form an interconnected network of dunite channels serving as pathways for melts to the surface (Kelemen et al. 1995). The separate pieces of lherzolites and dunites dredged from the Stalemate FZ can thus represent disintegrated parts of shallow oceanic mantle strongly modified by melt percolation and serpentinized by rock -seawater interaction at shallow depth. The later process overprinted nearly completely primary bulk composition of the studied rocks. It caused strong enrichment of the rocks in fluid mobile elements (U, Li, Sb, Ba) and U-shaped patterns of REE with strong negative Ce anomaly reflecting precipitation of REE from the seawater and very large water-rock ratios during alteration.

References

Dick HJB, Fisher RL, Bryan WB (1984) Mineralogic variability of the uppermost mantle along mid-ocean ridges. Earth and Planetary Science Letters 69: 88-106

McDonough WF, Sun SS (1995) The composition of the Earth. Chemical Geology 120: 223-253

Kelemen PB, Shimizu N, Salters VJM (1995) Extraction of mid-ocean-ridge basalt from the upwelling mantle by focused flow of melt in dunite channels. Nature 375: 747-753

Lonsdale P (1988) Paleogene history of the Kula plate: Offshore evidence and onshore implications. Geological Society of America Bulletin 100: 733-754

Climate effects of large explosive volcanism: tropical versus high latitude eruptions

Kirstin Krüger[1], Matthew Toohey[1], Davide Zachettin[2], Claudia Timmreck[2]

[1] IFM-GEOMAR, Leibniz Institute of Marine Sciences, Wischhofstrasse 1-3, 24148 Kiel, Germany; email: kkrueger @ ifm-geomar.de
[2] MPI-M, Hamburg, Germany

Large, explosive volcanic eruptions have a significant impact on the radiation balance of the atmosphere, leading to changes in atmospheric circulation patterns, chemical composition, and the Earth's surface climate. These impacts result from the volcanic injection of sulfur-containing gases into the stratosphere, converted to sulfate aerosols, which reflect solar radiation and absorb infrared radiation. Due to the large scale meridional overturning circulation in the stratosphere, volcanic aerosols from eruptions in the tropics can be spread globally, while aerosols from midlatitude eruptions are usually contained within one hemisphere.

This presentation will give an overview on climate effects of large Plinian eruptions, directly injecting volcanic material into the stratosphere. We will compare the global and regional impact of eruptions in the tropics with those from high latitudes depending on the seasons of the eruption. Finally we will show first model results from a Kamchatka eruption.

Compositional variations of volcanic glasses from Kamchatka

Olga Kuvikas[1], Maxim Portnyagin[2,3], Vera Ponomareva[1]

[1] IVS FEB RAS, Institute of Volcanology and Seismology FEB RAS, Piip Boulevard 9, Petropavlovsk-Kamchatsky, 683006, Russia; email: kuvikas@mail.ru
[2] IFM-GEOMAR, Leibniz Institute of Marine Sciences, Wischhofstrasse 1-3, 24148, Kiel, Germany
[3] GEOKHI RAS, Vernadsky Institute of Geochemistry and Analytical Chemistry, Kosygin Str. 19, 119991 Moscow, Russia

Volcanism in Kamchatka is highly explosive so most of the magma comes to surface as tephra. In order to characterize silicic magmas erupted over entire Kamchatka during the Holocene we attempted to assess multi-component systematics of volcanic glass from major Holocene Kamchatka tephras. These results are used for 1) fingerprinting of tephra from different sources; 2) comparison of silicic magmas across and along the volcanic arc, and 3) understanding the processes governing generation of silicic melts in Kamchatka. Within the framework of the German-Russian project KALMAR, we have analyzed 94 samples of volcanic glass from major Holocene Kamchatka tephras. The analyses were obtained in the IFM-GEOMAR (Kiel, Germany) at the JEOL JXA 8200 microprobe using a single analytical protocol (15 keV accelerating voltage, 6 nA current, and 5 micron beam size). In the result we have obtained a new self-consistent database of ~2500 high-quality analyses of silicic glass of known source and age.

Composition of the glass depends on a magmatic source and conditions of magma crystallization. There is large compositional variability of volcanic glasses from different volcanic zones and volcanic centers in Kamchatka (Fig. 1). Some spatial geochemical trends are, however, evident from our database. For example, mean glass compositions from different volcanoes demonstrate increase in K_2O contents, and decrease in FeO, MgO, CaO contents and Cl/K ratio from the volcanic front toward the rear-arc, i.e. with increasing depth to the subducting plate.

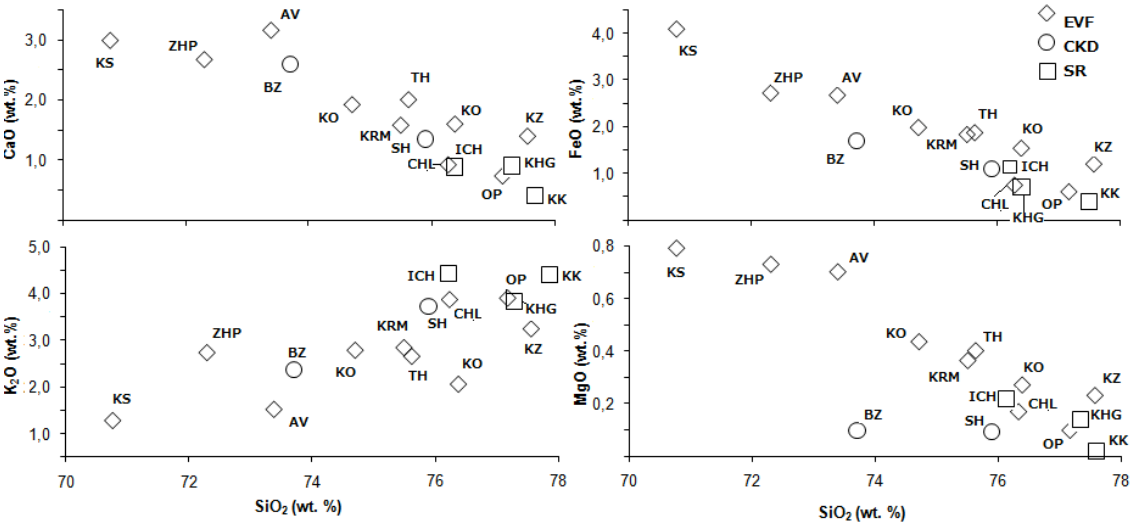

Fig. 1: Variations of major elements in volcanic glass. Average values for each volcanic center are use. Signs are labeled as follows: "SR" – Sredinny Range, "EVF" – Eastern Volcanic Front, "CKD" – Central Kamchatka Depression. Abbreviations of volcanoes: KO – Kurile Lake Caldera, AV – Avachinsky, KS – Ksudach, KRM – Karymskaya Caldera, ICH – Ichinsky, KHG – Khangar, KZ – Kizimen, OP – Opala, BZ – Bezymianny, SH – Shiveluch, TN-Taunshits, ZHP – Zhupanovsky, KS – Kosheleva, CHL – Chasha Lake, KK - Kekunaisky.

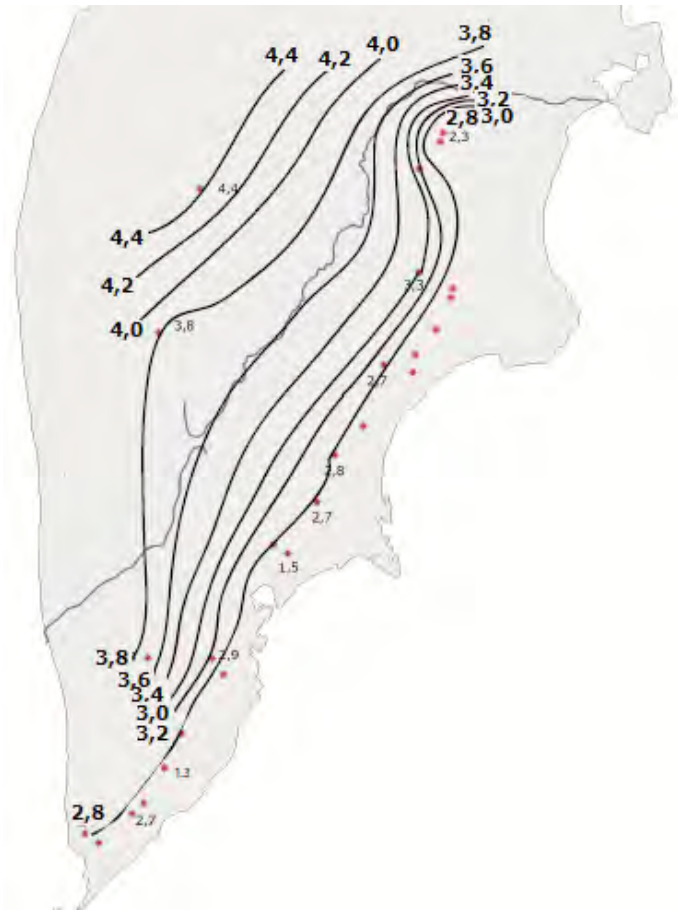

Fig. 2: Spatial variations of K_2O in silicic glasses from Kamchatkan tephras. Average values for each volcanic center and the most plausible contours of constant K_2O are shown.

In order to better analyze the spatial pattern of the geochemical variations, we have applied statistical 2D analysis to the existing database of volcanic glasses (Nakagawa 1992, Volynets 1994). Some preliminary results are shown in Fig. 2, where systematic increase in K_2O from frontal to rear-arc volcanoes is well seen. According to this data, silicic tephras originating from the Kliuchevskoy volcanic group have anomalously low content of K_2O compared to other Kamchatkan volcanoes located at similarly far distance from the trench. This may indicate specific conditions of magma generation beneath the Kliuchevskoy volcanic group such as unusually high degrees of melting and enhanced fluid flux from the subducting plate (Portnyagin et al. 2007).

References

Nakagawa M (1992) Spatial. Variation in chemical composition of Pliocene and Quaternary volcanic rocks in Southwestern Hokkaido, Northeastern Japan Arc. Jour. Fac. Sci., Hokkaido Univ. 23: 2

Portnyagin M, Hoernle K., Plechov P, Mironov N, Khubunaya S (2007) Constraints on mantle melting and composition and nature of slab components in volcanic arcs from volatiles (H_2O, S, Cl, F) and trace elements in melt inclusions from the Kamchatka Arc. Earth Planet. Sci. Lett. 255(1-2): 53-69

Volynets O (1994) Geochemical types, petrology and genesis of Late Cenozoic volcanic rocks from the Kurile-Kamchatka island arc system. Int. Geol. Reviews 36/4: 373-405

First results of component, grain-size and XRF analyses for sediment core SO201-2-101-KL (Shirshov Ridge)

Mikhail Levitan[1], Tatyana Kuzmina[1], Irma Roshchina[1], Kirill Syromyatnikov[1], Ralf Tiedemann[2], Dirk Nürnberg[3], Lars Max[2]

[1] GEOKHI RAS, V.I. Vernadsky Institute of Geochemistry and Analytical Chemistry RAS, Kosygina str. 19, 119991 Moscow, Russia; email: m-levitan@mail.ru
[2] AWI, Alfred Wegener Institute for Polar and Marine Research, Am Handelshafen 12, 27568, Bremerhaven, Germany
[3] IFM-GEOMAR, Leibniz Institute of Marine Sciences, Wischhofstrasse 1-3, 24148 Kiel, Germany

Quaternary sedimentation history of the Shirshov Ridge (the Bering Sea) is still poor known. Assemblages of heavy minerals in sediment core DM 2594 have been changed significantly near the boundary MIS 1/ MIS 2 (Levitan, Lavrushin 2009): large continental blocks adjacent to the Bering Sea have been changed by Aleutian Islands as the main sources of terrestrial matter. Opening of the Bering Strait near this boundary played a principally important role in a radical transformation of circulation pattern in the Bering Sea. We would like to emphasize the significance of Yukon River in this scenario because after the opening of the Bering Strait its discharge turned through the strait in the Chukchi Sea (relatively to supply in the Bering Sea before).

Sediment core SO201-02-101-KL retrieved from the board of RV "SONNE" in 2009 is the longest sediment core (ca. 18 m) from Shirshov Ridge up to date. Sediment description and measurements of physical properties during the cruise have been performed by R. Tiedemann and D. Nürnberg (e.g. Dullo et al. 2009). In coastal laboratories of GEOKHI RAS we have studied in same samples the component composition (M. Levitan, K. Syromyatnikov), grain-size composition (M. Levitan, L. Zadorina), inorganic geochemistry (by XRF analysis, I. Roshchina). Samples are spaced mainly in 20 cm. Total number of samples is 90. 2 mm, 0.063 mm, 0.002 mm are the boundaries between gravel, sand, silt and clay fractions, respectively. XRF analysis were performed using XRF spectrometer Axios Advanced by PANalytical Company (the Netherland) without of washing out of sea salts. Methods of mathematical statistics have been applied to XRF data by T. Kuzmina. L. Max proposed an age model.

Combination of lithological description, grain-size and component analyses revealed three types of lithologies: main, minor and rare. Main lithology is presented by silts and clayey silts, minor lithology – by silts with sand admixture (amount of sand fraction is 10-20 %), and rare – by mictite and sandy-clayey silt (amount of sand fraction is 20-60 %). Minor lithology is recorded in intervals: 234-354, 454-455, 854-855 cm. The only interval with rare lithology is 1594-1675 cm. In general component composition of the studied sediments is very uniform: light and clay minerals dominate (27-30 % each), color minerals and fragments of rock compose 11-18 % each; black ore minerals, volcanic glasses, remains of siliceous organisms (mainly, diatoms and sponges spicules) and carbonate organisms (mainly, foraminifers and nanofossils) can be considered as accessories. In rare lithology one can observe the increasing of quartz content, rock fragments and spicules. Interestingly, that volcanic glass of brown color dominates beneath the level 920 cm, and green volcanic glass – above. We consider the sand fraction as result of sea ice (sometimes icebergs?) melting. It seems that sand maxima fit with glaciation events practically in all cases.

Chemical composition of sediments demonstrates very uniform pattern which are disrupted only within "sandy" interval (1594-1675 cm). Only here chemical composition recalculated for SiO_2-free basis shows the result different from other sediment sections. Comparison of average chemical composition of Shirshov Ridge sediments with data from (Ronov et al. 1990) showed that it is very close to chemical composition of clays and shales from Paleozoic fold belts. So, we propose that some Paleozoic complexes from the central Alaska supplied

their matter to Yukon River and its tributors and served as main source province for studied Quaternary sediments of the Shirshov Ridge. But the source for "sandy" interval is still under discussion.

Correlation matrix with Pearson coefficients allowed to reveal a number of geochemical associations: 1) SiO_2, Sr, Zr, Ni which are linked with the mineral part of the sand fraction; 2) Al_2O_3, Ti, Fe, Mn, K, Mg, P, V, Co, Cu, Zn, Rb, Y, Nb, Ba, Pb, LOI which are in connection with fine clastics in the silt and, partly, clay fractions, organic matter, oxy-hydroxides of Fe and Mn; 3) CaO, Sr from biogenic carbonates; 4) S, As, LOI (partly, Al) – organic matter with clay and pyrite.

Q-mode of factor analysis with Varimax rotation gave three main factors. Their distribution along the core showed that first factor fits well with distribution of silt fraction, the second one – with distribution of clay fraction, and the third one – with sand fraction.

Such way, it looks very probable that sedimentation history of the Shirshov Ridge for the last 145 kyr. was ruled mainly by the history of Yukon River discharge within Beringia Land with some admixture from activity of sea ice in the Bering Sea proper.

References

Dullo WC, Baranov B, van den Bogaard C (Eds.) (2009) FS Sonne Fahrtbericht / Cruise Report SO201-2 KALMAR: Kurile-Kamchatka and ALeutian MARginal Sea-Island Arc Systems: Geodynamic and Climate Interaction in Space and Time, Busan/Korea - Tomakomai/Japan, 30.08. - 08.10.2009 [Fahrtbericht]. In: IFM-GEOMAR Report, 35. IFM-GEOMAR, Kiel

Levitan MA, Lavrushin YA (2009) Sedimentation history in the Arctic Ocean and Subarctic Seas for the last 130 kyr. Berlin, Springer: 387

Ronov AB, Yaroshevsky AA, Migdisov AA (1990) Chemical composition of the Earth crust and geochemical balance of the main elements. Moscow, Science: 182

Climate change, sea ice and productivity responses in magnetic parameters of sediments from Western Bering Sea and NW Pacific

Mikhail Malakhov[1], Sergey Gorbarenko[2], Dirk Nürnberg[3], Ralf Tiedemann[4], Galina Malakhova[1], Jan-Rainer Riethdorf [3], Aleksandr Bosin[2], Marina Cherepanova[5]

[1] NEISRI, Northeastern Integrated Scientific-Research Institute Far East Branch RAS, Portovaya 16, 685000 Magadan, Russia; email: malakhov@neisri.ru
[2] POI FEB RAS V.I. Il'ichev Pacific Oceanological Institute Far East Branch RAS, Baltiyskaya 43, 690041 Valadivostok, Russia
[3] IFM-GEOMAR, Leibniz Institute for Marine Sciences, Wischhofstrasse 1-3, D-24148 Kiel, Germany
[4] AWI, Alfred Wegener Institute for Polar and Marine Research, Am Handelshafen 12, 27570 Bremerhaven, Germany
[5] PIG, Pacific Institute of Geography Far East Branch RAS, Radio 7, 690041 Vladivostok, Russia

The set of the main rock-magnetic parameters in sediments from cores SO201-2-85, -81, -77, -40 -12 recovered in the Bering Sea during R/V Sonne cruise SO 201-2 was measured every 2 cm. All parameters were combined in: a) petromagnetic group -magnetic susceptibility (K), anhysteretic remanent magnetization (J_{ri}); saturation isothermal remanent magnetization (J_{rs}); magnetization (J_p) of paramagnetic component in the field of 0.5 T; saturation magnetization (J_s) without the paramagnetic component; b) coercive group -coercive force (B_c) of saturation magnetization without the paramagnetic component; coercive force (B_{cr}) of remanent saturation magnetization; and position of the maxima (B_{da} and B_{db}) on the coercive spectrum (isothermal magnetization along the *a* and *b* axes, respectively, of the Preisach–Neel diagram (Dunlop, Ozdemir 1997) and c) lithophysical group - J_p, color, K and biogenic components- diatom abundance and chlorine content. On the base of detailed magnetic studying of the Okhotsk Sea sediment it was established that parameters of these groups changed along core depth vary in concert with climate changes in the past (Malakhov et al. 2009). For example, during warm MIS content of the coarse magnetic grains in the basin sediment decrease due to decrease of IRD and production of the magnetotactic bacteria increase. It allows us to correlate broad oscillations of these groups with global climate changes recorded in ^{18}O LR04 stack of Lisiecki and Raymo (2005) and marine isotope stages MIS boundaries. Correlation of variability of the petromagnetic parameters of core SO201-2-85 sediments with MIS boundaries was demonstrated in Fig. 1 as example.

This work was supported by Russian-German project KALMAR (BMBF grant 03G0201A), grant 10-05-00160a from the Russian Foundation for Basic Research, grant 09-II-CO-07-003 from the Far Eastern Branch of the RAS, and Basic Research Program 7 from the Geoscience Department of the RAS.

References

Dunlop DJ, Ozdemir O (1997) Rock Magnetism: Fundamentals and Frontiers. Cambridge Univ.Press, New York, 573

Malakhov MI, Gorbarenko SA, Malakhova GY, Harada N, Vasilenko YP, Bosin AA, Goldberg EL, Derkachev AN (2009) Petromagnetic Parameters of Bottom Sediments as Indicators of the Climatic and Environmental Changes in the Central Zone of the Sea of Okhotsk During the Last 350 kyr.. Russian Geology and Geophysics 50: 973

Lisiecki LE, Raymo ME (2005) A Pliocene-Pleistocene Stack of 57 Globally Distributed Benthic ^{18}O Records. Paleoceanography 20: PA 1003

Geomagnetic reletive paleointensity of sediment cores of the Western Bering Sea and NW Pacific

Mikhail Malakhov[1], Sergey Gorbarenko[2], Dirk Nürnberg[3], Ralf Tiedemann[4], Galina Malakhova[1], Jan-Rainer Riethdorf[3]

[1] NEISRI, Northeastern Integrated Scientific-Research Institute Far East Branch RAS, Portovaya 16, 685000 Magadan, Russia; email: malakhov@neisri.ru
[2] POI, V.I. Il'ichev Pacific Oceanological Institute Far East Branch RAS, Baltiiskaya 43, 690041,Vladivostok, Russia
[3] IFM-GEOMAR, Leibniz Institute for Marine Sciences, Wischhofstrasse 1-3, D-24148 Kiel, Germany
[4] AWI, Alfred Wegener Institute for Polar and Marine Research, Am Handelshafen 12, 27570 Bremerhaven, Germany

The set of the main paleomagnetic parameters in sediments from cores SO201-2-85, -81, -77, -40 -12 recovered in the Bering Sea and far NW Pacific during R/V Sonne cruise SO 201-2 was measured through every 2 cm.

In order to evaluate Relative Paleointensity (RPI) of geomagnetic field in the studied cores, the characteristic remanent magnetization (ChRM) of sediments was measured. To exclude the dependence of the geomagnetic signal on climatic factors, the ChRM values were normalized by anhysteretic remanent magnetization (ARM).

The curves SINT-800 (Guyodo, Valet 1999), PISO-1500 (Channell et al. 2009) and the record RPI for the last ~ 400 ka (Thouveny et al. 2004) were used as dated reference curves of geomagnetic field paleointensity. The correlation of the RPI in sediments of core SO 201-2-85KL with above mentioned dated reference curves of paleogeomagnetic field are shown in Fig. 1 as example.

According to RPI record of core SO 201-2-81KL, the sediments of this core were accumulated during last 400 kyr. The additional investigation of the characteristic magnetization formation in tephra layers it is need to study RPI in sediments of core SO 201-2-40KL influenced by strong volcanic activity.

The ages of key time points of studied core determined by correlation of RPI with dated reference curves of geomagnetic field are consistent with location of MIS boundaries defined by correlation of the petromagnetic, coercive and lithophysical groups with standard oxygen isotopic record.

This work was supported by German - Russian project KALMAR, grant 10-05-00160a from the Russian Foundation for Basic Research, grant 09-II-CO-07-003 from the Far Eastern Branch of the RAS, and Basic Research Program 7 from the Geoscience Department of the *RAS.*

References

Channell JET, Xuan C, Hodell DA (2009) Stacking Paleointensity and Oxygen Isotope Data for the Last 1.5 Myr (PISO-1500). Earth and Planetary Science Letters 283: 14

Guyodo Y, Valet J-P (1999) Global Changes in Intensity of the Earth's Magnetic Field During the Past 800 Kyr. Nature 399: 249

Thouveny N, Carcaillet J, Moreno E, Leduc G, Nerini D (2004) Geomagnetic Moment Variation and Paleomagnetic Excursions Since 400 Kyr. BP: A Stacked Record from Sedimentary Sequences of the Portuguese Margin. Earth and Planetary Science Letters 219: 377

Late Quaternary micropaleontology and paleoceanography in the southeastern Beringia: new results from the KALMAR project

Alexander Matul[1], Khadyzhat Saidova[1], Tatyana Khusid[1], Maria Chekhovskaya[1], Natalia Oskina[1], Maria Smirnova[1], Sergei Korsun[1]

[1] IO RAS, P.P. Shirshov Institute of Oceanology RAS, Nakhimovsky prospekt 36, 117997 Moscow, Russia; email: amatul @ ocean.ru

The micropaleontological studies of the sediment cores, obtained within the Russian-German project KALMAR, provide new detailed information about the paleoenvironmental changes in the southeastern Beringia during the transition from the last glacial maximum to the Holocene. We intend to analyze the Late Quaternary paleoceanography on the northern Shirshov Ridge – sediment core SO201-2-101-KL, on the Kamchatka slope at the Kronotzky Peninsula – SO201-2-12-KL, and on the Obruchev Rise in the Northwest Pacific – SO201-2-40-KL. Foraminiferal diatoms and radiolarian were analysed.

Sample processing and slide preparation was made according to the standard micropaleontological methods. Benthic and planktonic foraminifera: washing out through the sieve of 0.05 mm. Diatoms and radiolarians: boiling with the hydrogene peroxide and natrium pyrophosphate, for radiolarians – washing out through the sieve of 0.04 mm.

Sediment core SO201-2-40-KL from the Obruchev Rise gives subtle paleoinformation as foraminifera are not abundant or even absent in our samples. Most samples are composed of the volcanic material which dilutes the biogenic material in a very high degree.

Sediment core SO201-2-12-KL from the Kamchatka slope contains both benthic and planktonic foraminifera suitable for the quantitative study. Two large core intervals of ca. 250-350 and 450-650 cm exhibit very pronounced peaks in the total foraminiferal abundances. We may correlate them with the two warming steps within the Termination I. Such occurence of maxima in the biogenic calcite and foraminifera distribution in the Late Pleistocene sediments of the North Pacific and its marginal seas is typical for the Termination I, and suggested by many recent publications (e.g. Gorbarenko 1996, Cook et al. 2005, Khusid et al. 2006). Paleoenvironments during that time are also indicated by changes both in the species and high-rank foraminiferal taxa record.

Sediment core SO201-2-101-KL from the northern Shirshov Ridge in the western Bering Sea, compared to core SO201-2-12-KL, has lower sedimentation rates, thus provides lower resolution results. It also exhibits two foraminiferal abundance peaks at ca. 0-20 and 50-170 cm, which could be assigned to the Termination I. Unfortunately, this evidence is not supported by the micropaleontological counts of the biogenic silica as diatoms and radiolarians in our slides were found only in the uppermost core interval of 0-47 cm.

References

Cook MS, Keigwin LD, Sancetta CA (2005) The deglacial history of surface and intermediate water of the Bering Sea. Deep-Sea Research II 52: 2163–2173

Gorbarenko SA (1996) Stable Isotope and Lithologic Evidence of Late-Glacial and Holocene Oceanography of the Northwestern Pacific and its Marginal Seas. Quaternary Research 46: 230-250

Khusid TA, Basov IA, Gorbarenko SA, Chekhovskaya MP (2006) Benthic Foraminifers in Upper Quaternary Sediments of the Southern Bering Sea: Distribution and Paleoceanographic Interpretations. Stratigraphy and Geological Correlation 14(5): 538–548

Deep roots of Klyuchevskoy volcano, Kamchatka

Nikita Mironov[1], Maxim Portnyagin[2,1]

[1] GEOKHI RAS, V.I.Vernadsky Institute of Geochemistry and Analytical Chemistry RAS, Kosygin Str. 19, 119991 Moscow, Russia; e-mail: nmironov@geokhi.ru
[2] IFM-GEOMAR, Leibniz Institute of Marine Sciences, Wischhofstrasse 1-3, 24148 Kiel, Germany

Klyuchevskoy is a magnificent ~5 km-high stratovolcano famous for its frequent eruptions and vigorous (>60*10^6 t/year) magma output. This study was aimed at elucidating evolution of Klyuchevskoy magmas from their origin in the mantle wedge to eruption. We have studied >400 melt inclusions in olivines (Fo_{92-67}), which were separated from all Klyuchevskoy rock varieties. The age of the samples ranged from 6.9 cal ka to 1966 AD. The melt inclusions were analyzed for major, volatile and trace elements using electron and ion microprobes and infrared spectroscopy. To quantify conditions of magma origin, the data on melt inclusions were combined with those on composition of crystal and fluid inclusions in minerals and with the results of numerical modeling.

Primary magmas of Klyuchevskoy volcano have basaltic high-Mg and Ne-normative composition and originate in the upper mantle at pressure of 12 to 21 kbar (40-70 km depth) and temperature of 1300-1320 °C through 10-20 % fluid-fluxed melting of lithologically heterogeneous peridotite. On the way from the source region to the crust, the primary magmas interact with previously metasomatized lithospheric mantle, that causes enrichment of primitive magmas in many incompatible trace elements (K, Ba, Th, U, Sr, REE, Zr and Hf). The extent to which primary Klyuchevskoy melts assimilate metasomatized mantle varied through time and decreased during periods of high magma production rate in the deep mantle and likely faster magma passage to the crust. The primary magmas start to crystallize at 1250-1300 °C temperature, oxygen fugacity of ΔNNO~0 and 10-12 kbar pressure corresponding to the Moho depth beneath the Central Kamchatka Depression (35-40 km) (Balesta 1981). The following fractional crystallization occurs at magma decompression with different ascent rate for high-Mg and high-Al basalts. A change of the rates of magma cooling and crystallization at the depth <20 km suggests magma stalling in the upper crust beneath the volcano (Fig. 1). Assimilation of country rocks and processes of Ol-Cpx fractional crystallization and accumulation in the upper crust modify significantly the major and trace element composition of Klyuchevskoy magmas (Mironov 2009). Crystallization at the lower to upper crustal levels was accompanied by release of carbonate-rich fluids. Final stages of magma evolution are characterized by exsolution of predominantly H_2O-rich fluid (see also Mironov and Portnyagin this volume) and accompanied by massive degassing-driven crystallization.

The estimated conditions of magma evolution beneath Klyuchevskoy volcano agree well with independent data based on seismic tomography studies and distribution of epicenters of the earthquakes in the crust (Gorel'chik et al. 2001, Lees et al. 2007). This allowed us to constrain a consistent model of the magma plumbing system beneath Klyuchevskoy volcano utilizing data from petrology, geochemistry and geophysics (Mironov 2009, Fig. 1). Our future studies are to focus on the temporal evolution of the plumbing system and the role of crustal assimilation at generating diversity of Klyuchevskoy magmas.

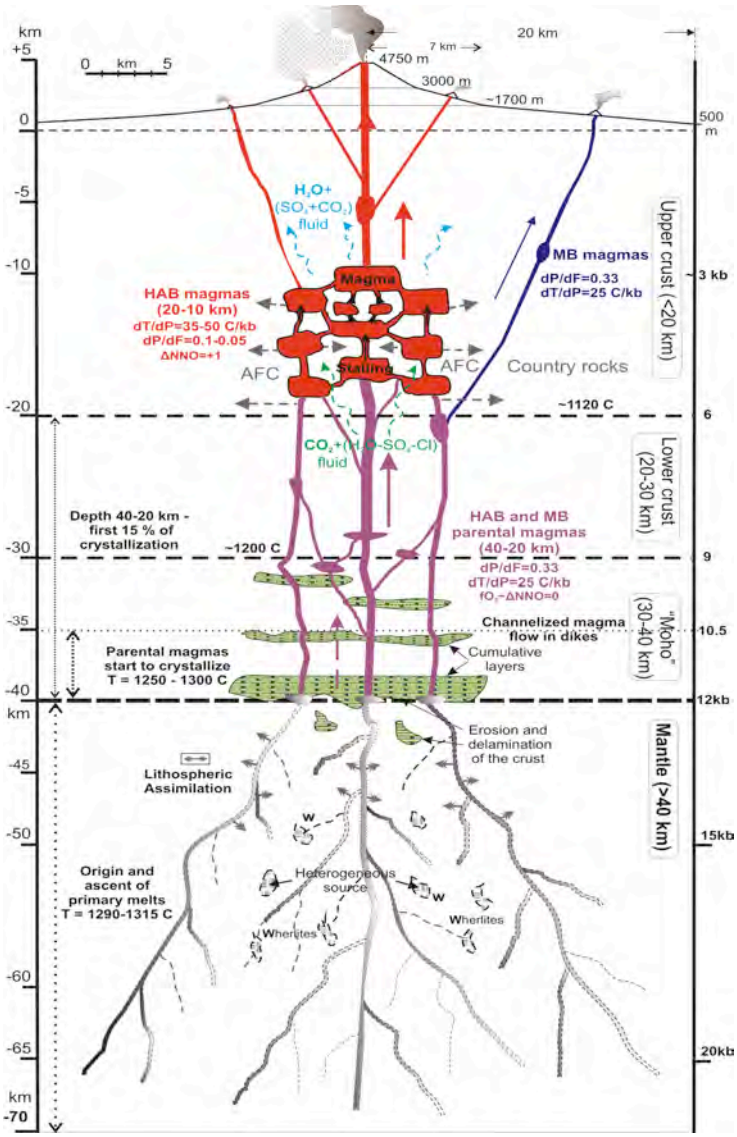

Fig.1: Magmatic feeding system of Klyuchevskoy volcano inferred from petrological and geophysical data

References

Balesta ST (1981) Earth crust and magma chambers in regions of modern volcanism. Nauka, Moscow. 134 p. In Russian

Gorel'chik VI, Garbuzova VT, Gorel'chik VI, Storcheus AV (2001) Seismicity and earthquakes beneath Klyuchevskoy volcano. In: Geodynamics and volcanism of Kurile-Kamchatka island arc system. IVGG FEB RAS, Petropavlovsk-Kamchatsky. P. 159-189. In Russian

Lees JM, Symons N, Chubarova O, Gorelchik V, Ozerov A (2007) Tomographic images of Klyuchevskoy volcano p-wave velocity. In: Eichelberger J, Gordeev E, Izbekov P, Lees J (eds) Volcanism and Subduction: The Kamchatka Region. AGU, Washington, DC: 293-302

Mironov NL (2009) The origin and evolution of Klyuchevskoy volcano magmas from study of melt inclusions in olivine. PhD Thesis, Vernadsky Institute of Geochemistry and Analytical Chemistry RAS, Moscow, 325 p. In Russian. (Http://geo.web.ru/db/msg.html?mid=1182249)

Volatile flux from Klyuchevskoy volcano, Kamchatka

Nikita Mironov[1], Maxim Portnyagin[2,1]

[1] GEOKHI RAS, V.I.Vernadsky Institute of Geochemistry and Analytical Chemistry RAS, Kosygin St. 19, 119991 Moscow, Russia; e-mail: nmironov@geokhi.ru
[2] IFM-GEOMAR, Leibniz Institute of Marine Sciences, Wischhofstrasse 1-3, 24148 Kiel, Germany

Klyuchevskoy is famous for its frequent eruptions and vigorous (>60 Mt/year) magma output. This study was aimed at characterization of fluid regime of Klyuchevskoy magmas and quantification of volatile fluxes resulted from its volcanic activity. The results were submitted for publication in Special volume of the Russian Geology and Geophysics devoted to fluid inclusion studies (Mironov and Portnyagin 2011). To estimate the pre-eruptive content of volatiles in magmas and co-existing

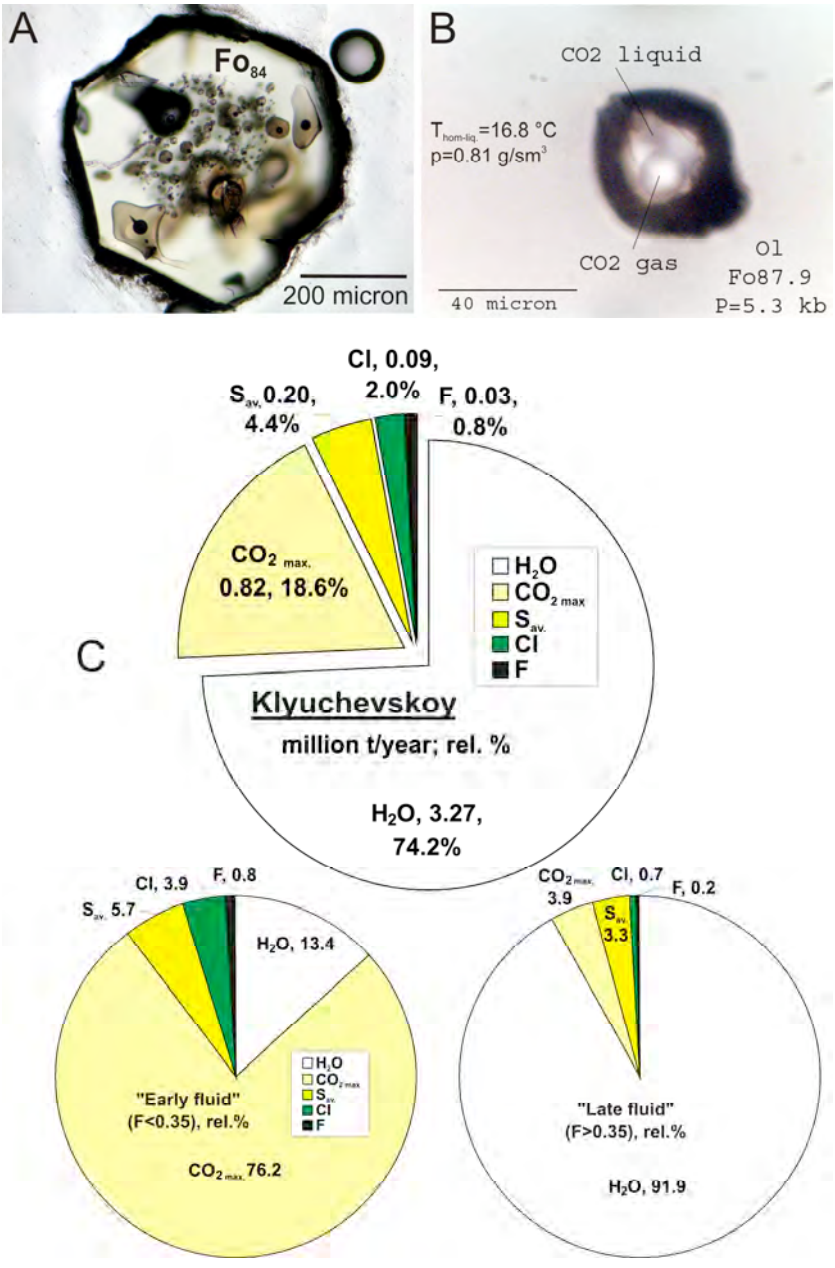

Fig. 1: Naturally quenched melt inclusions (A) and high density CO_2 fluid inclusion (B) in Klyuchevkoy olivine phenocrysts. (C) Volatiles annual emission estimate and composition of Klyuchevskoy fluids.

fluids, more than 400 melt and fluid inclusions in olivine (Fo_{92-67}) from different rock varieties were studied (Fig. 1a,b). Volatiles in melt inclusions were analyzed using electron microprobe (S, Cl), ion microprobe (H_2O, F) and infrared spectroscopy (CO_2, H_2O). Fluid inclusions were studied criometrically. Careful examination of melt inclusions for possible loss of water, redistribution of CO_2 between melt and fluid phases and sulfide immiscibility was undertaken prior interpretation of the analytical data.

The data selected to be representative for magmatic conditions suggest that parental Klyuchevskoy magmas are very rich in volatile components (minimum-maximum, average, wt. %): H_2O=2.8-3.6, 3.2; CO_2=0.35-0.8; S=0.13-0.23, 0.16; Cl=0.02-0.13, 0.08; F=0.022-0.051, 0.032). Substantial amount of the volatiles initially dissolved in the primitive melts is released to fluid phase at subsequent magma evolution. The early stage crystallization in the lower to upper crust (~30-15 km depth) is accompanied by release of chlorine-, sulphate- and water-bearing carbonate-rich fluid (CO_2>60 %) from fractionating magma. The later magma evolution (at depth ~<10 km) is characterized by exsolution of predominantly carbonate- and sulphate-bearing water-rich fluid (H_2O>90 %) (Fig. 1c) and accompanied by massive degassing-driven crystallization. The high pre-eruptive water content in evolved Klyuchevskoy magmas (up to 5-6 wt.%) is likely the main reason for highly explosive eruptions of this volcano.

The data on volatile/K_2O ratios in parental magmas and magmatic K_2O flux (calculated on the base of mean K_2O content in erupted rocks and productivity) were used to estimate the total flux of volatiles resulted from Klyuchevskoy volcano activity during the Holocene. The composition of bulk fluid was estimated to contain 83-74 wt% of H_2O, 9-19 wt% of CO_2 and 7-8 wt. % of S, Cl and F (Fig. 1c), that is close to the average fluid composition of the Earth island-arc volcanism (Wallace 2005, Sadofsky et al. 2008). The estimated annual flux of volatiles from Klyuchevskoy Volcano is however ca. 10 times higher compared to typical arc volcano. This massive emission of volatiles can account for up to 1.5 % of the average annual flux from all island-arc volcanoes. Large Klyuchevskoy eruptions can inject huge amounts of volatiles to the troposphere and therefore have climatic effect. Particularly large effect is anticipated during periods of enhanced Klyuchevskoy activity, for example ~7 and 3 ka BP (Portnyagin et al. this volume).

This study was supported by the KALMAR project (BMBF grant 03G0640A) and RFBR project # 09-05-01234a.

References

Mironov NL, Portnyagin MV (2011) Volatiles (H_2O, CO_2, S, Cl, F) in Klyuchevskoy volcano magmas from study of melt inclusions in olivine. Russian Geology and Geophysics, submitted

Sadofsky SJ, Portnyagin M, Hoernle K, van den Bogaard P (2008) Subduction cycling of volatiles and trace elements through the Central American volcanic arc: evidence from melt inclusions. Contributions to Mineralogy and Petrology 155(4): 433-456

Wallace PJ (2005) Volatiles in subduction zone magmas: concentrations and fluxes based on melt inclusion and volcanic gas data. Journal of Volcanology and Geothermal Research 140(1-3): 217-240

Glacial – interglacial environmental changes on the Shirshov Ridge, Western Bering Sea: micropaleontological and sedimentary records from Core SO 201-2-85KL

Ekaterina Ovsepyan[1], Elena Ivanova[1], Ivar Murdmaa[1], Tatyana Alekseeva[1], Alexander Bosin[2]

[1] IO RAS, P.P. Shirshov Institute of Oceanology RAS, Nakhimovsky prospect 36, 117997 Moscow, Russia; email: ameli_cat@mail.ru

[2] POI FEB RAS, V.I. Il`ichev Pacific Oceanological Institute, Far Eastern Branch RAS, Baltiyskaya Str. 43, 690041 Vladivostok, Russia

Environmental changes in the surface and bottom water layers are reconstructed for the upper 4,5 m of the core SO201-2-85KL (57°30.30 N, 170°24.79 E, w.d. 968 m) retrieved from the Shirshov Ridge, Western Bering Sea in the framework of the KALMAR project. Benthic and planktic foraminiferal assemblages are studied in grain size fractions 63-100 μm and >100 μm. Content of coarse fractions (>63 μ m) is determined by wet sieving throughout the core whereas the complete grain size analysis of fine fractions has been done for selected samples using Sedigraph 5100. Chlorine content is measured throughout the core SO201-2-85KL with 2-cm sampling interval. The core recovers the last 40 kyr. BP according to the preliminary age model (Riethdorf et al. 2010). Several prominent faunal changes are identified within this interval (Ovsepyan et al. 2010). The glacial and postglacial benthic foraminiferal assemblages are distinguished by changes in species percentages and by factor analysis (Fig. 1). Glacial assemblage corresponding to MIS 3-2 and the early deglaciation, consists of several common species including *Alabaminella weddellensis*, *Islandiella norcrossi, Trifarina angulosa, Uvigerina akitaensis, Cassidulina reniforme* and *Islandiella californica*. It indicates low bottom-water temperature and moderate surface bioproductivity with high seasonal pulses. The moderate surface bioproductivity is also supported by relatively high values of planktic foraminiferal species *Globigerina bulloides* (up to 20%). However, small numbers of both planktic and benthic foraminifers, as well as a reduced chlorine content point to low productivity conditions. This discrepancy might be linked to a significant dissolution of calcareous microfossils in the glacial sediments and to some special burial conditions unfavorable for chlorine preservation. High values of the "oxic" benthic group (according to Kaiho 1994) suggest moderate bottom-water ventilation during the glacial time span due to vertical mixing induced by brines release during the winter sea ice formation. The maximum percentage of this benthic group mirrors a strong bottom-water ventilation around the last glacial maximum (LGM). It seems to be related to intensification of winter sea-ice formation over the region at the LGM. Coarse detrital material attributed to ice rafted debris (IRD) is dominated by sand, with sporadic gravel grains. It demonstrates sizable fluctuations in abundance and grain-size, with maximum amplitudes during MIS 2-3, thus implying a considerable sea ice influence on the studied area at that time. The relationship between prevailing fine fractions (<63 μm) does not show any significant changes pointing to independent behavior of IRD. The abundance of planktic and benthic foraminifers show maximum and high values, respectively, at the early deglaciation, just after the LGM. The postglacial benthic assemblage is characterized by a dominance of high-productivity species *Buliminella tenuata* and *Bolivina seminuda* from Bølling/Allerød to early Holocene. Two peaks of chlorine content coincide with maxima of these benthic species. This might imply a significant rise in productivity during the so-called Northern Hemisphere melt-water pulses (MWP) 1a and 1b. The maximum abundance of these benthic species also points to the two-steps weakening of bottom-water ventilation at Bølling/Allerød (B/A) warming and the late deglaciation-early Holocene time span.

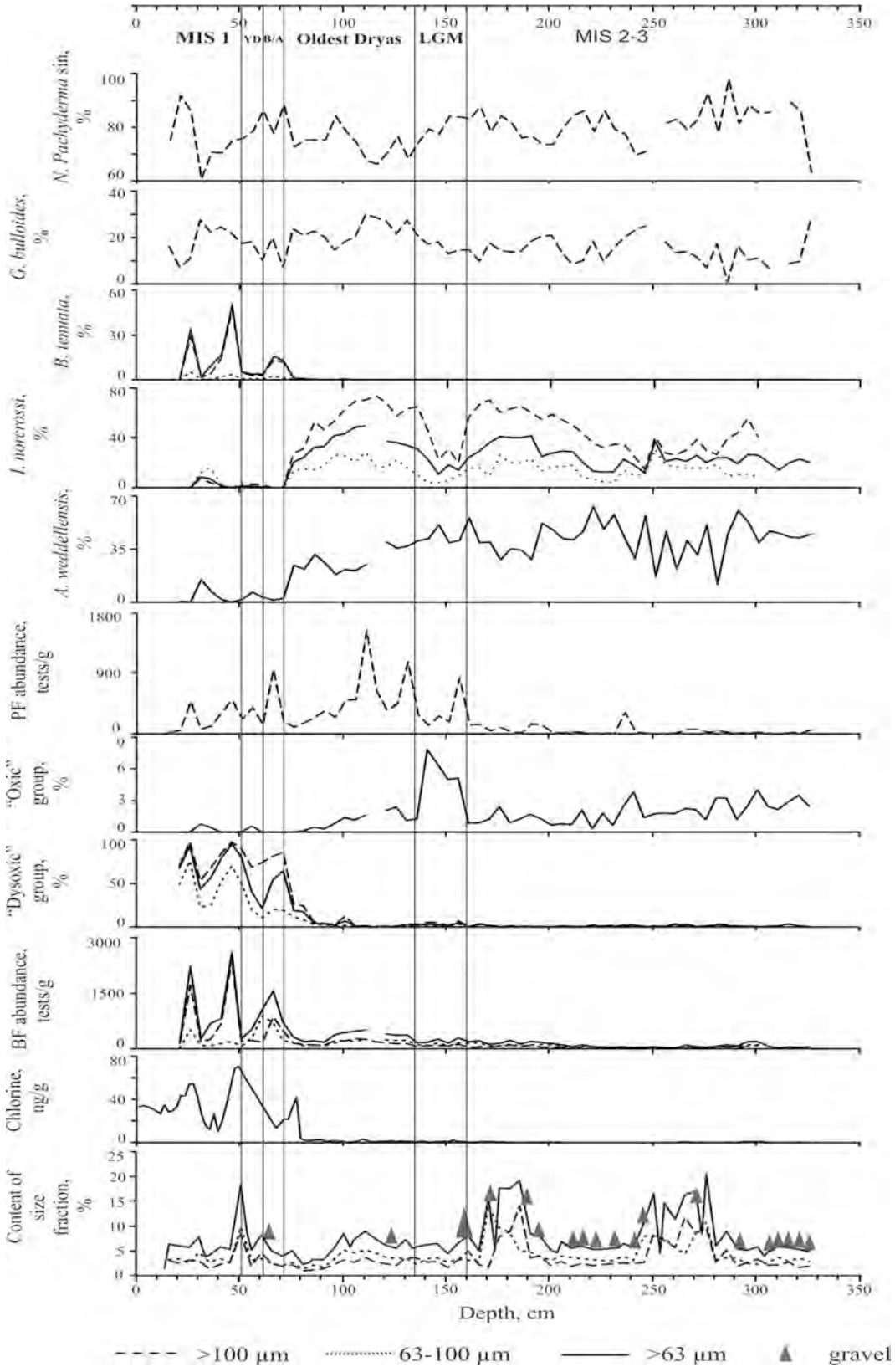

Fig. 1: Proxy time series in Core SO201-2-85-KL discussed in the text. Preliminary time scale according to (Riethdorf et al. 2010) and to faunal data from this study.

The maximum percentages of "dysoxic" benthic group within the same intervals support a strong oxygen depletion likely resulted from the enhanced O_2 consumption during the increased organic matter supply to the seafloor. Decrease in weight percentages

of sandy-silty sediment fraction and absence of gravel-size IRD grains were determined over the B/A. Around the Younger Dryas, appearance of gravel-size IRD grains and an increase in sand fraction suppose the return from interglacial conditions to glacial ones. A slight increase in oxygen content of bottom waters inferred from a decrease in percentage of "dysoxic" group and a slight increase in that of "oxic" group are linked to a better ventilation due to intensification of sea ice formation over the site.

Because of a strong disturbance of the upper 15- cm layer in core SO201-2-85KL, the Late Holocene was studied in the nearby multicore SO201-2-79MUK (56°43.12 N, 170°29.85 E, w.d. 1150 m). The sediments contain a huge amount of radiolarians and diatoms which points to a high surface-water productivity. Meanwhile, the scarcity of planktic and benthic foraminifers most likely indicates an extensive dissolution of calcareous microfossils during the Late Holocene.

This work was supported by grants OSL-10-14, OSL-11-11 and the Program 'Basic problems in Oceanology' by the Russian Academy of Sciences and by the German KALMAR project, BMBF grant 03G0201A

References

Kaiho K (1994) Benthic foraminiferal dissolved-oxygen index and dissolved-oxygen levels in the modern ocean. Geology 22: 719-722

Ovsepyan E, Ivanova E, Max L, Riethdorf J, Tiedemann R, Nürnberg D (2010) Reconstruction of bottom water ventilation and export production based on benthic foraminiferal assemblages from the Shirshov Ridge (Bering Sea) during MS1-2. Forams2010. International Symposium on Foraminifera. Rheinische Friedrich-Wilhelms-Universität Bonn: 152

Riethdorf JR, Max L, Nürnberg D. Tiedemann R (2010) Sea surface temperature, marine productivity and terrigenous fluxes in the western Bering Sea during the last 150 kyr. Abstracts of the ICP 10, La Jolla, USA, Aug 29-Sept 3, 2010

Tsunami and active tectonics along the western margin of the Bering Sea - impact on the coastal zone environment and evolution

Tatiana Pinegina[1], Andrey Kozhurin[2]

[1] IVS FEB RAS, Institute of Volcanology and Seismology FEB RAS, Piip Boulevard 9, 683006 Petropavlovsk-Kamchatsky, Russia; email: tsunami@kscnet.ru
[2] Geological Institute, RAS, Pyzhevsky per. 7, 119017 Moscow, Russia

Over the last about 20 years, the Bering coast of Kamchatka was not considered as an area with a high level of earthquakes and tsunami risks, despite the 1969 Mw 7.7 tsunamigenic earthquake near the Ozernoi Peninsula. However, the 1991 Khailinskoe (Mw 6.6) earthquake in the southern part of the Koryakia, and especially the 2006 Olytorskoe earthquake (Mw 7.6) had raised the public and scientific concern about the possibility of large (including tsunamigenic) earthquakes in this area.

The western Bering Sea overlies a tectonically complex region. The plate

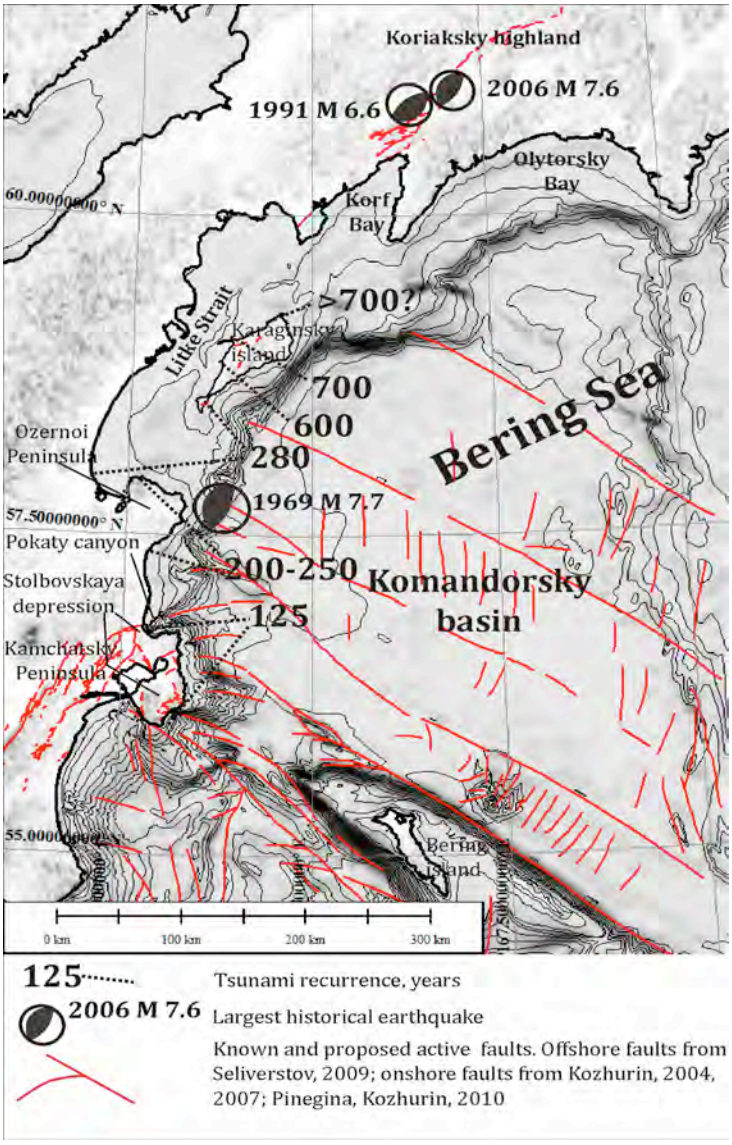

Fig. 1: Recurrence interval of tsunami with runup >5 m at the different parts of the Bering Sea coast (based on tsunami deposits for the last ~2000 years).

in this region are not well established - geoscientists have proposed several different plate configurations. Multiplate models (Cook et al. 1986, Lander et al. 1994, Mackey et al. 1997, Apel et al. 2006) more easily explain the location and mechanisms of the 1969, 1991 and 2006 earthquakes that occurred on the inferred Okhotsk/ Bering/ and Bering/ North America plate boundaries.

During 1998-2003 field seasons we studied paleotsunami deposits along the southwestern coasts of the Bering Sea. First, we examined geological evidence for the 1969 Ozernoy earthquake and tsunami (Bourgeois et al. 2006, Martin et al. 2008). Then, we used these data as well as data on other historical tsunamis, as a guide for analyzing more than 4000 years of paleoseismic record in the southwestern Bering Sea. In this area we have documented evidence for 12-15 tsunamis during about 4500 years. Based on tsunami runup (4-8 m) and tsunami inundation (≤300-400 m), we think that these events were produced by local earthquakes with Mw ~7.5±0.5. Possibly, by kinematics, they are underwater analogues of the Olytorskoe Mw 7.6 earthquake of April 20, 2006 in Koryakia (Pinegina, Konstantinova 2006, Pinegina, Kozhurin 2010).

In 2009-2010 we extended the paleoseismological investigation to the west and northwest coast of the Bering Sea. A number of active faults, deforming late Pleistocene-Holocene marine terraces were identified. These faults, probably, have a submarine continuation in the Bering Sea. Slip along these faults may generate tsunamigenic earthquakes. Based on our data, the recurrence interval of slips along a single active fault may be as long as several thousands to ~10 thousands of years. The recurrence interval of tsunami (with runup >5 m) at the different parts of the Bering Sea coast vary, in average, from 125 years up to ~1000 years (Fig. 1). Historical data show that the tsunamis with sources situated along the Kurile-Kamchatka subduction zone do not influence the Bering Sea coast significantly. So, we suppose that most of the Bering Sea tsunamis come from local sources (Bourgeois et al. 2006). They may be generated by several zones located along the margins of the Komandorsky basin. The analysis of historical seismicity (1937-2010) clearly shows that possible tsunamigenic zones may be 1) at the western shelf of Komandorsky basin, its slope and foot, and 2) at the western end of the Aleutian Island Arc. To that, seismogenic and tsunamigenic zones may be 3) at the extension of active faults of the Stolbovskaya depression in the Pokaty canyon, and 4) at the continuation of active structures of Koriaksky highland in the Litke Strait. These last two zones are less clearly pronounced in the modern seismicity, and were identified mostly by our paleoseismological study. Still, we have no data, either historical or paleoseismological, about tsunami from local earthquakes in the Olytorsky and Korf Bays. One known historical tsunami in these Bays with ~4 m runup was transoceanic (from Chili 1960). It is no question that such events if there were any, influenced geologic history of the coastal area. For example, the coastal coseismic deformations may cause rapid fluctuations in relative sea level and produce therefore great environmental changes in the lake's and lagoon's sedimentation as a whole. Tsunami waves can inject a large amount of allogenic material into the coastal area and modify it drastically. Study of earthquakes- and tsunami-related imprints on coastal sequences should give us possibility to better understand the interaction between onshore and offshore processes in context of reconstruction of the paleoenvironmental conditions and their evolution.

References

Apel EV, Burgmann R, Steblov G, Vasilenko N, King R, Prytkov A (2006) Independent active microplate tectonics of northeast Asia from GPS velocities and block modeling. Geophysical Research Letters 33: L11303

Bourgeois J, Pinegina T, Ponomareva V, Zaretskaia N (2006) Holocene tsunamis in the southwestern Bering Sea, Russian Far East, and their tectonic implications. GSA bulletin 118: 449-463

Cook DB, Fujita K, McMullen C (1986) Present-day plate interactions in northeast Asia: North American, Eurasian, and Okhotsk plate. J. Geodynamics 6: 33-51

Kozhurin AI (2004) Active faulting at the Eurasian, North American and Pacific plates junction. Tectonophysics 380: 273-285

Kozhurin AI (2007) Active Faulting in the Kamchatsky Peninsula, Kamchatka-Aleutian Junction. In: Eichelberger J, Gordeev E, Izbekov P, Lees J (eds) Volcanism and Subduction: The Kamchatka Region. American Geophysical Union, Washington, DC: 263-282

Lander AV, Bukchin BG, Droznin DV, Kiryushin AV (1994) Tectonic Position and focal parameters of the Hailinskoe (Koryaskoe) earthquake on 8 March, 1992: Is there a Bering Plate? Geodynamics and Earthquake Forecasting: Computational Seismology edition 26: 104-122

Mackey KG, Fujita K, Gunbina L, Kovalev V, Imaev V, Kozmin B (1997) Seismicity of the Bering Straight region: evidence for a Bering block. Geology 25: 979-982

Martin ME, Weiss R, Bourgeois J, Pinegina TK, Houston H, Titov VV (2008) Combining constraints from tsunami modeling and sedimentology to untangle the 1969 Ozernoi and 1971 Kamchatskii tsunamis. Geophysical Research Letters 35: L01610

Pinegina TK, Konstantinova TG (2006) Macroseismic observation of consequences from April 21, 2006 “Olytorskoe” earthquake. Bulletin of Kamchatka regional association "Educational-scientific center". Earth Sciences 7: 169-173 (in Russian)

Pinegina TK, Kozhurin AI (2010) A new data on Olytorsky earthquake fault (Mw 7.6, April 21, 2006, Koriakia, Russia). Bulletin of Kamchatka regional association "Educational-scientific center". Earth Sciences 16: 231-241 (in Russian)

Seliverstov NI (2009) Geodynamic zones at the junction between the Kuril-Kamchatka and Aleutian Island Arcs. Petropavlovsk-Kamchatsky, KamGU Vitusa Beringa: 191 (in Russian)

Diatom stratigraphy and paleogeography of the Western Bering Fluxes of volatiles from volcanoes of Kamchatka

Anastasiya Plechova[1], Maxim Portnyagin[1,2] , Nikita Mironov[1]

[1] GEOKHI RAS, V.I.Vernadsky Institute of Geochemistry and Analytical Chemistry RAS, Kosygin St. 19, 119991 Moscow, Russia; email: aplech@geokhi.ru
[2] IFM-GEOMAR, Leibniz Institute of Marine Sciences, Wischhofstrasse 1-3, 24148 Kiel, Germany

Evaluation of short and long-term effects of volcanism on the global climate requires quantitative estimates of the volcanic emission of volatiles. One cannot directly measure the amount of volatiles emitted by volcanoes in the past but can estimate it using petrologic methods based on study of melt inclusions. In this work we estimate emission of volatiles resulted from basaltic volcanism in Kamchatka since the last Ice Age using data on volatiles in olivine-hosted melt inclusions.

We studied about 900 glassy and experimentally homogenized olivine-hosted (Fo_{92-65}) melt inclusions from 10 volcanic centers representative for 3 volcanic zones of the Eastern Volcanic Belt of Kamchatka: volcanic front (Ksudach, Zheltovsky, Vysoky, Krasheninnikov, Karymsky and Zhupanovsky volcanoes), rear-arc (Zavaritsky volcano and Tolmachev Dol) and the southern segment of the Central Kamchatka Depression (SCKD) (Klyuchevskoy volcano and Tolbachinskiy Dol). The compositions of rocks studied range from low- to high-K basalts and basaltic andesites and are representative for major magma types of the Eastern Volcanic Belt. Inclusions were analyzed for volatiles (S, Cl, H_2O, F), major and trace elements using electron and ion microprobes.

H_2O content in the most primitive inclusions is 2-3.5 wt% for EVF, 2.5-3.5 wt% for SCKD volcanoes and ~1.5 wt% for rear-arc Zavaritsky volcano. This difference in water content between frontal and rear-arc EVF volcanoes can be explained by decreasing water concentrations in parental melts and their sources with increasing depth from volcano to the subducting plate (Portnyagin et al. 2007). H_2O concentrations in EVF melts decrease with increasing K_2O and indicate degassing of water during crystallization. The rate of water degassing is much slower than that of sulfur. No more than ~ 50% of the initial water content is lost from magmas at 70% of crystallization. H_2O content in SCKD melts increases up to 5-5.5 wt.% during first 30-35 % of fractionation (Fo_{82-83}) and then decreases due to degassing at shallow pressure.

Sulfur content in high-magnesian (Fo_{88-80}) olivines is 2500-3000 ppm from Zheltovsky and Zhupanovsky volcanoes from EVF, Zavaritsky and Tolmachev Dol from rear-arc zone and slightly less in olivines Fo_{81-73} from Ksudach (1700 ppm), and in olivines Fo_{78-75} from Vysoky and Krasheninnikov (1500 ppm). SCKD melts also have high S concentrations ranging from 1700 to 4000 ppm. Sulfur content correlates inversely with K_2O in all samples and decreases to less than 200 ppm in groundmass glasses. Fast depletion of fractionating melts in sulfur and high proportion of sulfate species (measured S^{6+}/S^{Total} is 0.40±0.16 on average) dissolved in melts suggest that sulfur preferentially partitions into fluid phases during magmatic evolution. We estimated that magmas in Kamchatka lose more than 90% of sulfur after 70% crystallization.

Average chlorine and fluorine content in primitive magmas of Kamchatka volcanoes are shown at the Table 1. Concentrations of these components slightly increase during crystallization but Cl/K_2O and F/K_2O ratios decrease that indicates partial loss of chlorine and fluorine into fluid phase.Volcanic fluxes of volatiles to the exosphere (total flux to atmosphere, crust and hydrosphere) were estimated from published data on productivity of all EVF volcanoes during the Holocene (80×10^6 t/y) and CKD (Klyuchevskoy-Tolbachik: 10^7 t per year) (Ponomareva et al. 2007) and data on the volatile content in parental melts. The estimated minimum total and normalized to the length of the arc segments volatile fluxes are shown in Table 1.

Table 1. Average amounts of volatiles in mafic magmas of Kamchatka and their long-term fluxes.

	EVF	BVF	SCKD
H_2O (wt%)	2.6	1.5	2.8
S (wt%)	0.25	0.3	0.35
Cl (wt%)	0.05	0.08	0.09
F (wt%)	0.01	0.01	0.034
H_2O (t/year)/(t/km/year)	$2.0x10^6/3.7x10^3$		$2.7 x10^6/2.7x10^4$
S (t/year)/(t/km/year)	$2.0x10^5/3.7x10^2$		$3.4x10^5/3.4x10^3$
Cl (t/year)/(t/km/year)	$4.1 x10^4/75$		$8.7 x10^4/8.7x10^2$
F (t/year)/(t/km/year)	$8.0 x10^3/14.5$		$3.3 x10^4/3.3x10^2$

The flux estimated for the EVF is comparable to the average global flux from island arcs (Sadofsky et al. 2008). Significantly larger fluxes of volatiles from the SCKD volcanoes on the regional scale and globally reflect exceptionally high volcanic productivity of this region hosting Klyuchevskoy Volcano, the most productive volcano in the Pacific Ring of Fire. The estimated long-term sulphur flux for Kamchatka is at least 5 times higher than COSPEC measurements for this region (Hilton et al. 2002). The difference indicates that results of short period measurements cannot be representative for the long-term flux. Large eruption occurred during the period of satellite monitoring of gas emission from volcanic area can in turn lead to large overestimate of the long-term flux.

In summary, we conclude that primitive magmas of Kamchatka are very rich in volatiles and particularly in sulfur which concentrations in primitive Kamchatkan magmas are among the highest measured so far in island arcs (3000-6000 ppm). Given the large productivity of Kamchatkan volcanism during the last post-glacial period, its contribution to the volcanic forcing of the Earth climate should be discernable on the global scale.

This work was supported by the KALMAR project (BMBF grant 03G0640A) and the RFBR grant # 05-09-01234a.

References

Hilton DR, Fischer TP, Marty B (2002) Noble gases and volatile recycling in subduction zones. In: Porcelli D, Ballentine C, Weiler R (eds) Noblegases in geochemistry and cosmochemistry, reviews in mineralogy and geochemistry. Mineralogical Society of America, Washington, DC, 47: 319–370

Ponomareva VV, Melekestsev IV, Braitseva OA, Pevzner MM, Sulerzhitsky LD (2007) Late Pleistocene- Holocene Volcanism on the Kamchatka Peninsula, Northwest Pacific region. In: Eichelberger J, Gordeev E, Kasahara M, Izbekov P, Lees J (Eds) "Volcanism and Tectonics of the Kamchatka Peninsula and Adjacent Arcs". Geophysical Monograph Series, 172: 169-202 Geophysical Monograph Series, 172: 169-202

Portnyagin, MV, Hoernle, K, Plechov, PY, Mironov NL, Khubunaya, SA (2007) Constraints on mantle melting and composition and nature of slab components in volcanic arcs from volatiles (H_2O, S, Cl, F) and trace elements in melt inclusions from the Kamchatka Arc. Earth and Planetary Science Letters, 255 (1-2): 53-69

Sadofsky S, Portnyagin M., Hoernle K, van den Bogaard P (2008) Subduction Cycling of Volatiles and Trace Elements Through the Central American Volcanic Arc: Evidence from Melt Inclusions. Contributions to Mineralogy and Petrology, 155(4): 433-456

Tephra links for the NW Pacific, Asian mainland and Kamchatka regions

Vera Ponomareva[1], Maxim Portnyagin[2,3], Alexander Derkachev[4], Maarten Blaaw[5], Andrey Kozhurin[6], Maria Pevzner[6], Tatiana Pinegina[1], Christel van den Bogaard[2], Dieter Garbe-Schönberg[7]

[1] IVS FEB RAS, Institute of Volcanology and Seismology FEB RAS, Piip Boulevard 9, 683006 Petropavlovsk-Kamchatsky, Russia; email: ponomareva@kscnet.ru
[2] IFM-GEOMAR, Leibniz Institute of Marine Sciences, Wischhofstrasse 1-3, 24148 Kiel, Germany
[3] GEOKHI RAS, V.I.Vernadsky Institute of Geochemistry and Analytical Chemistry RAS, Kosygin St. 19, 119991 Moscow, Russia
[4] POI FEB RAS, V.I. Ilichev Pacific Oceanological Institute FEB RAS, Baltiyskaya Street 43, 690041 Vladivostok, Russia
[5] School of Geography, Archaeology and Palaeoecology, Queen's University Belfast, 42 Fitzwilliam Street, Belfast, BT9 6AX, UK
[6] Geological Institute RAS, Pyzhevsky per. 7, 119017 Moscow, Russia
[7] Institute of Geosciences, Christian-Albrechts-University of Kiel, Ludewig-Meyn-Str. 10, 24118 Kiel, Germany

Numerous Pleistocene-Holocene tephra layers derived from Kamchatkan volcanoes are buried in various deposits on the Kamchatka Peninsula as well as in the adjacent seas and NE Asia mainland. About 1000 tephra samples collected from soil-pyroclastic sequences, peat, deep-sea and lake sediments were characterized geochemically with the help of >10,000 electron microprobe and LA-ICP-MS glass analyses obtained within the frame of the KALMAR Project. This extensive and novel database permits long-distance correlations of individual tephra layers, which directly link various geological records and permit comparison of paleoclimatic, paleoceanological, volcanological and paleoseismological records. In addition, these correlations allow us to evaluate eruptive volumes and areas of ash dispersal for a number of large eruptions and thus contribute to the global record of explosive volcanism. These data have allowed us to preliminary identify a number of "correlation chains" each including a set of terrestrial and submarine samples characterized by very close glass compositions, for example:

cinder from Plosky Dalny (Ushkovsky) volcano → SR1 tephra found in Bering Sea cores SO201-77 and 81;

pumice from Karymsky caldera → tephra WP1 in a pilot core SO201-2-40;

pumice from Gorely caldera-forming eruption → WP5 tephra from the core SO201-2-40;

younger pumice from Gorely volcanic center (~40 kyr BP) → WP4 tephra in the Pacific cores at Meiji and Detroit Mts. → tephra in Ledovy Bluff outcrop (Chukotka); in this case we suggest two eruptions closely spaced in time from the same volcano because this tephra was not found in the Bering Sea cores (Fig. 1);

Rauchua tephra from the Chukotka Arctic coast → SR6 tephra (Shirshov Ridge, Bering Sea) → WP14 tephra (Meiji Mt., Pacific Ocean). This tephra may represent one of the largest explosive eruptions from Kamchatka comparable with the 8.5 kyr old Kurile Lake caldera-forming eruption (KO) and the eruption that produced ~120 kyr old Old Crow tephra with a bulk volume amounting to ~200 km^3 (Fig. 1) (Ponomareva et al. 2004, Preece et al. 2011).

These examples will allow us to discuss implications of these correlations for linking various paleoenvironmental records and consider tephrochronological pitfalls stemming from occasional similarity of the volcanic glass composition for different eruptions. Correlation of the Holocene marker tephra layers over Kamchatka has allowed us to link C^{14}-dated eruptive histories of different volcanoes and compare obtained paleovolcanic record to the emerging paleoseismological record, which is based on tephrochronological dating of tsunami deposits and faulting events (Bourgeois et al. 2006, Kozhurin et al. 2006).

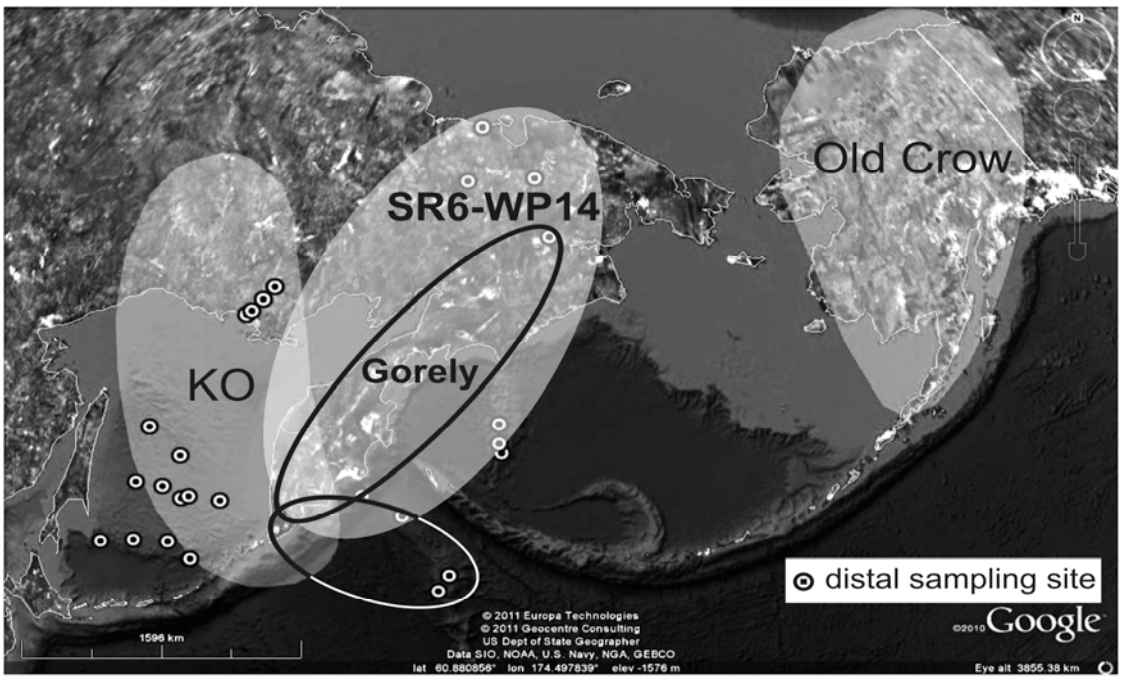

Fig. 1: Preliminary estimate of the tephra dispersal area for the newly identified largest eruptions in comparison with earlier studied KO (Ponomareva et al. 2004) and Old Crow (Preece et al. 2011) tephra.

The 12-m thick tephra sequence at the Klyuchevskoy volcano has been continuously accumulating during the last ~11 ka. It contains over 200 visible individual tephra layers and no datable organic material. The section is dominated by dark-gray mafic cinders related to Klyuchevskoy activity. In addition, it contains 30 light-colored thin layers of silicic tephra from distant volcanoes including 11 layers from Shiveluch volcano. We have used EMPA glass analysis to correlate most of the marker tephra layers to their source eruptions dated earlier by C^{14} (Braitseva et al. 1997), and in this way linked Klyuchevskoy tephra sequence to sequences at other volcanoes including Shiveluch.

The C^{14} dates and tephras from the northern Kamchatka are then combined into a single Bayesian framework taking into account stratigraphical ordering within and between the sites. This approach has allowed us to enhance the reliability and precision of the estimated ages for the eruptions. Age-depth models are constructed to analyse changes in deposition rates and volcanic activity throughout the Holocene. This detailed chronology of the eruptions serves as a basis for understanding temporal patterns in the geochemical variations of magmas and for dating major tectonic events. This research could prove important for the long-term forecast of eruptions and volcanic and seismic hazards.

Acknowledgements. The authors thank A.V. Lozhkin for providing the samples from Rauchua and Ledovy Bluff outcrops (Chukotka).

References

Bourgeois J, Pinegina TK, Ponomareva VV, Zaretskaia NE (2006) Holocene tsunamis in the southwestern Bering Sea, Russian Far East and their tectonic implications. The Geol. Soc. Amer. Bull. 11 (3/4): 449–463

Braitseva OA, Ponomareva VV, Sulerzhitsky LD, Melekestsev IV, and Bailey J (1997) Holocene key-marker tephra layers in Kamchatka, Russia. Quaternary Res 47: 125-139

Kozhurin A, Acocella V, Kyle PR, Lagmay FM, Melekestsev IV, Ponomareva V, Rust D, Tibaldi A, Tunesi A, Corazzato C, Rovida A, Sakharov A, Tengonciang A, and Uy H (2006) Trenching studies of

active faults in Kamchatka, eastern Russia: paleoseismic, tectonic and hazard implications. Tectonophysics, 417: 285-304

Ponomareva VV, Kyle PR, Melekestsev IV, Rinkleff PG, Dirksen OV, Sulerzhitsky LD, Zaretskaia NE, and Rourke R (2004) The 7600 (^{14}C) year BP Kurile Lake caldera-forming eruption, Kamchatka, Russia: stratigraphy and field relationships. J Volcanol Geotherm Res 136: 199–222

Preece SJ, Pearce NJG, Westgate JA, Froese DG, Jensen BJL, Perkins WT (2011) Old Crow tephra across eastern Beringia: a single cataclysmic eruption at the close of Marine Isotope Stage 6. Quaternary Science Reviews, in press. doi:10.1016/j.quascirev.2010.04.02

Geochemical systematics of submarine glasses from the Volcanologists Massif, Far Western Aleutian Arc

Maxim Portnyagin[1,2], Folkmar Hauff [1], Kaj Hoernle[1], Gene Yogodzinski[3], Reinhard Werner[1], Boris Baranov[4], Dieter Garbe-Schönberg[5]

[1] IFM-GEOMAR, Leibniz Institute of Marine Sciences, Wischhofstrasse 1-3, 24148 Kiel, Germany; email: mportnyagin@ifm-geomar.de
[2] GEOKHI RAS, V.I.Vernadsky Institute of Geochemistry and Analytical Chemistry RAS, Kosygin St. 19, 119991 Moscow, Russia
[3] Department of Earth & Ocean Sciences, University of South Carolina, 701 Sumter St., EWSC617, Columbia SC 29208, USA
[4] IO RAS, P.P. Shirshov Institute of Oceanology RAS, Nakhimovsky prospekt 36, 117997 Moscow, Russia
[5] Institute of Geosciences, Christian-Albrechts-University, Ludewig-Meyn-Strasse 10, 24118 Kiel, Germany

The Volcanologists Massif is located ca. 50 km north of Medny Island between Alpha and Bering FZ in the axial part of the Komandor Graben, the southernmost spreading center of the Komandorsky Basin (Baranov et al. 1991). Piip Volcano occupies the central part of the massif and considered to be the westernmost active volcano in the Aleutian Arc. Here we report first results of geochemical investigation of volcanic rocks obtained during R/V Sonne cruise SO201-KALMAR (Leg 2, 30.08. - 08-10.2009). The goals of the study are development of a model of the geodynamic evolution of the Volcanologists Massif and Piip Seamount, and testing of petrogenetic models proposed for the origin of active volcanism in the Western Aleutian Arc.

Dredging at the Volcanologists Massif during SO201-KALMAR followed three previous sampling campaigns at this volcanic structure in 1985-1989 with Russian research vessels "Vulcanolog" and "Akademik Keldish" (summarized in Yogodzinski et al. 1994). The SO201-2 expedition focused primarily on detailed bathymetric mapping of the massif and dredging of structural units of different ages within the volcanic complex. The rocks obtained at 10 dredge stations ranged from aphyric to olivine-plagioclase-pyroxene-phyric basaltic and andesitic lavas and dacitic pumice. Our investigations have focused on major, trace element and isotope compositions of volcanic glasses from the dredged rocks, which represent magmatic melts quenched by contact with seawater. Several samples obtained by R/V Vulcanolog during Legs 26 and 35 were also included in this study. Based on dredge location, petrography and geochemistry we subdivided all studied samples into 3 groups.

Group 1 is comprised of aphyric and rare olivine-plagioclase-phyric basalts and basaltic andesites dredged at the greatest depths, possibly representing the oldest rocks in the massif (DR53, DR61, V35-10). These rocks correspond to the Komandor Series after Yogodzinski et al. (1994). Volcanic glasses from the Group 1 have moderately evolved (Mg#=0.50-0.52), low-K (K_2O=0.44-0.56 wt %), relatively rich in FeO (7.1-7.6 wt %) and TiO_2 (1.3-1.7 wt %) andesitic compositions (SiO_2=54-56 wt %). These glasses have the highest S content (140-450 ppm) and the lowest Cl (510-640 ppm) compared to the other groups. The glasses have relatively high HREE and Y concentrations similar to MORB-like lavas from the Gamma FZ in the Komandorsky Basin (Fig. 1). Concentrations of more incompatible elements are higher compared to the Komandorsky Basin basalt, and their fractionated pattern suggests small to moderate contribution from slab-derived fluid to their mantle source (Ba/La=6.0-8.8, Pb/Ce=0.07-0.10). The Group 1 glasses have relatively low $^{87}Sr/^{86}Sr$ (0.70256-0.70271), high εNd (10.6) and slightly elevated $^{206}Pb/^{204}Pb$ (18.07-18.11) compared to other samples. Groups 2 and 3 correspond to the Piip Series after Yogodzinski et al. (1994). The Group 2 is comprised by olivine-pyroxene-plagioclase-phyric basaltic andesites and andesites dredged on both flanks of the Volcanologists Massif and from the foot of Piip volcano (DR48, DR51, DR55-60). Quenched glasses of this group have primitive (Mg#=0.54-0.68) low- to middle-K (K_2O=0.45-0.96 wt %), relatively low-FeO (6.6-4.7 wt %) and low-TiO_2 (0.73-1.21 wt %) andesitic compositions.

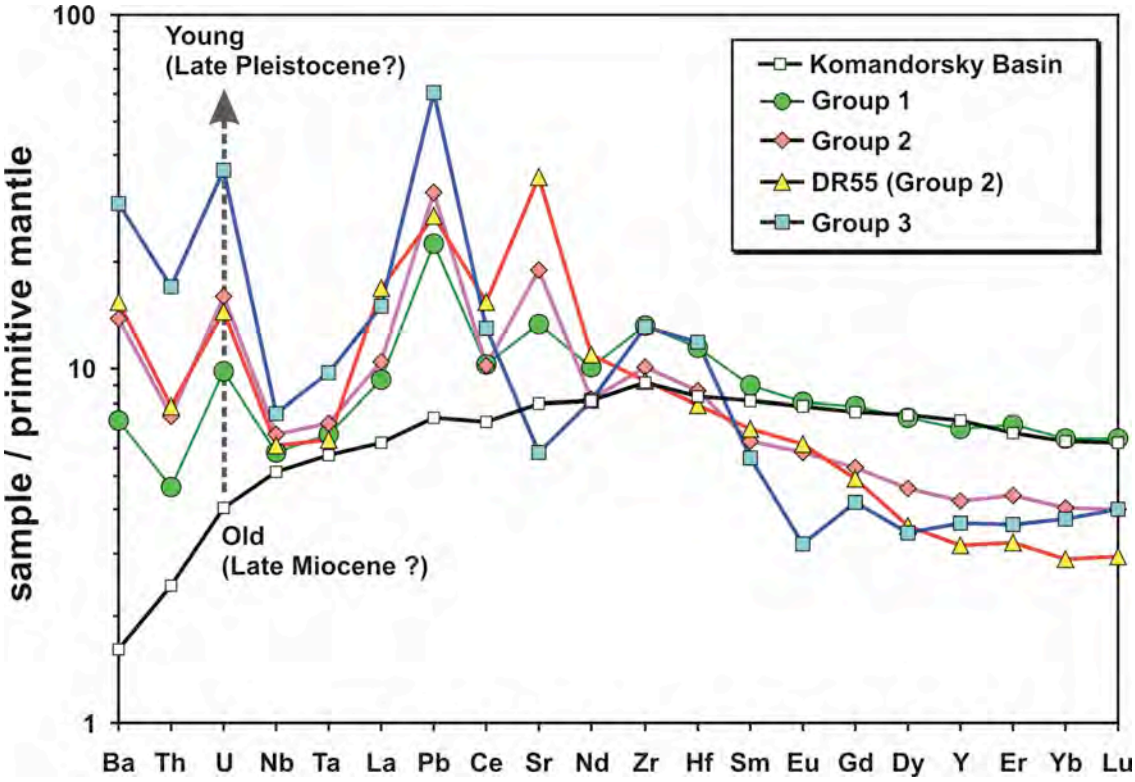

Fig. 1: Average trace element compositions of three groups of volcanic glasses from the Volcanologists Massif. Composition of Komandorsky Basin basalt from the Gamma FZ (SO201-2, DR118-1) is shown for reference.

Compared to the Group 1, these glasses are remarkably depleted in S (30-150 ppm), all REE (except La and Ce), enriched in Cl (600-1030 ppm) and highly incompatible elements and have more pronounced subduction-related signature (e.g., Ba/La=9.2-18.3, Pb/Ce=0.09-0.16) (Fig. 1). The $^{87}Sr/^{86}Sr$ ratios (0.70264-0.70279) are similar, and εNd (9.6-10.4) are lower compared to glasses of the Group 1. $^{206}Pb/^{204}Pb$ ratios (17.98-18.15) show greater variation but completely enclose Group 1. Among the Group 2 glasses, samples DR55 have specific compositions. They are enriched in Cl (1300 ppm), Sr (~740 ppm), LREE (La/Yb~8.5) and highly depleted in HREE. DR55 glasses have relatively low $^{87}Sr/^{86}Sr$ (0.70264) and εNd (9.6) compared to other Group 2 glasses and likely contain a large proportion of MORB-eclogite melt component (A-type adakite).

Glasses of the Group 3 have evolved (Mg#=0.28-0.46) middle-K (K_2O=1.66-1.81 wt %) dacite rhyolitic (SiO_2=70.4-74.3 wt %) compositions. The glasses occur at chilled margins of some andesitic lavas (DR59) and in dacitic pumice (DR60), which were dredged at the foot of the Piip Volcano and likely represent the youngest rocks in the massif. As indicated by negative Eu and Sr anomalies and flat HREE pattern of these glasses (Fig. 1), they originated by significant fractionation of plagioclase and amphibole from more primitive melts. These silicic glasses have the most pronounced slab-related signature (e.g., Ba/La=9.2-18.3, Pb/Ce=0.09-0.16) and also higher $^{87}Sr/^{86}Sr$ (0.70277-0.70284) and lower εNd (10.0-10.2) compared to the other groups.

In summary, the compositions of volcanic glasses from the Volcanologists Massif suggest clear temporal evolution of the mantle sources from weakly modified in subduction zone (Group 1) to more strongly modified (Groups 2 and 3). This transition can be explained if the distance from the volcano to the subducting plate has shortened and more slab-derived fluids and melts reached the source region of younger magmas. Possible tectonic models to explain the geochemical evolution of the Volcanologists Massif are trench advance,

migration of the massif closer to the trench and changes of the slab dip.

References

Baranov BV, Seliverstov NI, Murav'ev AV, Muzurov EL (1991) The Kommandorsky basin as a product of spreading behind a transform plate boundary. Tectonophysics 199: 237-270

Yogodzinski GM, Volynets ON, Koloskov AV, Seliverstov NI, Matvenkov VV (1994) Magnesian andesites and the subduction component in a strongly calc-alkaline series at Piip volcano, Far Western Aleutians: J. Petrology 35: 163-204

The origin of primary magmas at the Kamchatka-Aleutian Arc junction by melting of mixed pyroxenite and peridotite mantle sources

Maxim Portnyagin[1,2], Alexander Sobolev[2,3,4], Nikita Mironov[2], Natalya Gorbach[5], Dmitri Kuzmin [4], Kaj Hoernle[1]

[1] IFM-GEOMAR, Leibniz Institute of Marine Sciences, Wischhofstrasse 1-3, 24148 Kiel, Germany; email: mportnyagin@ifm-geomar.de
[2] GEOKHI RAS, V.I.Vernadsky Institute of Geochemistry and Analytical Chemistry RAS, Kosygin St. 19, 119991 Moscow, Russia
[3] Laboratoire de Géodynamique des Chaînes Alpines (LGCA), University Joseph Fourier, 1381 rue de la Piscine, 38401 Grenoble, France
[4] Max-Plank-Institute for Chemistry, J.-J. Becherweg 27, 55128 Mainz, Germany
[5] IVS FEB RAS, Institute of Volcanology and Seismology FEB RAS, Piip Boulevard 9, 683006 Petropavlovsk-Kamchatsky, Russia

A key feature of magmatism associating with the Kamchatka-Aleutian junction is occurrence of young high-magnesian andesites (Shiveluch and Kharchinsky Volcanoes, Shisheisky Complex in Kamchatka, Volcanologists Massif in the Aleutian Arc), a rare type of island-arc rocks, which share somewhat incompatible geochemical features such as high SiO_2 content and high Mg#. The close association of high-magnesian andesites with the Kamchatka-Aleutian junction has been related to (1) slab edge melting and interaction of the eclogite-derived melts with mantle peridotite, (2) low temperature hydrous mantle melting, (3) melting of olivine-free pyroxenites in the mantle wedge, (4) mixing of primitive basaltic and evolved silicic magmas (e.g. Yogodzinski et al. 2001, Portnyagin et al. 2007; Gorbach, Portnyagin 2011).

To test these hypotheses and to characterize mantle sources at the Kamchatka-Aleutian junction, we have carried out a high precision analysis (Sobolev et al. 2007) of major and trace elements (Ca, Ni, Mn, Cr, Co, Al) in olivine phenocrysts from primitive rocks of Kamchatka and the Western Aleutian Arc.

Our study was initially focused on the largest Kamchatkan volcanoes, where we studied olivines from 6 volcanoes along the Central Kamchatka Depression (CKD), from the Klyuchevskoy (Klyuchevskoy and Tolbachik volcanoes) and Shiveluch (Shisheisky Complex, Shiveluch, Zarechny and Kharchinsky volcanoes) volcanic groups. The rocks ranged in composition from high-magnesian basalts (all localities) to high-magnesian andesites (Shiveluch Group). Our results revealed a systematic difference between the compositions of the most magnesian olivines (Fo89-92.5) along CKD. Klyuchevskoy Group olivines have systematically higher Ca/FeO (112-140), Mn/FeO (124-130) and lower Ni/MgO (35-60) (all in ppm/wt%) compared to Shiveluch Group olivines (61-111, 107-117, 51-91).

These results suggest that the systematic difference between the Klyuchevskoy and Shiveluch Group olivines and rocks can originate from different proportion of pyroxenite and peridotite-derived melts contributed to the parental magmas (Portnyagin et al. 2007). By using the approach of Sobolev et al. (2007, 2008), we estimate that the Klyuchevskoy parental melts contain no more than 20% pyroxenite-derived component, whereas its amount increases to 35-60% in the Shiveluch Group parental melts, which range from high-magnesian basalts to andesites.

Analysis of olivine from rocks obtained during the R/V Sonne SO201-2 KALMAR cruise at the Volcanologists Massif was crucial to confirm the genetic link of andesitic parental magmas to pyroxenite mantle sources. We found that olivines from the Komandor Series basalts (V35-D10/1, DR53) have relatively high Mn/FeO (125-128; sample averages) and low Ni/MgO (26-28) compared to the Piip Series high-magnesian andesites from DR48, 51, 55 and 60 (119-125, 39-55). These data imply that the amount of pyroxenite component was relatively small in the parental melts of the Komandor Series basalts (0-8%) and significantly larger for the Piip series andesites (~20% on average). The largest

amount of pyroxenite-derived component (~30%) was estimated for DR55 andesites, which have distinctive trace element and isotope composition and require significant contribution from eclogite-melt component (Portnyagin et al. 2011 this volume).

In summary, our extensive, consistent and precise data set on composition of olivines from volcanic rocks of Kamchatka and the Western Aleutian Arc suggests a variable contribution from non-peridotitic (most likely, pyroxenitic) mantle sources to the composition of primary magmas at the Kamchatka-Aleutian junction. Particularly large fraction of pyroxenite-derived component is estimated for high-magnesian andesites. The andesites have strong (Kamchatka) to moderate (Western Aleutian Arc) trace-element subduction-related signature. It is therefore plausible that the pyroxenites have been formed *in-situ* beneath the modern volcanic arcs due to reaction of eclogite-derived melts with mantle wedge peridotite. The large amount of pyroxenite-derived component in the Shiveluch Group and Piip Series parental melts can be related to the concurring effects of the large amount of slab melts generated at the edge of the subducting Pacific plate (Yogodzinski et al. 2001) and the relatively low mantle temperature which limited amount of peridotite melting (Portnyagin et al. 2007).

References

Gorbach NV, Portnyagin MV (2011) Geology and petrology of the lava complex of Young Shiveluch volcano, Kamchatka. Petrology 19 (in press)

Portnyagin M, Bindeman I, Hoernle K, Hauff F (2007) Geochemistry of primitive lavas of the Central Kamchatka Depression: Magma Generation at the Edge of the Pacific Plate. In: Eichelberger J, Gordeev E, Kasahara M, Izbekov P, Lees J (eds) Volcanism and Subduction: The Kamchatka Region. Geophysical Monograph 172. American Geophysical Union, Washington D.C., pp 199-239

Sobolev AV, Hofmann AW, Brügmann G, Batanova VG, Kuzmin DV (2008) A Quantitative Link Between Recycling and Osmium Isotopes. Science 321:536

Sobolev AV, Hofmann AW, Kuzmin DV, Yaxley GM, Arndt NT, Chung SL, Danyushevsky LV, Elliott T, Frey FA, Garcia MO, Gurenko AA, Kamenetsky VS, Kerr AC, Krivolutskaya NA, Matvienkov VV, Nikogosian IK, Rocholl A, Sigurdsson IA, Sushchevskaya NM, Teklay M (2007) The Amount of Recycled Crust in Sources of Mantle-Derived Melts. Science 316 (5823): 412-417

Yogodzinski GM, Lees JM, Churikova TG, Dorendorf F, Woerner G, Volynets ON (2001) Geochemical evidence for the melting of subducting oceanic lithosphere at plate edges. Nature 409(25 January 2001): 500-504

Late Pleistocene to Holocene changes in sea surface temperature, marine productivity and terrigenous fluxes in the Western Bering Sea

Jan-Rainer Riethdorf[1], Lars Max[2], Dirk Nürnberg[1], Ralf Tiedemann[2]

[1] IFM-GEOMAR, Leibniz Institute of Marine Sciences, Wischhofstrasse 1-3, 24148 Kiel, Germany; email: jriethdorf@ifm-geomar.de
[2] AWI, Alfred Wegener Institute for Polar and Marine Research, Am Handelshafen 12, 27570 Bremerhaven, Germany

As the Bering Sea links the Pacific with the Arctic Ocean and the N-Atlantic via the Bering and Kamchatka Straits, it is thought to contribute to changes in Earth's climate, especially the quasi-regular glacial-interglacial cycles of the Quaternary. However, assessment of paleoceanographic changes is limited within most of the Bering Sea sediments due to a relatively shallow CCD and corrosive bottom waters, prohibiting the preservation of calcareous microfossils.

Here, we present sediment records from the western Bering Sea recovered on a north-south transect from intermediate water levels well above the lysocline. Our age model is based on high-resolution spectrophotometric measurements (color b*) on these sediment archives, which showed similar changes and strong correlations with the NGRIP oxygen isotope record (NGRIP Members, 2004). This has been validated by radiocarbon datings and comparison of benthic oxygen isotopes with the global reference stack LR04 (Lisiecki, Raymo 2005; Fig. 1). Thus, our cores resolve the last ca. 190 ka on centennial to millennial timescales.

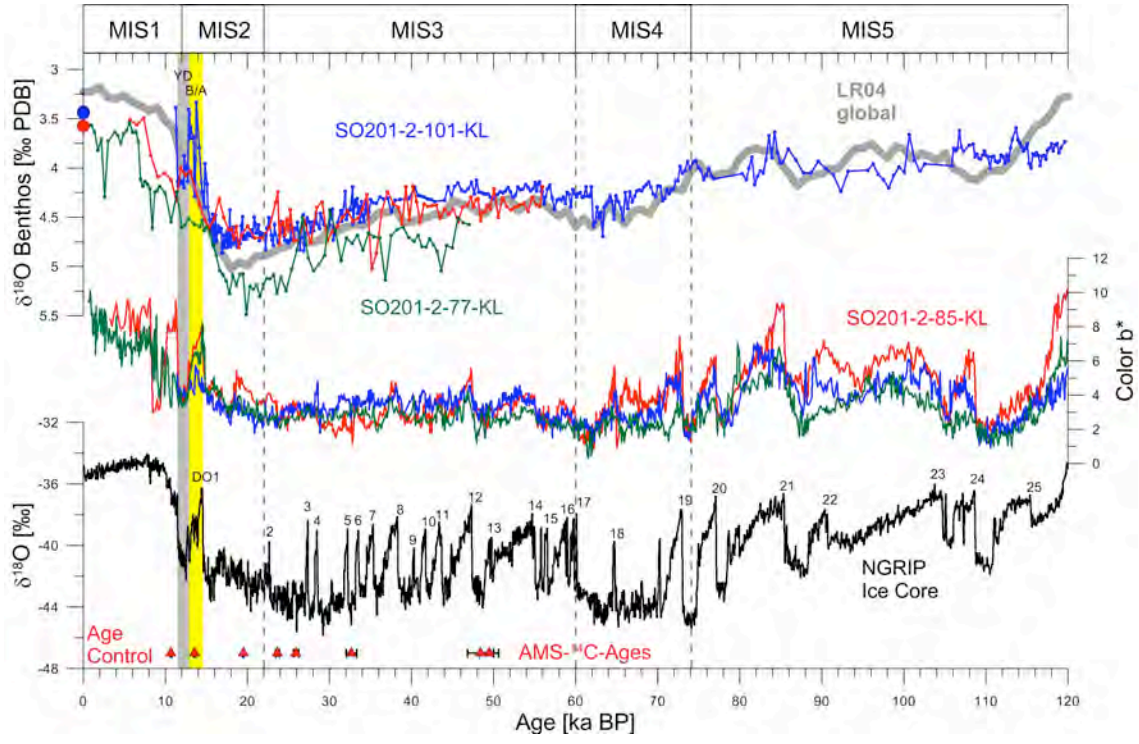

Fig. 1: Stratigraphy of our western Bering Sea sediment records. Benthic oxygen isotopes of cores SO201-2-77-KL, -85-KL, -101-KL compared to the global LR04 stack (Lisiecky & Raymo, 2005), as well as temporal variations of color b* for the same cores and oxygen isotopes from the NGRIP ice core. Age control points are indicated.

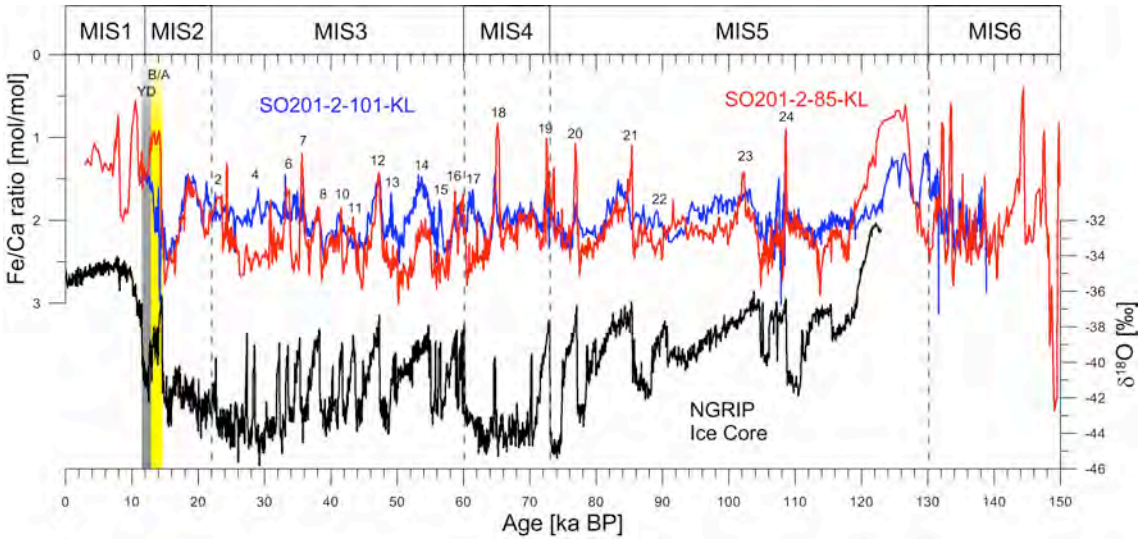

Fig. 2: Variability in Fe/Ca ratios in cores SO201-2-85-KL and -101-KL compared to the NGRIP oxygen isotope record (NGRIP Members, 2004). Interstadials are mirrored by minima in Fe/Ca.

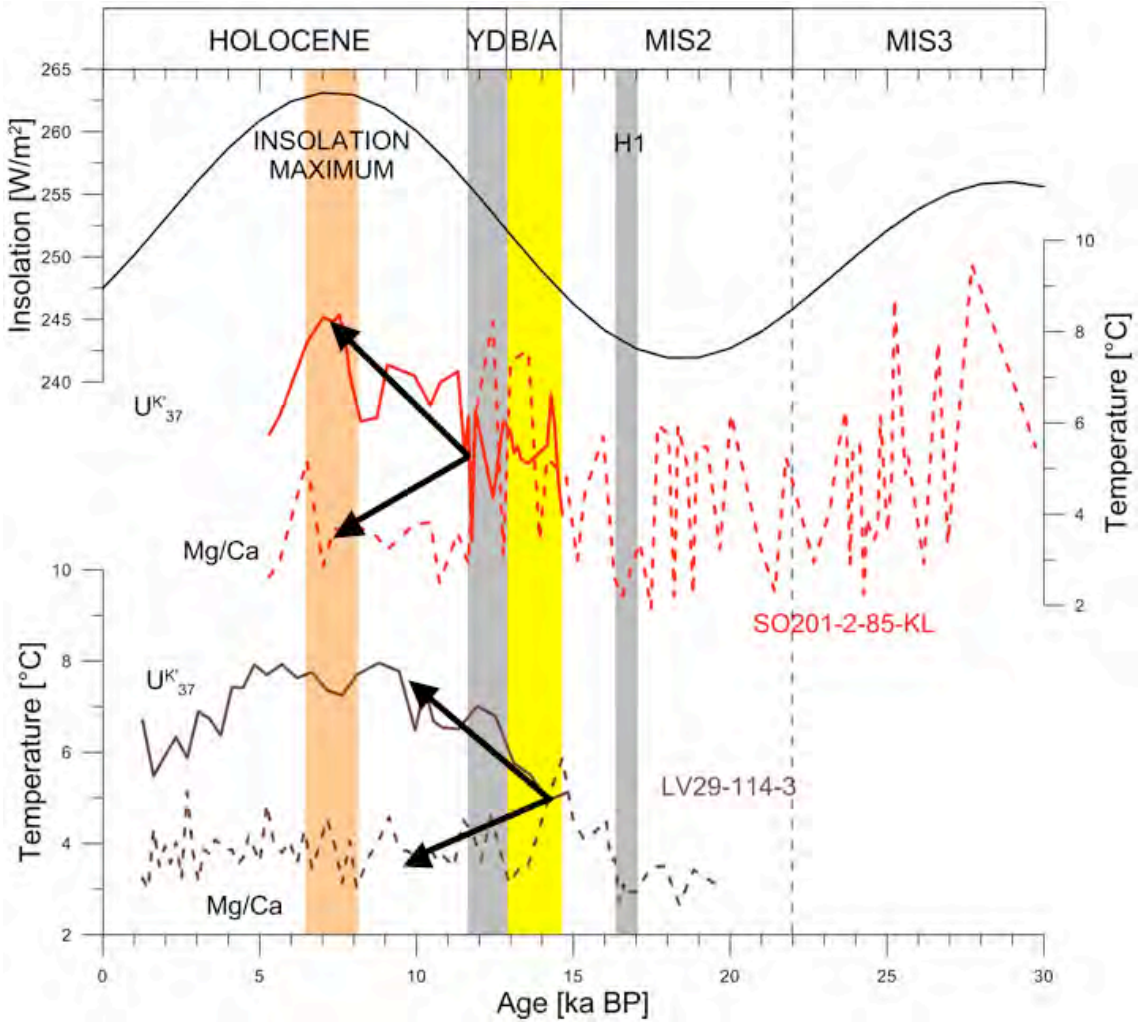

Fig. 3: Late summer insolation at 65°N (Laskar et al. 2004), compared to temperatures derived from planktonic Mg/Ca and $U^{K'}_{37}$ in cores SO201-2-85-KL from the western Bering Sea and LV29-114-3 from the Sea of Okhotsk.

We assess past terrigenous fluxes and marine productivity by XRF-element scanning and by the determination of TOC, $CaCO_3$ and biogenic opal. Deglacial and interglacial sediments show high contents of TOC, $CaCO_3$ and biogenic opal, while contents of typically terrigenous elements like Zr and Ti are low. This suggests enhanced surface water productivity under ice-free conditions. Interstadials are mirrored by minima in Fe/Ca ratios and sudden decreases in contents of Ti, indicating an atmospheric coupling mechanism between the N-Atlantic and the N-Pacific (Fig. 2). During the last glaciation the situation is reversed. Primary productivity is prohibited in the western Bering Sea, possibly due to a (perennial) sea-ice coverage. However, changes in marine productivity and terrigenous fluxes are clearly anticorrelated and show different intensity along the north-south transect. Terrigenous influence becomes weaker towards the south, while productivity increases, and vice versa. Sea surface temperatures (SST) are reconstructed using planktonic foraminiferal Mg/Ca ratios. Results for the western Bering Sea show that temperatures follow late summer insolation at 65°N until a sudden decrease at 11.5 ka (Fig. 3). Compared to results from the Sea of Okhotsk and temperature reconstructions using the alkenone index, there is the possibility, that a seasonal thermocline develops in the Bering Sea at the beginning of the Holocene, ca. 2-3 ka later than in the Sea of Okhotsk. If this interpretation is correct, the formation of N-Pacific intermediate water masses was still active in the Bering Sea during the Bølling-Allerød and Younger Dryas.

References

Laskar J, Robutel P, Joutel F, Gastineau M, Correia, ACM, Levrard B (2004) A long-term numerical solution fort he insolation quantities of the Earth. Astronomy & Astrophysics 428, 1: 261-285

Lisiecki LE, Raymo ME (2005) A Pliocene-Pleistocene stack of 57 globally distributed benthic $\delta^{18}O$ records. Paleoceanography 20, PA1003, doi:10.1029/2004PA001071

NGRIP Members (2004) High-resolution record of Northern Hemisphere climate extending into the last interglacial period. Nature 431: 147-151

Epithermal alteration of volcanic rocks of Kamchatka – onshore, offshore

Ulrich Schwarz-Schampera[1], Nikolay Tsukanov[2], Christoph Gaedicke[1], Boris Baranov[2],Gennadi Cherkachev[3], Nikolay Seliverstov[4]

[1] BGR, Federal Institute for Geosciences and Natural Resources, Geozentrum Hannover, Stilleweg 2, 30655 Hannover, Germany; email: Ulrich.Schwarz-Schampera@bgr.de
[2] IO RAS, P.P. Shirshov Institute of Oceanology RAS, Nakhimovsky prospekt 36, 117997 Moscow, Russia
[3] VNII Oceanologia, 1, Maklin Ave, 19012 St. Petersburg, Russia
[4] IVS FEB RAS, Institute of Volcanology and Seismology FEB RAS, Piip Boulevard 9, 683006 Petropavlovsk-Kamchatsky, Russia

Subduction processes and melt generation in island arc systems produce large amounts of intermediate to felsic lavas showing characteristic geochemical signatures with enrichments in incompatible, volatile and fluid-mobile elements. Metallogenetic processes commonly are closely associated with the production of island arc melts. It is accepted that assimilation, fractionation, sulphur fugacities, and redox conditions control the enrichment of a distinct group of volatile metals and metalloids usually found in island arc-associated ore deposits. Metallogenetic processes are associated with the fluids expelled from intermediate to felsic lavas; the fluid evolution is critical for mobilization, transport and precipitation of volatile elements. It is accepted that geothermal fields and associated alteration occur as a consequence of fluid mixture between meteoric water and juvenile water expelled from a crystallizing differentiated magma. Subaearial epithermal-type alteration and fluid discharge show a distinct alteration pattern which is indicative for associated magmatic processes, emplacement, fluid-rock interaction and fluid evolution. Shallow submarine hydrothermal systems, however, share many geochemical, mineralogical and isotopic similarities with subaerial geothermal fields despite distinct differences in crustal composition, lithologies, fluid origin and fluid composition. The proposed project aims at the comparison of both end-members in subaerial and shallow seawater systems in terms of fluid flow, fluid evolution and fluid-rock interaction. End-members may be defined by the volcanic centers of Kamchatka and the offshore Piip Seamount.

The majority of fluid-induced alteration processes are located within Tertiary paleovolcanic centres which are composed in their basal parts of andesites and diorites and are overlain by sequences of basalts, andesites and dacites. Paleovolcanic centres at Aginskoe, Ozernovskoe and Baranievskoe, for instance, are host to remnants of silicic sinters and low-temperature alteration assemblages whereas fault-controlled epithermal veins are spatially related to subvolcanic rocks of volcanic centres at Mutnovskoe. Furthermore, solutions from discharge areas of recent hydrothermal systems commonly contain a wide range of incompatible elements. The vapour-dominated system at the Mutnovskoe volcano show fluids and precipitates which are rich in highly volatile elements like mercury, antimony, arsenic, thallium and tellurium. Alteration at the active submarine Piip volcano is different in terms of the mineralogical composition but shows large similarities in the enrichment in the same element suite.

We propose a detailed sampling campaign with regard to alteration processes within different lava types of the volcanic edifices both, on Kamchatka and at the Piip Seamount.

Silification of peridotites from the Stalemate Fracture Zone, NW Pacific: Tectonic and geochemical applications

Sergei Silantyev[1], Elisaveta Krasnova[1], Maxim Portnyagin[1,2], Alexey Novoselov[1]

[1] GEOKHI RAS, V.I.Vernadsky Institute of Geochemistry and Analytical Chemistry RAS, Kosygin St. 19, 119991 Moscow, Russia; email: silantyev@geokhi.ru
[2] IFM-GEOMAR, Leibniz Institute of Marine Sciences, Wischhofstrasse 1-3, 24148 Kiel, Germany

One of the most significant achievements of the R/V Sonne cruise SO201-1b KALMAR is a very successful sampling at the Stalemate Fracture Zone (SFZ) because no data on bedrocks existed for this area in the NW Pacific. Bathymetric surveying during the cruise confirmed earlier data that SFZ includes a partially disintegrated NW-SE trending transverse ridge situated along a fracture zone. Dredging during the SO201-1b was performed at several locations on the northern slope of the ridge. Dredge 37 was carried out just north of the characteristic bend of the ridge where SFZ turns clockwise to NNW-SSE as it approaches the Aleutian trench (FS Sonne Fahrbericht, 2009). The dredge track sampled the east-facing slope from 4,360 to 3,995 mbsl and recovered highly altered rocks, which were recognized at onboard examination to have ultramafic protoliths of mantle origin (dunites, harburguites and lherzolites), testifying significant vertical uplift along the fault that probably also enhanced deep fluid migration.

Data on geochemistry and petrology of these ultramafic rocks obtained at IFM-GEOMAR as well as in the Vernadsky Institute during the last year are presented in work by Krasnova et al. (2011 this volume). The close association of dunites and moderately depleted lherzolites in the SFZ has been interpreted to result from interaction of lherzolitic shallow mantle with Ti- and Na-rich melts that leaded to reactive replacement of lherzolites by dunites along the melt channels. On the later stage, both dunites and lherzolites were modified by seawater alteration. Although extensive alteration is typical for abyssal peridotites, a very enigmatic geochemical feature of the rocks formed after dunites is their extremely low MgO (1.4-10.2 wt%) and high SiO_2 (71-89 wt%) contents. We assign this phenomenon to specific and rare type of low temperature sea-floor alteration (silification). Possible mechanism and processes responsible for the silification of the SFZ dunites are discussed in this presentation.

Comparative analyses of co-variations between SiO_2 (presumably, the most mobile major component in the system) and major and trace element contents in studied rocks allow us to outline some geochemical and mineralogical trends related to silification of the SFZ dunites. (1) Co-variations of SiO_2 vs. Sc, Zr and Ti contents confirm primary dunitic origin of these strongly altered ultramafic rocks. (2) Co-variations between SiO_2 and Ni, MgO, and LOI (weight loss on ignition) evidence for low temperature dehydration (e.g. deserpentinization) of dunitic serpentinites. Such geochemical features as mentioned above for the SFZ dunites were not described in abyssal peridotites from the contemporary oceanic basins, where relatively high silica content in so called soap-stones originates by talc formation. Dislike talk-bearing soap-stones, the SFZ dunites are composed by quartz (!), chlorite, spinel (relic) and serpentine (trace).

Other remarkable peculiarity of the ultramafic assemblage obtained at the site DR37 is close association of strongly silificated dunites and non-silificated spinel lherzolites. This contrasting assemblage implies three possible scenarios: (i) a very different, perhaps, spatially heterogeneous conditions of alteration for dunites and lherzolites, (ii) different position of dunites and lherzolites in geological sequence different age of alteration for dunites and lherzolites.

Our next step to reconstruct the processes and conditions leading to silification of the SFZ dunites will be numerical simulation. To model the complex processes of seawater-rock interaction, we are going to use thermodynamic calculations with kinetic parameters implemented within the computer program GEOCHEQ (thermodynamic data base derived from SUPCRT92) (Mironenko

et al. 2008). The simulations will be performed for a range of P-T and time conditions using the least altered SVZ peridotite composition and the seawater and/or its fluid derivatives as starting materials. The data obtained by the modeling are anticipated to suggest new interpretations for the currently enigmatic silification of the SFZ dunites and will be reported at the workshop.

References

FS Sonne Fahrtbericht / Cruise Report SO201-1b, KALMAR, Yokohama, Japan – Tomakomai, Japan, 10.06-06.07.2009, 62p.

Mironenko MV, Melikhova TYu, Zolotov MYu and Akinfiev NN (2008) GEOSHEQ_M: program complex for thermodynamic and kinetic modeling of geochemical processes in rock-water-gas systems. Version 2008/Vestn. Otdelenia nauk o Zemle RAN, 26.

Krasnova E, Portnyagin M, Silantiev S, Werner R, Hauff F, Hoernle K (2010) Petrology and geochemistry of mantle rocks from the Stalemate Fracture Zone (NW Pacific)

Quaternary Glaciations in NE Russia

Georg Stauch[1], Olga Glushkova[2], Frank Lehmkuhl[1], Bernhard Diekmann[3]

[1] RWTH Aachen University, Geographical Institute, Templergraben 55, 52056 Aachen, Germany; email: gstauch@geo.rwth-aachen.de
[2] North-East Interdisciplinary Science Research Institute, FEB RAS, Portovaya 16, 685000 Magadan, Russia
[3] AWI, Alfred Wegener Institute for Polar and Marine Research, Telegrafenberg A43, 14473 Potsdam, Germany

Climatic changes during the late Quaternary led to the development of major glaciations on earth. While the waxing and waning of the large northern hermispheric ice sheets basically reflect global climate changes, the extent of mountain glaciations strongly reflects regional and local environmental boundary conditions. Therefore, reconstruction of mountain glaciation can give insight into local climate development, especially in regard to temperature and precipitation estimates. Compared to other regions on earth, the glacial history of the widely distributed mountain ranges of northeastern Siberia is not well constrained. Open questions concern both, the timing and duration of repeated glaciation as well as their meaning for palaeoclimatic interpretations.

Former research led to the identification of up to five glaciations in the westernmost mountain range, the Verkhoyansk Mountains, and only two glaciations on the eastern seaboard of Eurasia, the Koryak Mountains and on the Kamchatka Peninsula (Fig. 1) as well as three in the Pekulney Mountains (Stauch, Gualtieri 2008). Beside the number of glaciations also the timing differs throughout the late Quaternary. In nearly all areas at least one major glaciation is recognized for the previous glacial cycle. In the Verkhoyansk Mountains glaciers reached more than 100km in length. Age control on this glaciation is generally poor. In the Verkhoyansk Mountains four glaciations occurred early in the last glacial cycle (Stauch et al. 2007; Stauch, Lehmkuhl 2010) and no ice advances has been attributed to the timespan of the global Last Glacial Maximum (gLGM, 18 to 24ka). Rough estimations of the ELA (equilibrium line altitude) for these glaciers indicate values of 1000 to 1200m asl (above sea level) which would correspond to a ELA lowering of roughly 1000m. Further to the east the number of glaciations during the last glacial cycle decreased and only one or two glaciations are recognized in central (Glushkova 2001) and eastern NE Russia and Kamchatka (Stauch, Gualtieri 2008). Interestingly Kamchatka is the only area where no glaciation is recognized for the middle part of the last glacial cycle, the MIS 3 (Marine Isotope Stage). ELA estimates for the time of the gLGM in the Pekulney Mountains in the northeast gave values of 650 to 850m asl (Barr, Clark 2011). These values are considerably lower than those in the Verkhoyansk Mountains due to a different moisture source. While the Verkhoyansk Mountains receive their moisture from the west and therefore from the Atlantic Ocean glaciers on the eastern seaboard are fed by precipitation originating in the northern Pacific Ocean. Slightly higher values come from the Sredinny Mountains in central Kamchatka further to the south. Paleo-ELA estimates yield values between 700 and 1100m (Barr, Clark 2011). Higher values are caused by higher insolation values, however, the highest values are supposedly caused by local effects like precipitation shielding from neighboring mountains.

Generally precipitation in the area of NE Siberia seemed to have significantly decreased during the last glacial cycle, resulting in progressively smaller mountain glaciers and leading to an opposite trend in comparison e.g. to the Scandinavian Ice Sheet in northern Europe. As moisture sources in eastern Siberia vary from west to east, the interpretation of glacial dynamics has to invoke different climatic processes. In the western part of the area the most important factor, beside changes in insolation, was the moisture blocking by the development of large ice sheets in western

Eurasia (Stauch, Gualtieri 2008; Krinner et al. 2011). While the Scandinavian Ice became large during the different glaciations in the last glacial cycle, moisture transport to the west was restrained leading to smaller glaciations in the Verkhoyansk Mountains. During the maximum extent of the ice sheet during the gLGM only little moisture reached NE Russia from the Atlantic Ocean and despite very low temperatures no mountain glaciation has been developed. Further to the east also the reduction of moisture was leading to smaller glaciations. The lowering of the sea level and the increased sea ice-extent restricted the transport of moisture to the area (e.g. Barr, Clark 2011). However, especially in the Pacific influenced sector of NE Russia the understanding of the timing of mountain glaciations needs to be improved to decipher the different climatic factors in more detail.

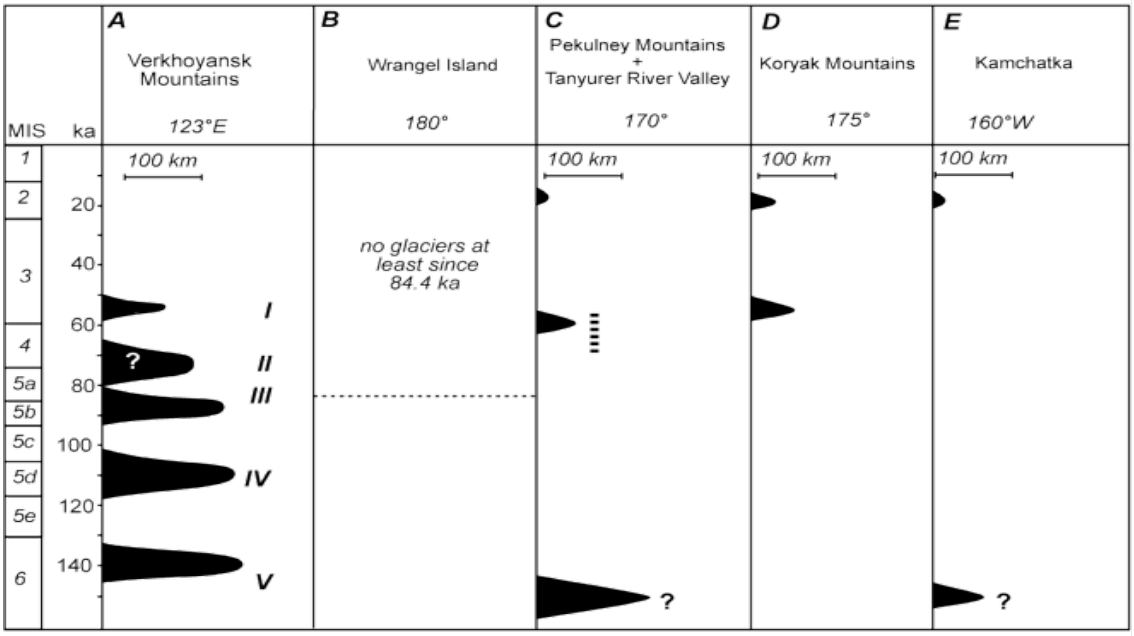

Fig. 1: Quaternary glaciations in NE Russia (Stauch, Gualtieri 2008, reprinted with permission).

References

Bar ID, Clark CD (2011) Glaciers and climate in Pacific Far NE Russia during the Last Glacial Maximum. Journal of Quaternary Sciences (in press). doi: 10.1002/jqs.1450

Glushkova G (2001) Geomorphological correlation of Late Pleistocene glacial complexes of Western and Eastern Beringia. Quaternary Science Reviews 20:405-417. doi:10.1016/S0277-3791(00)00108-6

Krinner G, Diekmann B, Colleoni F, Stauch G (2011) Global, regional and local scale factors determining glaciation extent in Eastern Siberia over the last 140,000 years. Quaternary Science Reviews (accepted). doi:10.1016/j.quascirev.2011.01.001

Stauch G, Gualtieri L (2008) Late Quaternary Glaciations in northeastern Russia. Journal of Quaternary Science 23:545-558. doi: 10.1002/jqs.1211

Stauch G, Lehmkuhl F (2010) Quaternary Glaciations in the Verkhoyansk Mountains, Northeast Siberia. Quaternary Research 74:145-155. doi:10.1016/j.yqres.2010.04.003

Stauch G, Lehmkuhl F, Frechen M (2007) Luminescence chronology from the Verkhoyansk Mountains (North-Eastern Siberia). Quaternary Geochronology 2:255-259. doi:10.1016/j.quageo.2006.05.013

Oceanic and atmospheric teleconnections between the North Pacific and the North Atlantic during the past 25 ka

Ralf Tiedemann[1], Dirk Nürnberg[2], Lars Max[1], Jan-Rainer Riethdorf[2], Julia Gottschalk[3], Andrea Abelmann[1], Sergey Gorbarenko[4], Elena Ivanova[5], Alexander Matul[5]

[1] AWI, Alfred Wegener Institute for Polar and Marine Research, Am Handelshafen 12, 27570 Bremerhaven, Germany; email: Ralf.Tiedemann@awi.de
[2] IFM-GEOMAR, Leibniz Institute of Marine Sciences, Wischhofstrasse 1-3, 24148 Kiel, Germany
[3] University of Bremen, Department 5 Geosciences, Klagenfurter Straße, 28359 Bremen, Germany
[4] POI FEB RAS, V.I.'Ilichev Pacific Oceanological Institute FEB RAS, Baltiyskaya Street 43, 690041 Vladivostok, Russia
[5] IO RAS, P.P. Shirshov Institute of Oceanology RAS, Nakhimovsky prospekt 36, 117997 Moscow, Russia

Our high-resolution sediment records from the NW-Pacific continental margin and the Bering Sea provide an excellent opportunity to verify hypothesized oceanic and atmospheric teleconnections between the North Pacific and the North Atlantic. Results from coupled atmosphere-ocean general circulation models suggest fundamental inter-oceanic teleconnections during the Holocene and the last glacial termination.

For the Holocene, Kim et al. (2004) proposed a sea surface temperature (SST) seesaw pattern between the North Atlantic and the North Pacific with a continuous cooling in the North Atlantic and a warming in the North Pacific over the past 7 kyr. This inverse SST pattern has been connected to an atmospheric circulation field that comprises the elements of the Pacific North American (PNA)/Pacific Decadal Oscillation (PDO) and the North Atlantic Oscillation (NAO) atmospheric circulation patterns in opposite phases. These atmospherical modes, acting on decadal to centennial timescales, have been suggested as a mechanism to explain the simulated inverse long-term SST trends between the North Pacific and the North Atlantic.

Another model study (Okazaki et al. 2010) suggests an atmospheric-oceanic teleconnection between the North Pacific and the North Atlantic, proposing a seesaw in deepwater formation between the North Atlantic and the North Pacific during the early stages of the last glacial termination, including H1 and the Bølling-Allerød. During H1, the Atlantic meridional overturning circulation (AMOC) weakened substantially in response to large meltwater discharges from the Northern Hemisphere ice cap. During this time, the model results suggest significant deep-water formation in the Northwest Pacific due to cooling and increased sea surface salinities (SSS). The mechanism has been related to air-sea interaction in the N-Atlantic and emanating atmospheric teleconnections, which led to a decrease in North Pacific SST and an increase in SSS. The cooling in the North Atlantic during H1 may have resulted in both, a weakening in the moisture transport from the Atlantic into the Pacific and a southward shift of the Pacific Intertropical Convergence Zone, leading to a reduction of pecipitation and thus an overall increase in North Pacific SSS. An inverse pattern would characterize the Bølling-Allerød.

To verify these hypotheses, we use a multi-proxy approach to assess changes in SST, SSS, upper water column stratification, sea ice distribution, productivity and intermediate to deep-water ventilation in the Bering Sea and the adjacent Northwest Pacific. In comparison to other paleoceanographic studies our KALMAR sediment records (Fig. 1) combine three necessary preconditions for such reconstructions: (1) millennial to decadal scale time resolution, (2) carbonate-rich sediments allowing to use the full library of carbonate proxies, and (3) finally the best stratigraphy so far available for the northwest Pacific region, which represents the backbone for all interpretations (see figure of abstract Riethdorf et al. this volume).

Our alkenone-based reconstructions of SST variability at cores SO201-2-77-KL, -85-KL, and -12-KL (see Fig. 1, red spots) suggest a complex pattern of changes in Holocene SST variability, which does not

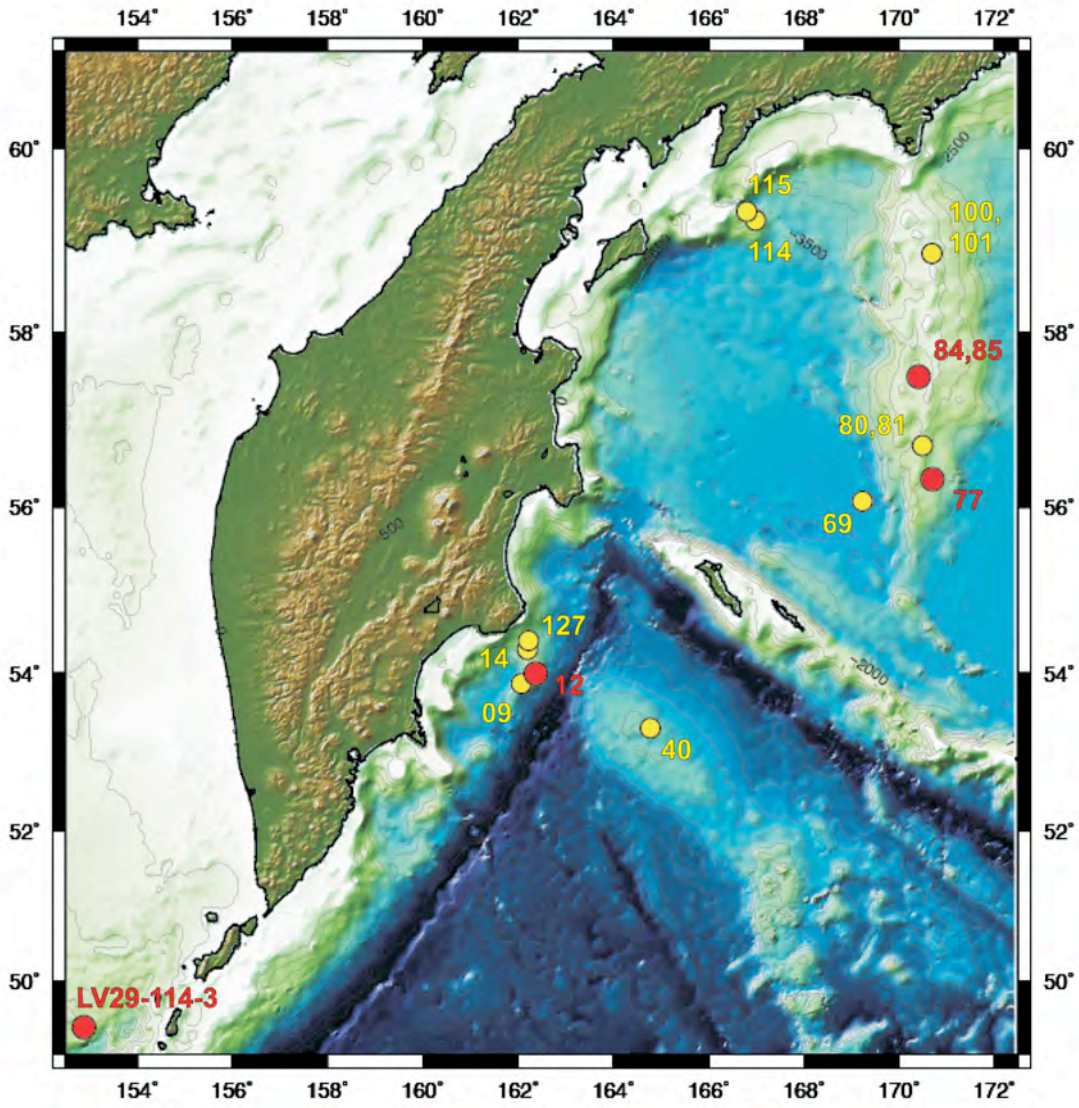

Fig. 1: Locations of sediment cores recovered during SO201-2 and core LV29-114-3

corroborate a Holocene warming since 7 ka as suggested by Kim et al. (2004). Instead, it shows an early Holocene increase in SST culminating in a temperature maximum at 7 ka, which parallels the local insolation maximum. Temperatures decreased from 7 to 1 ka and slightly increased again during the last thousand years. This long-term trend is also reflected in core LV29-114-3 from the southeastern Okhotsk Sea (generated during the KALMAR project) but is opposite to the temperature trend registered at a more northwestern position in the Okhotsk Sea. Another interesting feature of SST development in the western Bering Sea and the northwest Pacific is a temperature minimum around 8 ka. This cooling event is widely regarded as the strongest Holocene cooling episode, with clear expressions in Greenland, the North Atlantic, Europe, and North America (Alley et al. 1997). So far this cooling event has not been detected in the North Pacific. Explanations usually involve a perturbation in AMOC by increased freshwater inputs associated with the decay of the Laurentide ice sheet.

First results about changes in deep water ventilation and thus hints for deep-water formation in the Northwest Pacific are provided by epibenthic $\delta^{13}C$ records and the occurrence of laminated sediment deposits in the Bering Sea. These laminated sediment deposits mark the interval of the Bølling-Allerød and the early Holocene. Since these sediment layers almost lack indications of bioturbation, benthic live was

strongly reduced, most likely as a result of extremely low bottom water oxygen concentrations. This is consistent with low epibenthic $\delta^{13}C$ values, monitored at core SO201-2-85-KL from the Shirshov Ridge, and suggests a strong decrease in deep water ventilation. During the cold stages H1 and the Younger Dryas, $\delta^{13}C$ values are about 1 per mill higher and indicate well ventilated intermediate water masses. At the same time alkenone-based and Mg/Ca-derived temperature reconstructions suggest significantly reduced upper ocean stratification. Hence, this chain of evidence identifies the Bering Sea as a potential location of intermediate to deep-water formation during H1 and the Younger Dryas. This evidence supports the model results from Okazaki et al. (2010) as well as model simulations that were performed within the KALMAR project, suggesting the operation of a Pacific-Atlantic seesaw in overturning circulation.

The measured relative variability of the elemental composition of the seasonally resolved laminated horizons, using ultra high-resolution XRF-scanning (100 µm measuring distance), revealed further insights into the decadal to centennial climate variability and atmospheric teleconnections. Frequency analysis of the elemental variability suggests a dominant decadal climate impact of the Pacific Decadal Oscillation and revealed also an influence of the ENSO-variability. The frequency spectra also reveal that external forcing by variations in insolation cannot be neglected.

References

Alley RB, Mayewski PA, Sowers T, Stuiver M, Taylor KC, Clark PU (1997) Holocene climatic instability: A prominent, widespread event 8200 yr ago. Geology 25: 483-486

Kim JH, Rimbu N, Lorenz SJ, Lohmann G, Nam SI, Schouten S, Rühlemann C, Schneider RR (2004) North Pacific and North Atlantic sea-surface temperature variability during the Holocene. Quaternary Science Reviews 23: 2141-2154

Okazaki Y, Timmermann A, Menviel L, Harada N, Abe-Ouchi A, Chikamoto MO, Mouchet A, Asahi H (2010) Deepwater Formation in the North Pacific During the Last Glacial Termination. Science 329: 200-204

Structure of the uppermost sedimentary layers in Kamchatka and Aleutian island arcs junction area and northern Emperor Seamounts and Emperor Trough - new insights from high resolution echosound data (SO-201 Leg 1a, Leg 2 KALMAR)

Nikolay Tsukanov[1], Christoph Gaedicke[2], Ralf Freitag[2], Karina Dozorova[1]

[1] IO RAS, P.P. Shirshov Institute of Oceanology RAS, Nakhimovsky prospekt 36, 117997 Moscow, Russia; email: paleogeo@ocean.ru

[2] BGR, Federal Institute for Geosciences and Natural Resources, Geozentrum Hannover, Stilleweg 2, 30655 Hannover, Germany

Geological and geophysical investigations have been carried out from board of RV "Sonne", cruises SO-201leg1a, leg 2 (Cruise Report 2009, SO-201, Leg 1a, Leg 2) from summer to autumn 2009. Study areas were located in Kamchatka and Aleutian island arcs junction area, Komandor Basin of the Bering Sea and northern Emperor Seamounts (ESM) and Emperor Trough (ET). The work was performed in the frame of the Russian-German Project KALMAR and included acoustic profiling by on-board profilograph PARASOUND P70. This report presents obtained data on structure of the upper part (up to 100 m) of the sedimentary cover in different structures of the Kamchatka continental margin, northwestern Pacific Plate and the Bering Sea. The data were recorded in PS3 and SEGY formats and were processed by R. Lutz (BGR) in REFLEXW for consequent interpretation (Cruise Report 2009, SO-201, Leg 1a).

(1) The areas away from the influence of the continental slope and seamounts is generally dominated by an acoustic faces characterized by numerous distinct, closely spaced and continuous parallel reflectors, about 2-3 m in thickness. As usual, these reflectors are conformable with the surface topography and can be traceable over tenth of kilometers. The acoustic penetration is often around 50-75 m and some times about 100 m. The draping character and the layered internal reflection pattern suggest undisturbed pelagic or hemipelagic depositional conditions. This style of acoustic reflection is dominated in the top of Shirshov Ridge and Meijia Swell. (2) Similar acoustic faces generally dominate in the deepest areas of Komandorsky basin of Bering Sea but thickness of internal layers is bigger (about 5-7 m). The acoustic transparencies of the observed layers showed internal homogenization and very high acoustic reflection. It is probably the result of disintegration of slope-failed masses and their transport by turbiditic or debri flow. These layers are separated from each other by continuous parallel reflectors which are about 2-3 m thick. In some places near the slope and other topographic highs the uppermost sedimentary sequence is about 7 - 10 m thick and has irregular structure and a hummocky surface. It is traceable over tens of kilometers and is characterized by lens-shaped forms of layers that are separated by layers with good stratification from others lenses. Possibly, there are shear slides. (3) The uppermost sedimentary sequence along the Shirshov Ridge is different at the West and East flank. Acoustic facies at the East flank is characterized by numerous continuous or lens-parallel reflectors, closely spaced with diffuse acoustic reflections. The thickness of these layers is 7-10 m. The visible thickness is about 50-75 m. The sediment cover is disturbed by normal folds with a vertical offset of about 5-10 m. Erosional canyons crossing this area. In this case sediment layers are lens-shaped and feather out to the side of these canyons. The Western flank of Shirshov Ridge is characterized by steeper relief with many erosional canyons and topographic highs. Diffuse reflections obtained from these areas provide little information about the uppermost sedimentary sequence. The normal faults separate Shirshov Ridge from the Komandorsky Basin. The upper part of sediment cover is about 25 - 35 m thick and contains lens-strata and, as usual, feather out in thickness (15 -25 m) to topographic highs and faults. Very often the acoustic layers are folded. (4) Massif of Volcanologist is characterized by step fault and volcanic

cones relief. The sediments are less then 25-35 m in thickness and cover plain. In general, acoustic facies is characterized by numerous distinct, closely spaced lenses form layers, about several meters in thickness. They are separated by layers about 5-7 m in thickness with homogeneous internal structure. Reflectors are conformable with the basement surface topography. (5) Another type of section is typical for ESM and ET having dissected bottom relief. Maximum visible thickness of the sedimentary cover reaches 80 m. Two types of records are distinguished; they alternate in the section and characterize different sedimentary complexes with different internal structure. The first complex is formed by lens-like sedimentary bodies with length varying from several kilometers up to several tens of kilometers. They are formed by acoustically transparent unstratified complexes. Usually, these sedimentary bodies are developed in bottom relief depressions. Their visible thickness varies from 10 m to 40 m and internal structure is conditioned by disintegration and mixing of sedimentary masses during their transportation by underwater currents and flows. The second complex is formed by well-stratified sedimentary horizons similar to those described above. Their thickness reaches 40-60 m becoming thinner in relief lows, where they are interstratified with deposits of the first complex. They are observed on ESM, on the plain between ESM and ET, on ESM flanks. Geometry and internal structure of these bodies and analysis of bottom relief justify that they were formed by debris flows. Besides, they are stratified by thin-bedded sedimentary complexes characterizing pelagic background sedimentation. (6) In the studied parts of Kamchatka continental slope (the Bering Sea, Kronotsky Bay) sediments on the echograms have a homogeneous coarsely-stratified structure. The internal structure on the echograms is characterized by chaotic structure. Considerably long frequently lens-like interlayers subdivided by thin layers with intensive reflective characteristics are distinguished. Visible thickness of the sedimentary cover is from 10-15 m to 60 m. Sedimentary unit developed in the central part of the profile and composing the scarp on the slope has different structure. Thickness of sedimentary body increases up to 40 m. The records are characterized by thin-bedded, lens-like internal structure with intensive reflectors. The sedimentary cover in depressions within Kronotsky Bay have similar structures. Characteristic features of its upper part are: absence of thin-bedded structure, presence of numerous interlayers with intensive reflection connected with their coarse composition and presence of numerous lens-like layers. These features are typical for sediments formed in conditions of active sedimentary material removal by turbiditic flows and underwater currents, which nearly completely smooth over background pelagic sedimentation.

Fulfilled study of sedimentary cover upper part structure in the investigated area shows that several types of acoustic complexes characterizing different facial sedimentation environments are distinguished here: 1 – pelagic and hemipelagic sedimentation typical for deep-water environment of oceanic plates of the ocean and marginal sea, 2 – deposits of debris flows developed near the ridge and on the plain dividing ESM and ET, in the ET valley and on the Shirshov Ridge, 3 – sedimentary complexes on the continental slope characterized by coarse and lens-like bedding with intensive reflectors and apparently formed under strong influence of turbiditic strands, 4 – sedimentary bodies of landslide nature. In general it may be noted that structure and composition of sedimentary cover is mainly conditioned by local bottom relief features and are formed by depositional, redistribution and/or erosional processes. Along with background sedimentation the important role belong to complexes formed by different underwater flows and currents.

Authors express gratitude to scientific staff that obtained and processed the PARASOUND P70 data and crew of RV “Sonne”. The investigations were funded by BMBF, grant No. 03G0201B.

References

*K*urile-Kamchatka and *AL*eutian *MAR*ginal Sea-IslandArc Systems: Geodynamic and Climate Interaction. CRUISE REPORT, NR, 32, Sonne Cruise SO-201, Leg 1a. 2009.Yokohama. P. 105

Dullo WC, Baranov B, van den Bogaard C. (Eds.) (2009) FS Sonne Fahrtbericht / Cruise Report SO201-2 KALMAR: Kurile-Kamchatka and ALeutian MARginal Sea-Island Arc Systems: Geodynamic and Climate Interaction in Space and Time, Busan/Korea - Tomakomai/Japan, 30.08. - 08.10.2009 [Fahrtbericht]. In: IFM-GEOMAR Report, 35. IFM-GEOMAR, Kiel

Effect of seawater alteration on trace element geochemistry of submarine basalts from the Bowers Ridge, Bering Sea

Maren Wanke[1,2], Maxim Portnyagin[1,3], Reinhard Werner[1], Folkmar Hauff[1], Kaj Hoernle[1], Dieter Garbe-Schönberg[2]

[1] IFM-GEOMAR, Leibniz Institute of Marine Sciences, Wischhofstraße 1-3, 24148 Kiel, Germany; email: mwanke@ifm-geomar.de
[2] Institute of Geosciences, Christian-Albrechts-University of Kiel, Ludewig-Meyn-Straße 10, 24118 Kiel, Germany
[3] GEOKHI RAS, V.I.Vernadsky Institute of Geochemistry and Analytical Chemistry RAS, Kosygin St. 19, 119991 Moscow, Russia

New oceanic crust unavoidably interacts with seawater. Previous field and experimental studies have shown that the effects of seawater – rock interaction are large and dependent on rock chemistry, temperature, water/rock ratio, duration of interaction and environment (e.g. Hart 1969). The evaluation of the behavior of major and trace elements, radiogenic and stable isotopes during these low-temperature alteration processes is essential for accurate interpretations of geochemical data for igneous oceanic crust and quantification of geochemical recycling of elements between the Earth ocean and mantle reservoirs.

Here we present new data on composition of altered olivine basalts from the Bering Sea, which exhibit very unusual trace element patterns for altered oceanic basalts. The rocks were dredged during KALMAR R/V SONNE 201 Leg 1b cruise in 2009 from a seamount located west of the Bowers Ridge (DR29, Wanke et al. this volume). These rocks are fragments of variably altered olivine-phyric pillow basalts with some fresh glass preserved at the pillow rims. The glasses have been analyzed for major elements by electron microprobe at IFM-GEOMAR (Kiel) and for trace element by laser ablation ICPMS in the Institute of Geosciences at the CAU (Kiel). Whole rock (WR) analyses of major and trace elements were made by XRF and ICPMS at ACME Lab (Vancouver, Canada).

The compositions of quenched rim glasses are very similar for all studied samples. This allowed us to suggest that the compositions of the whole rocks were also similar prior to seawater alteration and could be close to that of glass with some ca. 12% olivine (thereafter referred to as “the initial rock composition”). Comparison of the whole rocks to this initial rock composition allowed us to quantify the relative mobility of major and trace elements during the alteration (Fig. 1).

The strongest enrichment was found for P (up to 1300 % in the most altered samples), U (up to 1040%), Cs (up to 260%), Ba (up to 680%), La (up to 345%), Y (up to 275%) and all HREE (up to 130 %). Y appears to be more mobile compared to HREE, and the most altered rocks have a strong positive Y-anomaly ($Y_N/Dy_N = 2.1$). Ce and Eu exhibit a lower mobility compared to neighbouring REE. Consequently, the most altered samples have negative Ce- and Eu-anomalies ($Ce/Ce^* = 0.33$ and $Eu/Eu^* = 0.80 – 0.88$, where asterisk indicates concentration calculated from interpolation of neighbouring REE) in the normalized patterns of REE. Enrichment in Sr is moderate (35 - 60%). The elements with concentrations within 20 relative % of the initial rock composition are all HFSE (Nb, Ta, Zr, Hf, and Ti), some LILE (K, Rb), Th and Pb. These elements were likely not unaffected by the alteration. The alteration pattern of the studied basalts is drastically different from that of typical low-temperature seawater alteration of oceanic basalts which is associated with strong enrichments in K, Rb, Cs, U whereas REE, HFSE and Y are immobile (e.g., Cann 1970; Hart 1969). The reasons for the distinctive alteration pattern of the Bowers Ridge basalts are not clear to us at present. Precipitation from the seawater can be a possible explanation for the enrichment in U, Cs, Ba and REE including the negative Ce-anomaly (e.g. Li 1991). In such case, the absolute concentrations of other mobile elements including those with high concentrations in seawater (Rb, K and Sr) should not be affected. The slight enrichment of Y relative to Dy and Ho in seawater (Li 1991) might be too small to create a prominent positive anomaly in the studied rocks.

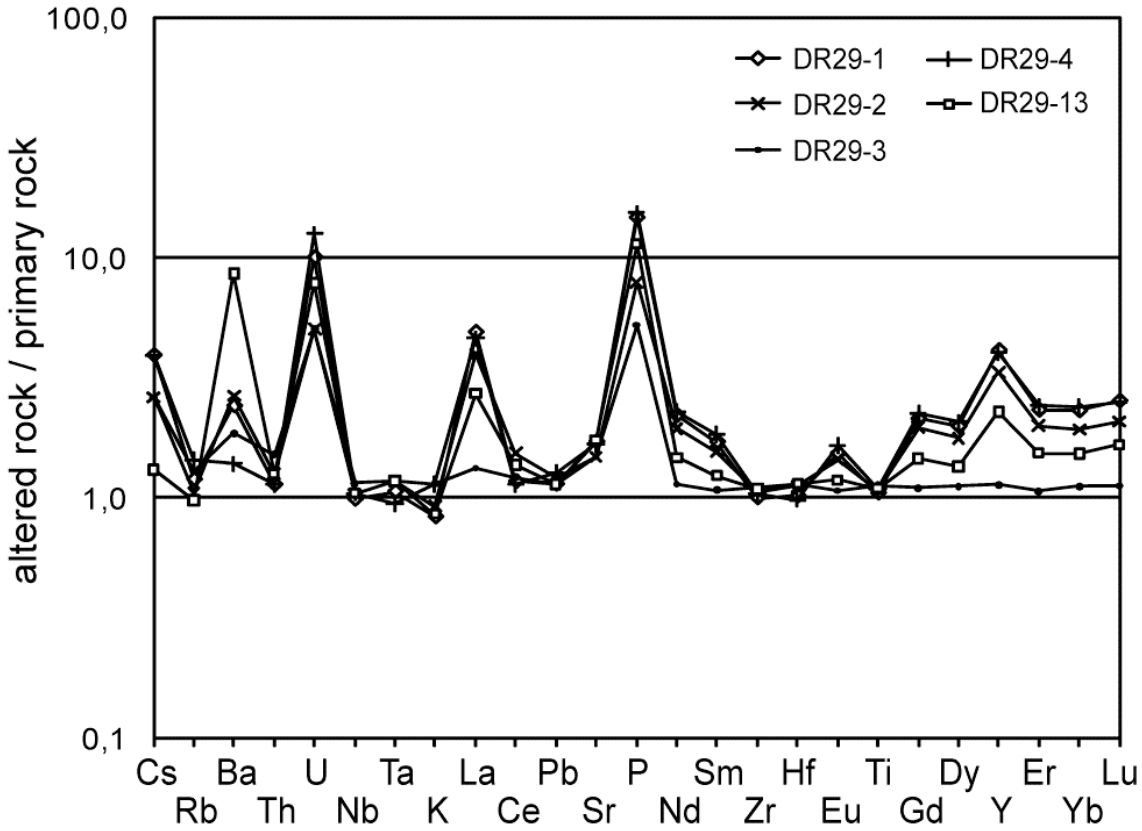

Fig. 1: Different patterns in the multielement diagram indicate changes in compositions of five altered basalts relative to the initial rock composition calculated.

The origin of the Y anomaly as well as the overall alteration pattern appears to require some specific reactions involving low-T complexes of trace and major elements (Bau 1999) and/or possibly effects of biogenic phosphorization.

Our future investigations will be focused on searching for possible mechanisms and reactions responsible for the alteration pattern of the Bowers Basalts and on the evaluation of isotopic effects of the alteration. The results are anticipated to provide new insights into seawater-rock alteration processes on the ocean floor and point to new proxies of recycled material in the sources of island-arc and ocean-island basalts.

References

Bau M (1999) Scavenging of dissolved yttrium and rare earths by precipitating iron oxyhydroxide: experimental evidence for Ce oxidation, Y-Ho fractionation, and lanthanide tetrad effect. Geochimica et Cosmochimica Acta 63: 67 - 77

Cann JR (1970) Rb, Sr, Y, Zr and Nb in some ocean floor basaltic rocks. Earth and planetary science letters 10: 7 - 11

Hart SR (1969) K, Rb, Cs contents and K/Rb, K/Cs ratios of fresh and altered submarine basalts. Earth and planetary science letters 6: 295 – 203

Li Y (1991) Distribution patterns of the elements in the ocean: A synthesis. Geochimica et Cosmochimica Acta 55: 3223 – 3240

Wanke M, Portnyagin M, Werner R., Hauff F, Hoernle K, Garbe-Schönberg D (2011) New geochemical data provide evidence for an island-arc origin of the Bowers and Shirshov Ridges (Bering Sea, NW Pacific) (this volume)

New geochemical data provide evidence for an island-arc origin of the Bowers and Shirshov Ridges (Bering Sea, NW Pacific)

Maren Wanke[1,2], Maxim Portnyagin[1,3], Reinhard Werner[1], Folkmar Hauff[1], Kaj Hoernle[1], Dieter Garbe-Schönberg[2]

[1] IFM-GEOMAR, Leibniz Institute of Marine Sciences, Wischhofstrasse 1-3, 24148 Kiel, Germany; email: mwanke@ifm-geomar.de
[2] Institute of Geosciences, Christian-Albrechts-University of Kiel, Ludewig-Meyn-Straße 10, 24118 Kiel, Germany
[3] GEOKHI RAS, V.I.Vernadsky Institute of Geochemistry and Analytical Chemistry RAS, Kosygin St. 19, 119991 Moscow, Russia

The Bowers and Shirshov Ridges (hereafter BR and SR, respectively) are two prominent submarine structures of unknown age and provenance in the Bering Sea (Fig. 1). So far only a few geochemical data exist on the composition of basement rocks from the SR (Silantyev et al. 1985) and none for the BR. Age and geochemical data are crucial to evaluate if the ridges represent remnant island arcs (Cooper et al. 1981, Scholl 2007), intra-oceanic rises, accreted onto the continental margin (Ben-Avraham and Cooper 1981), an ancient spreading center (SR: Kienle 1971) or parts of the Mesozoic Hawaiian hot-spot (Steinberger, Gaina 2007).

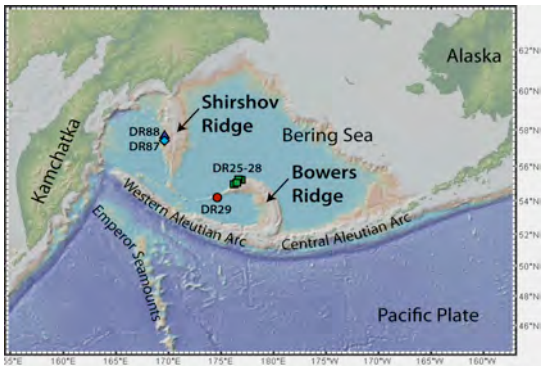

Fig. 1: Map of the study area. Colored symbols indicate dredge locations (DR) on the BR (green squares), the SR (blue triangle and diamond) and on a seamount next to the BR (red circle).

Here we report the first geochemical data on the composition of the basement rocks from the BR and SR, recovered during KALMAR R/V SONNE cruise 201 (Legs 1b and 2) in 2009. Fresh to moderately altered volcanic rocks were dredged from the northern slope of the BR, from seamounts on the western extension of the BR and from the western slope of the central part of the SR. We studied the petrography of the samples and carried out geochemical analyses of major and trace elements by XRF and ICPMS at ACME Lab (Vancouver, Canada) and CAU (Kiel). Sr-Nd-Pb(ds) isotopes were analyzed by TIMS at the IFM-GEOMAR (Kiel).

The rocks from the northwestern slope of the BR are clinopyroxene (cpx)-phyric basalts with minor amounts of olivine (ol) and plagioclase (plag) microphenocrysts, as well as hbl-plag-cpx-bearing basaltic andesites and trachyandesites. The rocks are strongly enriched in LREE (La_N/Yb_N = 3.2 – 8.5, N indicates normalization to primitive mantle), fluid-mobile elements (Pb, Ba, U, K) relative to NMORB and exhibit clear negative anomalies of HFSE (Nb, Ta and Ti) in primitive mantle-normalized incompatible element diagrams. The BR rocks also have a moderate adakitic signature, as indicated by elevated Sr_N/Y_N ratios (6.9 – 12.9). Hbl-cpx-plag trachybasalts from the SR have similar major and trace element compositions (La_N/Yb_N = 2.1 – 4.9) to the BR rocks. The other magmatic series from the SR comprises massive trachyandesites, trachytes and dacites with rare phenocrysts of plag and cpx. These rocks also have island-arc type incompatible element patterns and are distinct from other rock types from the BR and SR with less LREE enriched patterns (La_N/Yb_N ~ 1.8) and a strong negative Eu anomaly (Eu/Eu* = 0.74).

The rocks from BR have relatively unradiogenic Sr and Pb isotopes ($^{87}Sr/^{86}Sr$ = 0.70296 – 0.70311, $^{206}Pb/^{204}Pb$ = 18.22 – 18.30) and radiogenic Nd ($^{143}Nd/^{144}Nd$ = 0.51312 – 0.51314) compositions, which are well within the Aleutian Arc isotope array and intermediate between typical compositions of the Central and Western

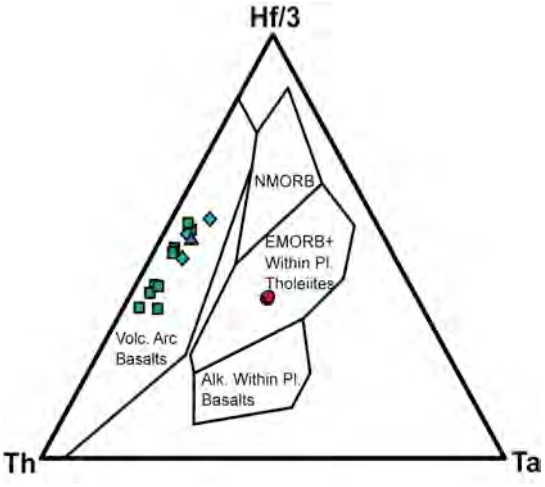

Fig. 2: Th-Hf-Ta diagram after Wood (1980) showing different tectonic settings for BR and SR and one seamount in between. Symbols refer to Fig. 1.

Aleutian rocks (Kelemen et al. 2003). The rocks from SR have slightly more radiogenic $^{87}Sr/^{86}Sr$ (0.70338 – 0.70414) and similar $^{143}Nd/^{144}Nd$ isotope compositions to the BR rocks. Silicic SR rocks have distinctively high $^{206}Pb/^{204}Pb$ (18.46 – 18.47) ratios compared to basalts from BR and SR.

Rocks dredged from a seamount on the western extension of the BR have very distinctive petrographic and geochemical characteristics. These are ol-phyric pillow basalts with minor (less than 5%) amounts of plag and cpx. The freshest whole rocks and pillow-rim glasses have relatively smooth patterns of incompatible trace elements, akin to intraplate oceanic basalts (Fig. 2) and in some characteristic incompatible element ratios (e.g. Th_N/Ba_N = 0.6, Sr_N/Ce_N = 1.2, La_N/Yb_N = 3.3) are similar to Hawaiian hotspot tholeiites.

In summary, petrography and geochemical results indicate an island-arc origin (Fig. 2) for major parts of the BR and SR. Isotope data suggest that the BR and parts of the SR could have developed as parts of the former Aleutian Arc. The discovery of intraplate basalts suggests that fragments of the Emperor Seamount Chain could also be preserved in the Bering Sea (Steinberger & Gaina 2007) as seamounts and in the BR and SR basement. Our further studies will be focused on obtaining absolute age data for the studied rocks, which will allow combining the petrologic data with tectonic and geodynamic models for the NW Pacific.

References

Ben-Avraham Z, Cooper AK (1981) Early evolution of the Bering Sea by collision of oceanic rises and North Pacific subduction zones. Geol. Soc. Am. Bull. 92: 485-495

Cooper AK, Marlow MS, Ben-Avraham Z (1981) Multichannel seismic evidence bearing on the origin of Bowers Ridge, Bering Sea. Geol. Soc. Am. Bull. 92: 474-484

Kelemen PB, Yogodzinski GM, Scholl DW (2003) Along-Strike Variation in the Aleutian Island Arc: Genesis of High Mg# Andesite and Implications for Continental Crust. In: Eiler J (ed): Inside the Subduction Factory. American Geophysical Union, Monograph 138: 223-276

Kienle J (1971) Gravity and magnetic measurements over Bowers Ridge and Shirshov Ridge, Bering Sea. Journal of Geophysical Research, 76: 7138-7153

Scholl D W (2007) Viewing the tectonic evolution of the Kamchatka-Aleutian (KAT) connection with an Alaska crustal extrusion perspective. In: Eichelberger JC, Gordeev E, Izbekov P, Kasahara M, Lees J (eds): Volcanism and subduction the Kamchatka region, American Geophysical Union, Monograph 172: 3-35

Silantyev SA, Baranov BV, Kolesov GM (1985) Geochemistry and petrology of amphibolites from the Shirshov Ridge (Bering Sea). Geochimiya 12: 1694-1704

Steinberger B, Gaina C (2007) Plate-tectonic reconstructions predict part of the Hawaiian hotspot track to be preserved in the Bering Sea. Geology 35: 407-410

Wood DA (1980) The application of a Th-Hf-Ta diagram to problems of tectnomagmatic classification and to establishing the nature of crustal contamination of basaltic lavas of the British Tertiary volcanic province. Earth and Planetary Science Letters 50: 11-30

Geochemistry of Seafloor Lavas of the Western Aleutian Arc

Gene Yogodzinski[1], Joshua Turka[1], Shawn Arndt[1], Peter Kelemen[2], Maxim Portnyagin[3,4], Kaj Hoernle[3]

[1] Department of Earth & Ocean Sciences, University of South Carolina, 701 Sumter St., EWSC617, Columbia SC 29208, USA; email: gyogodzin@geol.sc.edu
[2] Department of Earth & Environmental Sciences, Columbia University, Palisades, NY 10964, USA
[3] IFM-GEOMAR, Leibniz Institute of Marine Sciences, Wischhofstrasse 1-3, 24148 Kiel, Germany
[4] GEOKHI RAS, V.I.Vernadsky Institute of Geochemistry and Analytical Chemistry RAS, Kosygin St. 19, 119991 Moscow, Russia

Results of the 2005 Western Aleutian Volcano Expedition (WAVE) and the June 2009 cruise of the German-Russian KALMAR project (Kamchatka-Aleutian Margin) include the discovery of seafloor volcanism at the Ingenstrem Depression and at unnamed seamounts (hereafter referred to as the Western Cones) located 300 km west of Buldir Island, the westernmost emergent volcano in the Aleutian island arc. The newly discovered features fall on a volcanic line connecting Buldir and other emergent volcanoes to Piip Seamount, which is located in the far western Aleutian Komandorsky area. These discoveries indicate that the surface expression of active Aleutian volcanism slips below sea level at 175°E, but is otherwise continuous for more than 2000 km of arc length from 163°W to 167°E longitude.

Samples from the Ingenstrem Depression (60 km west of Buldir) define two broadly distinctive compositional groups based on Sr abundance. Low-Sr lavas (<700 ppm Sr) are basalts and andesites with moderately enriched trace element patterns (La/Yb 4-8, Sr/Y<30) and relatively radiogenic Sr ($^{87}Sr/^{86}Sr$ =0.7031-0.7033), typical of basalts and andesites in the eastern and central Aleutians and in island arcs worldwide. High-Sr lavas (>700 ppm) are mostly plagioclase, pyroxene and hornblende-phyric andesites and dacites with low Y (8-12 ppm), fractionated trace element patterns (Sr/Y=50-200) and relatively unradiogenic Sr isotopes ($^{87}Sr/^{86}Sr$ = 0.70262-0.70294). Lavas of the Western Cones are rhyodacites, which define the high-Sr end-member with 1280-1640 ppm Sr, 4-6 ppm Y, highly fractionated trace element patterns (Sr/Y=200-300), and unradiogenic (MORB-like) Sr isotopes ($^{87}Sr/^{86}Sr$ < 0.70266). Strontium isotopes for all western Aleutian seafloor lavas are inversely correlated with Sr/Y and SiO_2, so the most felsic samples, which have the highest Sr abundances and most fractionated trace element patterns, are also the most isotopically depleted.

The narrow range for Nd isotopes compared to Sr (epsNd=8.5-9.5 vs $^{87}Sr/^{86}Sr$=0.7026-0.7032) in western Aleutian sea floor lavas suggests that the source of these elements lies primarily in seawater-altered subducted oceanic crust, with little contribution from sediment. High SiO_2 and strongly fractionated trace element patterns in high-Sr lavas combined with MORB-like isotopic compositions are also consistent with a source predominantly in subducted oceanic crust and a melt residue that contained garnet. Their strongly calc-alkaline character (FeO*/MgO<1.5 at 60-70% SiO_2) indicates that western Aleutian andesites and dacites probably had high pre-eruptive H_2O contents (Zimmer et al. 2010), but the MORB-like isotopes indicate that the water was not derived from subducted sediment or seawater-altered oceanic crust, and instead may have been from serpentinite in the upper mantle portion of the subducting oceanic lithosphere.

These characteristics indicate that there is a combination of source chemistry, melting processes and residual mineralogy that distinguishes high-Sr lavas of the western Aleutians from most island-arc rocks worldwide; however, trace element patterns for the most incompatible elements in western Aleutian lavas of all compositions are typical of subduction-related lavas worldwide, with pronounced depletions in Ta and Nb and spikes at K, Pb and Sr. Isotopic constraints cited above rule out a significant role for hydrous fluids from the subducting plate as a source of K, Pb and Sr enrichments in the high-Sr rocks. Instead, and consistent with recent hydrous basalt-melting experiments (Klimm et al. 2008), these

classic signatures of subduction appear to be produced by melting of subducted basalt in the presence of accessory minerals such as garnet, rutile, allanite and zircon. The western Aleutian setting is particularly well suited to testing ideas about the possible role of accessory minerals in controlling trace element patterns in arc lavas because subducted sediment (which introduces tremendous geochemical complexity into the source of most arc lavas) is absent from the source of our high-Sr samples, and because the source of these samples lies predominantly in subducted basalt.

References

Klimm K, Blundy JD, Green TH (2008) Trace element partitioning and accessory phase saturation during H_2O-saturated melting of basalt with implications for subduction zone chemical fluxes, Journal of Petrology 49: 523-553

Zimmer MM, Plank T, Hauri EH, Yogodzinski GM, Stelling P, Larson J, Singer B, Jicha B, Mandeville C, Nye CJ (2010) The role of water in generating the calc-alkaline trend: New volatile data for Aleutian magmas and a new tholeiitic index, Journal of Petrology 51: 2411-2444

LIST OF AUTHORS

Participating Institutes

German Institutes

AWI - Bremerhaven
Alfred Wegener Institute for Polar and Marine Research
Am Handelshafen 12
27570 Bremerhaven
Germany

AWI - Potsdam
Alfred Wegener Institute for Polar and Marine Research
Telegrafenberg A43
14473 Potsdam
Germany

BGR
Federal Institute for Geosciences and Natural Resources, Geozentrum Hannover
Stilleweg 2
30655 Hannover
Germany

IFM-GEOMAR
Leibniz Institute of Marine Sciences
Wischhofstrasse 1-3
24148 Kiel
Germany

Leibniz University Hannover
Institute of Mineralogy
Callinstrasse 3
30167 Hannover
Germany

RWTH Aachen
University Geographical Institute
Templergraben 55
52056 Aachen
Germany

TU Bergakademie Freiberg
Saxonian Academy of Sciences Leipziger Str. 23
09596 Freiberg
Germany

University Jena
Institute of Earth Sciences,
Burgweg 11
07749 Jena
Germany

Russian Institutes

GEOKHI RAS
V.I.Vernadsky Institute of Geochemistry
and Analytical Chemistry RAS
Kosygin St. 19
119991 Moscow
Russia

Geological Institute RAS
Pyzhevsky per. 7
119017 Moscow
Russia

IO RAS
P.P. Shirshov Institute of Oceanology RAS
Nakhimovsky prospekt 36
117997 Moscow
Russia

IVS FEB RAS
Institute of Volcanology and Seismology
FEB RAS
Piip Boulevard 9
683006 Petropavlovsk-Kamchatsky
Russia

NEISRI FEB RAS
Northeastern Integrated Scientific-Research
Institute FEB RAS Portovaya St. 16
685000 Magadan
Russia

POI FEB RAS
V.I.'Ilichev Pacific Oceanological Institute
FEB RAS
Baltiyskaya Street 43
690041 Vladivostok
Russia

American Institute

USC
University of South Carolina
Department of Earth and Ocean Sciences
701 Sumter Street
Columbia, SC 29208
USA